Role of Aldosterone in Potassium Homeostasis and Pregnancy

Dissertation

zur

Erlangung der naturwissenschaftlichen Doktorwürde

(Dr. sc. nat.)

vorgelegt der

Mathematisch-naturwissenschaftlichen Fakultät

der

Universität Zürich

von

Abhijeet Pandurang Todkar

aus Indien

Promotionskomitee

Prof. Dr. med. Carsten A. Wagner (Vorsitz und Leitung der Dissertation)

Prof. Dr. med. Johannes Loffing (Leitung der Dissertation)

Prof. Dr. med. François Verrey

Prof. Dr. med. Dominique Eladari

Zürich, 2012

Contents

SUMMARY

Aldosterone is a mineralocorticoid hormone with pleiotropic actions in the body. Among others, aldosterone controls sodium and potassium excretion in kidney and colon and it was proposed to play an important role during pregnancy. Most of the previous studies examining the *in vivo* role of aldosterone have been performed in adrenalectomized animals. However, the often incomplete removal of adrenal tissue and the existence of local aldosterone producing systems in various organs complicated deciphering the precise role of aldosterone. In this thesis, we took advantage of the recently developed aldosterone-synthase-deficient ($AS^{-/-}$) mice to analyse the role of aldosterone in the control of potassium homeostasis and pregnancy. $AS^{-/-}$ mice lack any endogenous aldosterone production, have slightly elevated plasma corticosterone levels, a reduced bodyweight despite increased food intake, but are otherwise clinically normal.

$AS^{-/-}$ and $AS^{+/+}$ mice were kept for two days either on a standard diet (0.8% K^+), or diets enriched with potassium (2% K^+, 3% K^+ and 5% K^+). The $AS^{-/-}$ mice adapted well to 2% K^+ diet. Urinary K^+ excretion rose similar in $AS^{-/-}$ and $AS^{+/+}$ mice and plasma K^+ levels remained in the normal range. With 3% K^+ diet, $AS^{-/-}$ mice tended to become hyperkalemic and on 5% K^+ diet, the $AS^{-/-}$ mice were fully decompensated and exhibited severe hyperkalemia and K^+-food avoidance. Therefore, all following studies were performed on mice kept either on standard or on 2% K^+ diets. First, we analyzed the effect of dietary K^+ loading on the abundance and subcellular localization of the renal outer medullary potassium channel (ROMK) and the epithelial sodium channel (ENaC) in the kidney. ROMK and ENaC are expressed in the aldosterone-sensitive distal nephron (ASDN) comprising the late distal convoluted tubule (DCT2), the connecting tubule (CNT), and the collecting duct (CD). ROMK is thought to mediate most of renal K^+ excretion, while Na^+-reabsorption via ENaC provides the electrochemical driving force for K^+ secretion across the apical plasma membrane. Accordingly, we found that dietary K^+ loading (2% K^+) causes a translocation of ROMK and ENaC from intracellular compartments to the apical plasma membrane of the ASDN. The apical translocation of ENaC was accompanied by a proteolytic cleavage of the α- and γ-subunits of ENaC, which is thought to activate ENaC. Apical translocation of ROMK and ENaC, as well the proteolytic activation of ENaC was similar in $AS^{+/+}$ and $AS^{-/-}$ mice. Consistently, patch

clamp experiments on isolated split-open tubules revealed similar whole cell amiloride-sensitive Na^+ channel currents in the early ASDN of $AS^{+/+}$ and $AS^{-/-}$ mice. Likewise, on the 2% K^+ diet, $AS^{+/+}$ and $AS^{-/-}$ mice showed the same natriuretic response to a single amiloride injection. To address the possible mechanism for the aldosterone-independent activation of ENaC in the early ASDN, we treated $AS^{+/+}$ and $AS^{-/-}$ mice on 2% K^+ diet with the angiotensin II AT1 receptor antagonist losartan. While $AS^{+/+}$ mice tolerated losartan treatment without any problems, $AS^{-/-}$ mice decompensated and developed severe hypokalemia with K^+-food avoidance. Immunohistochemistry revealed that losartan-treatment of $AS^{-/-}$ mice impaired the apical translocation of ENaC. Interestingly, $AS^{-/-}$ mice showed reduced abundance and phosphorylation of the thiazide-sensitive NaCl-cotransporter (NCC), which was present already on standard diet and became even more pronounced on high K^+-diet. Consistent with lowered NCC activity, $AS^{-/-}$ mice on 2% K^+ diet showed lesser natriuresis than $AS^{+/+}$ mice in response to hydrochlorothiazide. Ussing-type chamber experiments on isolated colon mucosa from $AS^{+/+}$ and $AS^{-/-}$ mice showed that dietary K^+ intake (2% K^+ for 2-4 days) increases Ba^+-sensitive K^+ channel and amiloride-sensitive Na^+ channel currents only in $AS^{+/+}$ but not in $AS^{-/-}$ mice. Taken together our results suggest that aldosterone-deficiency does not prevent the K^+-intake-induced functional adaptation of ROMK and ENaC in the kidney, but impairs the homeostatic response of BK and ENaC in the colon. Angiotensin-II dependent activation of ENaC and functional downregulation of NCC in the renal tubule likely contribute to the maintenance of K^+ homeostasis in the absence of aldosterone. NCC downregulation in DCT enhances Na^+ delivery to the ASDN, which can be reabsorbed via angiotensin II activated ENaC and hence increases the driving force for K^+-secretion via ROMK.

During normal pregnancy, plasma volume expands to increase the perfusion of the placenta and support fetal growth. The extension of plasma volume coincides with a gradual increase in plasma aldosterone levels. Clinical studies revealed aldosterone deficiency in a subgroup of women in pregnancy-associated disorders like pre-eclampsia. Therefore, we aimed to test in our mouse model the hypotheses whether chronic aldosterone deficiency may contribute or cause pre-eclampsia or intra-uterine growth restriction (IUGR). In order to avoid differing genotypes of pups as a confounding factor, we used only two types of breeding ($AS^{+/+}$ male mating with

$AS^{-/-}$ female and $AS^{-/-}$ male mating with $AS^{+/+}$ female) giving heterozygous pups only. Hypertension and proteinuria are considered as cardinal signs of pre-eclampsia. Therefore, we measured systolic blood pressure (SBP) and proteinuria in $AS^{+/+}$ and $AS^{-/-}$ females to check for the development of pre-eclampsia. $AS^{-/-}$ mice did not develop hypertension or proteinuria but showed significantly decreased litter sizes. To investigate the possible mechanism for decreased litter sizes, pregnant mice were sacrificed on day 18 of pregnancy. At this stage, $AS^{-/-}$ females already showed a reduced number of fetuses that correlated with an increased number of necrotic placentas. Also, the weights of the fetuses and the placentas were lower in $AS^{-/-}$ than in $AS^{+/+}$ females. Histology of healthy placentas from $AS^{+/+}$ and $AS^{-/-}$ mice showed similar structures including a normal decidua basalis, junctional zone, and labyrinth, while necrotic placentas showed severe coagulative necrosis and infiltration of lymphocytes in all three layers. Consistently, necrotic placentas revealed increased mRNA levels of the pro-inflammatory cytokine tumor necrosis factor 1alpha (TNF1α), and the monocyte chemo-attractant protein 1 (MCP-1). We hypothesized that aldosterone deficiency decreases plasma volume and arterial perfusion, which finally compromise placental and foetal growth due to placental hypoxia. Consistent with placental hypoxia, we found a significantly increased protein expression of hypoxia inducible factor 1 (HIF1α) in placentas of $AS^{-/-}$ mice when compared with $AS^{+/+}$ mice.

In order to improve plasma volume during pregnancy, we fed a high salt diet (5% NaCl) to females. $AS^{+/+}$ and $AS^{-/-}$ female mice responded well to high salt diet as indicated by an increased SBP during high salt diet. During pregnancy, SBP decreased in both genotypes. Litter size was slightly improved but necrotic placentas were still observed in $AS^{-/-}$ mice. However, increased weight of pups was observed in $AS^{+/+}$ and $AS^{-/-}$ females on high salt diet during pregnancy compared to control diet. In mice of both genotypes, placental efficiency was significantly improved by the high salt diet suggesting a better perfusion of the placenta, which may have improved growth of the fetuses. Accoridingly, HIF1α expression levels were similar in placentas from $AS^{+/+}$ and $AS^{-/-}$ females on high salt diet.

In summary, using $AS^{-/-}$ mice, we revealed aldosterone-dependent and independent mechanisms for K^+ homeostasis in the kidney and the colon. The aldosterone-independent mechanisms allow for maintenance of K^+-homeostasis in the absence of any aldosterone by activation of ROMK and ENaC in the kidney and

perhaps down-regulation of NCC. In contrast to the kidney, the colonic adaptation to dietary K^+ intake appears to strictly depend on aldosterone. We also demonstrated, using $AS^{-/-}$ mice, that aldosterone deficiency affects placental function during pregnancy leading to reduced placental and fetal growth. Dietary salt supplementation during pregnancy can partially improve placental function.

DEUTSCHE ZUSAMMENFASSUNG DER DOKTORARBEIT

Aldosteron ist ein Mineralokortikoidhormon, das hauptsächlich in der Nebenniere gebildet wird und unterschiedlichste Körperfunktionen beeinflussen kann. Unter anderem spielt Aldosteron eine zentrale Rolle bei der Regulierung der Natrium- und Kaliumausscheidung durch Nieren und Dickdarm. Auch während der Schwangerschaft scheint Aldosteron eine wichtige Funktion zu haben.

Bisherige in vivo Untersuchungen zur physiologischen Bedeutung von Aldosteron wurden vor allem an adrenalektomierten Tieren durchgeführt. Die oft unvollständige Entfernung der Nebennieren und eine gewisse extraadrenale Produktion von Aldosteron erschwert aber eine eindeutige Interpretation der gewonnenen Daten. In dieser Doktorarbeit nutzten wir Aldosteronsynthase-defiziente ($AS^{-/-}$) Mäuse, die keine endogene Aldosteronproduktion mehr haben, um die Rolle von Aldosteron bei der Aufrechterhaltung der Kaliumhomöostase und während der Schwangerschaft genauer zu untersuchen. $AS^{-/-}$Mäuse weisen leicht erhöhte Plasma-Kortikosteron Werte auf, haben ein stark aktiviertes Renin-Angiotensin-System und ein reduziertes Körpergewicht, sind aber ansonsten weitgehend unauffällig.

Wir untersuchten die Fähigkeit von $AS^{-/-}$ Mäusen sich an unterschiedliche Kaliumaufnahmen anzupassen. Dazu fütterten wir $AS^{-/-}$ Mäuse und Wild-typ ($AS^{+/+}$) Mäuse für zwei Tage entweder mit einer Standard Diät mit einem Kaliumgehalt von 0.8% K^+ oder einer K^+-angereicherten Diät mit 2% K^+, 3%K^+ oder 5%K^+. Wir stellten fest, dass sich die $AS^{-/-}$ Mäuse gut an die 2% K^+-Diät anpassen können. Wie die $AS^{+/+}$ Mäuse erhöhten sie die K^+ Ausscheidung im Urin und hielten so ihre Plasma K^+-Konzentration auf einem normalen Wert. Ab einer K^+-Anreicherung von 3% zeigten die $AS^{-/-}$ aber erste Anzeichen einer Hyperkalämie. Wurde der Kaliumgehalt der Diät noch weiter auf 5% gesteigert dekompensierten die $AS^{-/-}$ Mäuse vollständig. Sie zeigten eine ausgeprägte Hyperkalämie und verweigerten die weitere Aufnahme der 5% K^+-Diät. Aufgrund dieser Beobachtungen wurden alle weiteren Untersuchungen nur noch an Mäusen, die mit der Standard Diät oder der 2% K^+-Diät gefüttert wurden, durchgeführt.

Zuerst untersuchten wir den Einfluss einer erhöhten Kalium Aufnahme auf die Menge und die subzelluläre Lokalisierung des K^+-Kanals ROMK und des

epithelialen Na^+-Kanals ENaC, die im Aldosteron-abhängigen distalen Teil des Nephrons, dem sogenannten ASDN, vorkommen. Im ASDN vermittelt ROMK die K^+-Ausscheidung über die apikale Plasmamembran. Die notwendige elektrochemische Triebkraft für die K^+-Sekretion wird durch eine ENaC-vermittelten Na^+-Aufnahme aufgebaut. Hierzu passend fanden wir nach einer erhöhten Kaliumaufnahme (2%K^+) eine Verlagerung von ROMK und ENaC aus intrazellulären Kompartimenten an die apikale Plasmamembran entlang des ASDN. Die Verlagerung von ENaC ging mit einer proteolytischen Spaltung und Aktivierung der alpha- und der gamma-Untereinheit von ENaC einher. Die apikale Translokation von ROMK und ENaC und die proteolytische Aktivierung von ENaC beobachten wir gleichermassen in $AS^{+/+}$ und in $AS^{-/-}$ Mäusen. Parallel zeigten Patch-Clamp Untersuchungen an isolierten Tubuli von $AS^{+/+}$ und $AS^{-/-}$ Mäusen ähnliche Na^+-Ströme, die mit Amilorid blockierbar waren. Beide Genotypen zeigten auch die gleiche natriuretische Antwort auf eine Amilorid-Injektion.

Um den möglichen Mechanismus der Aldosteron-unabhängigen Aktivierung von ENaC aufzuklären, behandelten wir die $AS^{+/+}$ und $AS^{-/-}$ Mäuse mit Losartan, einem Hemmer des Angiotensin II (AT1) Rezeptors. Während die $AS^{+/+}$ Mäuse diese Behandlung problemlos tolerierten, dekompensierten die $AS^{-/-}$ Mäuse. Sie entwickelten eine deutliche Hyperkalämie und verweigerten die K^+-Diät Aufnahme. Immunhistochemische Untersuchungen zeigten, dass bei den $AS^{-/-}$ Mäuse nach der Losartan-Behandlung die apikale Translokation von ENaC nicht mehr nachweisbar war.

Interessanterweise zeigten die die $AS^{-/-}$ Mäuse bereits unter Standard-Bedingungen eine geringere Menge und Phosphorylierung des renalen Natrium-Chlorid-Cotransporters (NCC) als die $AS^{+/+}$ Mäuse. Die Abnahme von NCC Menge und Phosphorylierung in den $AS^{-/-}$ Mäuse wurde noch deutlicher, wenn die K^+-Konzentration der Diät erhöht wurde. In Übereinstimmung mit diesen Beobachtungen zeigten $AS^{-/-}$ Mäuse auf der 2% K^+-Diät eine geringere natriuretische Antwort auf eine Thiazid-Injektion als die entsprechenden $AS^{+/+}$ Mäuse.

Ussing-Kammer-Untersuchungen am Colon zeigten, dass eine erhöhte K^+-Aufnahme (2% K^+) für 2-4 Tage sowohl Ba^+-hemmbare K^+-Kanäle als auch Amilorid-

hemmbare Na^+-Kanäle aktiviert. Diese Aktivierung der K^+ und Na^+ Kanäle war aber nur in den $AS^{+/+}$ und nicht in $AS^{-/-}$ Mäusen nachweisbar.

Zusammengefasst deuten unsere Resultate darauf hin, dass das Fehlen von Aldosteron die funktionelle Anpassunge der Niere an eine erhöhte K^+-Aufnahme nicht verhindert. Im Gegensatz dazu scheint die homeostatische Anpassung des Colons an eine erhöhte K^+-Aufnahme an Aldosteron gebunden zu sein. In der Niere scheint eine Angiotensin II-abhängige Aktivierung von ENaC und eine Herunteregulierung von NCC an der Aldosteron-unabhängigen Erhaltung K^+-Homöostase beteiligt zu sein. Die Herunterregulierung von NCC im DCT führt zu einer erhöhten Beladung des ASDNs mit Na^+, welches dann via ENaC resorbiert wird und damit die elektrochemische Triebkraft für die ROMK-abhängige K^+-Sekretion erhöht.

Während einer normalen Schwangerschaft vergrössert sich das mütterliche Plasmavolumen um die Durchblutung der Plazenta zu optimieren und damit das Wachstum des Fötus zu begünstigen. Die Ausdehnung des Plasmavolumens geht mit einer Erhöhung der Plasma-Aldosteron-Spiegel einher. In klinischen Studien wurde bei einzelnen werdenden Müttern mit Präeklampsie ein Aldosteron Mangel nachgewiesen. Daher testeten wir in unserem Maus-Modell die Hypothese, dass ein chronischer Aldosteron-Mangel die Schwangerschaft negativ beeinflusst und eine Präeklampsie und/oder einen intrauterinen Wachstumsverzug (IUGR) zur Folge haben kann.

Damit ausschliesslich heterozygote Jungtiere gezeugt wurden, wurden nur männliche $AS^{+/+}$ mit weiblichen $AS^{-/-}$ und männlich $AS^{-/-}$ mit weiblichen $AS^{+/+}$ verpaart. Bei den schwangeren Weibchen wurden dann während des gesamten Schwangerschaftsverlaufes der systolische Blutdruck (SBP) und die Proteinausscheidung im Urin gemessen, um zu kontrollieren, ob die Tiere die charakterischen Zeichen einer Präeklampsie (Bluthochdruck und Proteinurie) entwickelten. Wir konnten keine Anzeichen eines Bluthochdruckes oder einer Proteinurie bei den Mäusen entdecken. Die $AS^{-/-}$ Mütter hatten aber deutlich kleinere Würfe als die $AS^{+/+}$ Mütter. Das gehäufte Vorkommen nekrotischer Plazenten deutete an, dass die reduzierte Wurfgrösse auf ein intrauterines Absterben der Frucht zurückzuführen war. Nicht nur die Anzahl der Föten war bei $AS^{-/-}$ Müttern

geringer als bei $AS^{+/+}$ Müttern, sondern auch das Gewicht der entwickelten Föten und der dazugehörigen gesunden Plazenten war deutlich reduziert. Obwohl kleiner, zeigten die gesunden Plazenten der Mütter beider Genotypen einen strukturell unauffälligen histologischen Befund. Im Gegensatz dazu zeigten die nekrotischen Plazenten eine lymphozytäre Infiltration und eine erhöhte Transkription für das inflamatorische Zytokin Tumor-Necrosis-Factor 1 alpha (TNF1α) und das Monocyte Chemo-Attractant Protein1 (MCP-1). Wir nehmen an, dass der Aldosteronmangel das Plasmavolumen der schwangeren Mäuse verringert. Damit ist die optimale arterielle Blutversorgung der Plazenten nicht mehr gewährleistet, was zu einer plazentaren Hypoxie und damit zu einem beeinträchtigten plazentaren und damit fötalen Wachstum führt. Die Vermutung einer plazentaren Hypoxie in den $AS^{-/-}$ Mütter wird durch die Beobachtung einer signifikant erhöhten Expression des Hypoxie-Induzieren-Faktor 1 alpha (HIF1α) unterstützt.

Um das vermeintlich zu geringe Plasmavolumen der $AS^{-/-}$ Mäuse während der Schwangerschaft zu optimieren, fütterten wir die werdenden Mütter mit einer NaCl-angereicherten Diät (5% NaCl). Sowohl die $AS^{+/+}$ als auch die $AS^{-/-}$ Weibchen reagierten gut auf die Diät und zeigten vor und während der Schwangerschaft erhöhte Blutdruckwerte. Durch die NaCl-angereicherte Diät konnte die Wurfgrösse der $AS^{-/-}$ Mäuse deutlich erhöht werden. Auch das Gewicht der Jungtiere war sowohl bei den $AS^{+/+}$ Tieren als auch bei den $AS^{-/-}$ unter der NaCl-reichen-Diät deutlich erhöht. Trotzdem wurden bei den $AS^{-/-}$ Mäusen weiterhin nekrotische Plazenten gefunden. Um den möglichen Mechanismus der verbesserten Gewichtsentwicklung der Jungtiere zu verstehen berechneten wir die plazentäre Effizienz welche durch das Verhältnis von Plazentagrösse zu Jungtiergrösse bestimmt wird. Beide Genotypen zeigten eine deutliche erhöht Effizienz der Plazenta was darauf hindeutet, dass dem erhöhten Geburtsgewicht der Jungtiere eine verbesserte Durchblutung der Plazenta zugrunde liegt.

Zusammenfassend, konnten wir durch unsere Untersuchungen and den $AS^{-/-}$ Mäusen Aldosteron-abhängige und -unabhängige Mechanismen zur Erhaltung der K^+-Homöostase aufklären. Die Aldosteron-unabhängigen Mechanismen ermöglichen es durch eine Aktivierung von ROMK und ENaC und eine Herunterregulatierung von NCC in der Niere die K^+-Homöostase auch bei fehlendem Aldosteron aufrecht zu

erhalten. Im Gegensatz dazu scheint die Anpassung des Colons an eine erhöhte K^+-Aufnahme an Aldosteron gebunden zu sein.

Die Untersuchungen der $AS^{-/-}$ Mäuse zeigten auch, dass ein Aldosteronmangel in der Schwangerschaft die Funktion der Plazenta negativ beeinflusst und in der Folge zu einer Reduktion des plazentalen und fötalen Gewichts führt. Eine Supplementierung der Diät mit NaCl scheint die Effizienz der Plazenta zumindest teilweise zu verbessern.

1 INTRODUCTION

Aldosterone

Aldosterone is the main mineralocorticoid hormone produced in the glomerulosa cell layer of the adrenal glands. Aldosterone has pleiotropic actions in the body as shown in figure 1. One of its main functions is to participate to the hormonal control of ion and water homeostasis. Aldosterone stimulates sodium (Na^+) reabsorption and potassium (K^+) secretion by the kidney. As Na^+ is the primary active osmotic particle in the extracellular space and retains water, aldosterone finally determines the volume of extracellular fluid and hence blood pressure [1]. Aldosterone has also effects on many other organ systems including the cardiovascular system and metabolic organs. Moreover, local synthesis of aldosterone has been demonstrated in tissues such as those of the heart, blood vessels and brain [2-4]. The functions of aldosterone in these non-epithelial tissues are still a matter of debate. Recently aldosterone has been shown to play a role during pregnancy, in which it may contribute to plasma volume expansion, placental perfusion and hence improved placental and fetal growth [5, 6]. In our projects, we focussed on the role of aldosterone in K^+ homeostasis and in pregnancy. As aldosterone is produced by the enzyme aldosterone synthase (AS), AS knock out ($AS^{-/-}$) mice were used to study the role of aldosterone

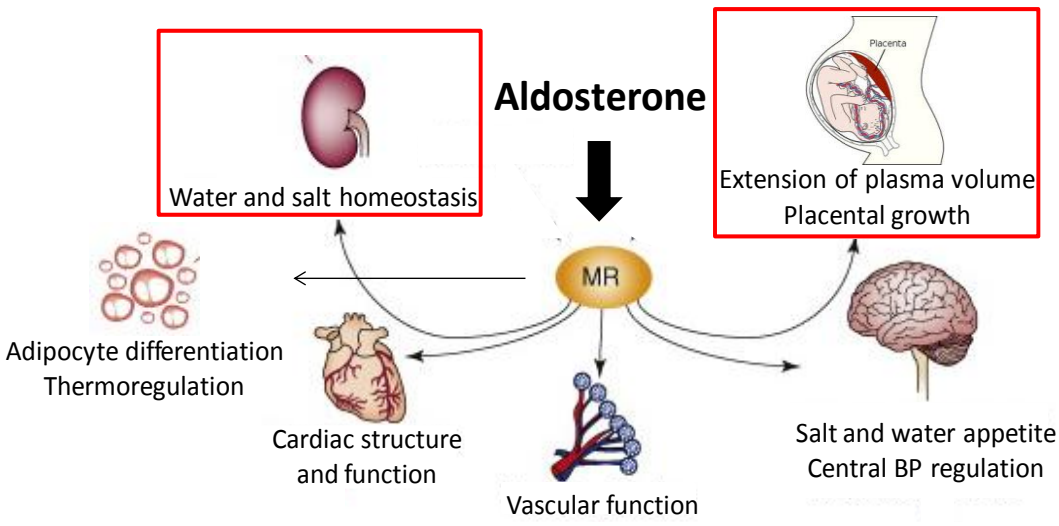

Figure 1. Pleiotropic role of aldosterone (adapted and modified from [7])

Aldosterone synthase (*Cyp11b2*)

Aldosterone is synthesized from cholesterol by a series of enzymatic reactions of which aldosterone synthase (AS, *Cyp11b2*) mediate the last two reactions using 11-deoxycorticosterone as a substrate (figure 2). Aldosterone synthase produces aldosterone by catalyzing first the hydroxylation of 11-deoxycorticosterone to corticosterone, then the 18-hydroxylation of corticosterone to 18-hydroxycorticosterone, and finally the oxidation of 18-hydroxycorticosterone to aldosterone [8] (figure 2). Aldosterone-deficient mice were generated by the Oliver Smithies group by targeted disruption of *Cyp11b2* gene and kindly provided to us. In these aldosterone-synthase knockout ($AS^{-/-}$) mice, the first two exons of the gene were replaced via homologous recombination with a nucleotide sequence coding for the expression of the enhanced green fluorescent protein (EGFP). $AS^{-/-}$ mice lack any endogenous aldosterone, have a reduced body weight (75% of the wild type mice), are hypotensive and show very high levels of plasma renin and angiotensin II, and slightly elevated levels of plasma corticosterone [9].

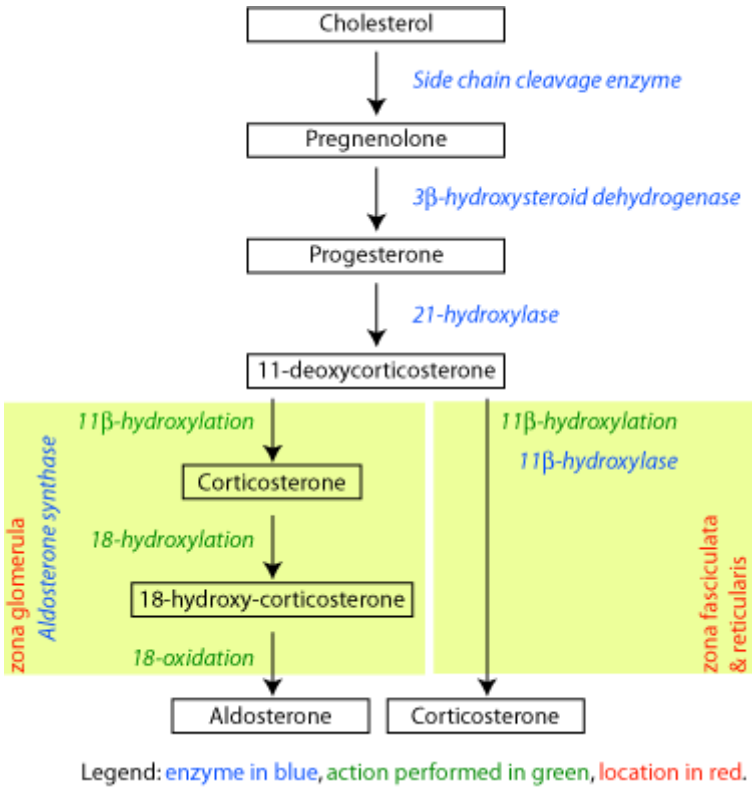

Figure 2. Flow chart showing function of aldosterone synthase enzyme in aldosterone production

1.1 Project 1. Role of aldosterone in renal potassium excretion

1.1.1 Aldosterone synthesis and regulation

The major role of aldosterone is to stimulate sodium (Na^+) reabsorption and potassium (K^+) secretion in target tissues. The zona glomerulosa cells from the adrenal cortex contain the aldosterone synthase enzyme involved in the final step of aldosterone production from deoxycorticosterone. The gene encoding for the aldosterone synthase is *Cyp11b2.*

There are three main factors that control aldosterone production, namely angiotensin II, plasma K^+ levels, and adrenocorticotropic hormone (ACTH). Angiotensin II is formed during extracellular volume depletion via an activation of the renin-angiotensin-system. In response to a decrease in the circulating blood volume renin is released from the granular cells in the renal juxtraglomerular apparatus. Renin converts angiotensinogen (produced mostly by the liver) into angiotensin I by proteolytic cleavage.Angiotensin I in turn is then converted by the angiotensin converting enzyme (ACE) into the physiologically active angiotensin II. Angiotensin II binds then to the AT1 receptor on the glomerulosa cells of the adrenal cortex to stimulate aldosterone production. An increase in extracellular K^+ concentrations directly stimulates aldosterone production in the glomerulosa cells by not yet well understood mechanism. ACTH is released from the anterior pituitary mainly to stimulate glucocorticoid productions. However, it does also promote aldosterone secretion although this effect is very weak [1].

1.1.2 Target tissues and specificity for the receptors

Aldosterone mediates its effect by binding to the type 1 corticosteroid or the mineralocorticoid receptor (MR). The MR is a ligand activated transcription factor and is a member of the steroid/thyroid hormone nuclear receptor superfamily of ligand inducible transcription factors [10]. The MR receptor is expressed in the epithelium lining the tubules in the distal nephron of the kidney, the distal colon, and the ducts of salivary and sweats glands. Glucocorticoids exert their effects through the glucocorticoid receptors (GR) [11]. Steroid binding studies showed that both, aldosterone and glucocorticoid, have similar high affinities for the MR [10]. Plasma levels of glucocorticoids hormones are 100 to 1000 times higher than that of

aldosterone (0.1 to 1nM) and theoretically expected to occupy MR. However, in aldosterone target tissues the MR is protected by the enzyme 11β-hydroxysteroid dehydrogenase type 2 (11β-HSD2) which converts cortisol and corticosterone, but not aldosterone, to their in-active 11-keto analog. These analog are unable to activate the MR [12]. Thus, in aldosterone target tissues specificity for the MR is mediated by the 11β-HSD2 enzyme.

Since the eighties of the last century, several additional target tissues for aldosterone have been defined. Expression of MR was reported in a number of non-epithelial tissues including the pituitary, neurons of the central nervous system (CNS), cardiac myocytes, and endothelial and smooth muscle cells of the large vessels [10-13]. Cardiac myocytes [14], vascular cells [15] and certain areas of the adult brain, related to control of blood pressure and salt appetite, appear to express 11β-HSD2 [16] suggesting that aldosterone may exert specific effects at this sites, despite the high circulating glucocorticoid levels. Nevertheless, the physiological role of the MR or aldosterone in these non-epithelial tissues has remained largely unknown whereas patho-physiological effects of aldosterone at these sites are the subject of intense studies [17]. Aldosterone was shown to contribute to cardiac fibrosis and cardiovascular remodelling in animals on high salt diet [18]. There is also evidence that aldosterone contributes to inflammation, fibrosis and progression of cardiovascular diseases, including hypertension and metabolic syndrome [19]. Interestingly, expression of the 11β-HSD2 and the MR in human placenta was also reported indicating a role of aldosterone in pregnancy [20]. The possible role of aldosterone in pregnancy will be discussed in more detail in a later part of the introduction.

1.1.3 Potassium homeostasis - External and internal K^+ balance

Control of K^+ homeostasis is vital for the function of many cells in the body. A high intracellular concentration of K^+ is important for cell growth whereas the maintenance of extracellular K^+ concentrations is important for normal functions of neurons, cardiac myocytes and skeletal muscle [1, 21]. Hypokalemia or hyperkalemia result in cardiac arrhythmias and dysfunction of neurons and muscle contraction (weakness and cramps). The amount of K^+ in the extracellular space is rather low. The K^+ content of a standard meal could be already sufficient to increase extracellular K^+

concentration. Thus, dietary K^+ intake has to be managed by rapid redistribution of taken-up, extracellular K^+ into intracellular tissue stores, particularly in muscle and liver cells. Eventually K^+ is released back into the extracellular fluid and gets excreted by the kidney into the urine [21]. Safeguarding of plasma K^+ is achieved by synchronised mechanisms of external and internal K^+ balance. External K^+ balance involves the rate of K^+ intake (approx.100 mEq/day) and the rate of K^+ excretion through urine (approx. 90 mEq/day) and faeces (approx. 10 mEq/day). The internal K^+ balance consists of distribution of K^+ between extracellular fluid (approx. 70 mEq/day) and intracellular spaces in bone, liver, muscle and red blood cells (figure 3). This distribution is regulated by several hormones like insulin, β-adrenergic agonists (e.g. epinephrine) and aldosterone all promoting the transport of K^+ from extracellular fluid to intracellular fluid compartments via the ubiquitous Na^+-K^+-ATPase pump. This process of distribution can be further affected by acid-base balance and the tonicity of the plasma [1, 22].

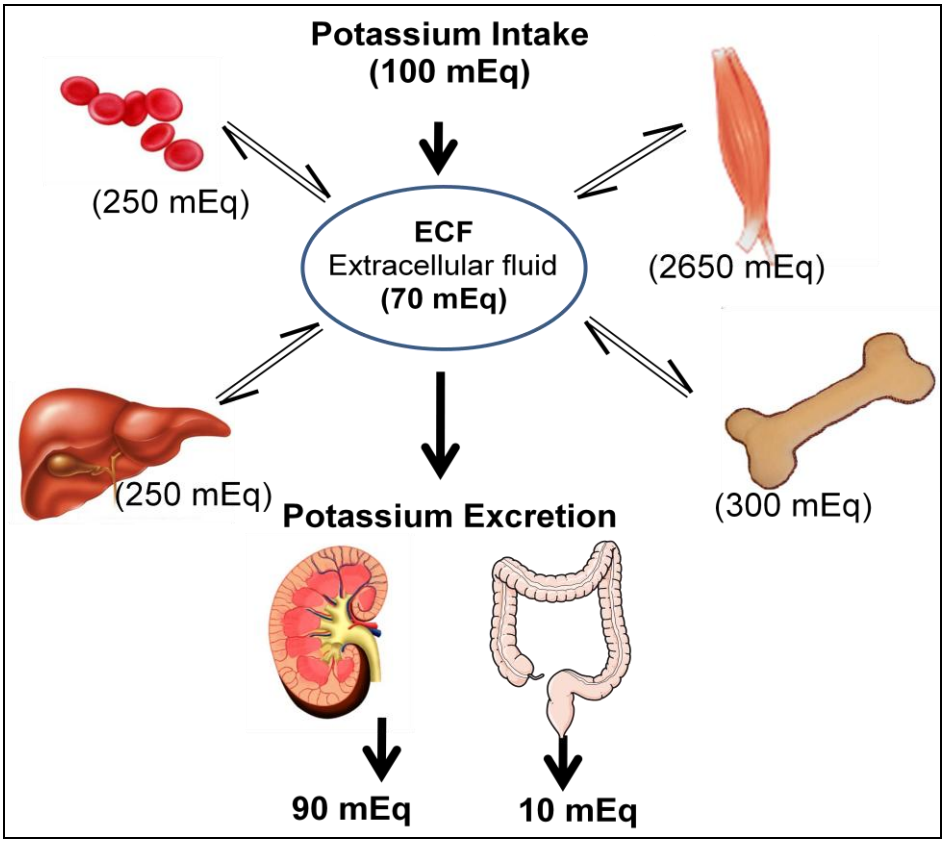

Figure 3. Potassium homeostasis. External and internal K^+ balances (adapted and modified from [22]). Detail description in text.

External K^+ balance is mainly determined by two organs, namely the kidney and the colon. The kidneys play a major role in K^+ homeostasis by excreting 90 to 95% of the daily K^+ intake while the colon excretes 5 to 10% of the daily K^+ intake. Although the colon can increase K^+ excretion under certain conditions like in response to adrenal hormones, decreased renal excretory capacity and high K^+ diet, the colon alone cannot excrete K^+ to the extent to maintain normal plasma K^+ levels [1]. K^+ secretion is under tight control of aldosterone, which acts as the final endocrine signal of the renin–angiotensin-aldosterone system and targets the epithelia in the kidney and colon [17].

1.1.4 Potassium handling in the kidney

In the kidney, potassium is freely filtered in the glomerulus, almost completely reabsorbed in the proximal tubule (almost 80%) and thick ascending limb (TAL) (10%), secreted in the connecting tubule (CNT) and cortical collecting duct (CCD) and reabsorbed in the outer medullary collecting duct (OMCD).

Potassium absorption

Figure 4 depicts the different cell models for K^+ absorption along the nephron.

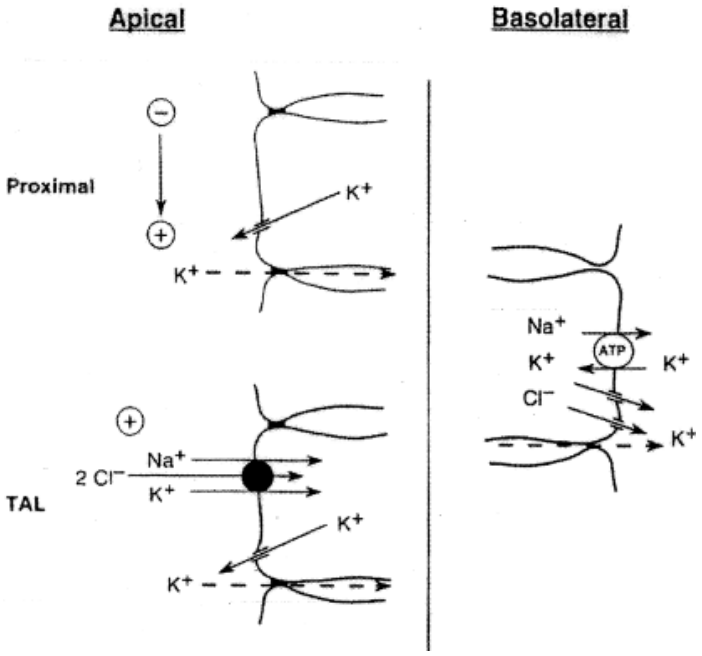

Figure 4. Potassium absorption along the nephron. Cell models showing similarities of transporters in the basolateral membrane and different transporters at the apical membrane, (adapted and modified from [23])

In the proximal tubule, K^+ is reabsorbed by two paracellular mechanisms: solvent drag and passive diffusion. Active Na^+ transport in the proximal tubule drives net fluid absorption and drags K^+ along with the fluid. The transcellular ion transport also generates at the end of the proximal tubule a lumen-positive transepithelial voltage that provides an electrochemical gradient for K^+ absorption through the low resistance paracellular pathway. In the TAL, K^+ is mostly recycledthrough the Na^+-K^+-$2Cl^-$ -cotransporter (NKCC2) and the ROMK channel [1, 23, 24].

1.1.5 Potassium secretion - Critical role of the ASDN

The amount of K^+ that finally becomes excreted in the urine critically depends on controlled K^+ secretion along the aldosterone-sensitive distal nephron (ASDN). The ASDN comprises the late distal convoluted tubule (DCT2), the connecting tubule (CNT), and the collecting duct (CD) [22, 24]. In the ASDN, two morphologically distinct cell types are present namely principal cells (PC) and intercalated cells (IC) [22, 25] (figure 5). The PCs are involved in K^+ secretion, whereas ICs are involved in K^+ absorption [26, 27]. Principal cells express epithelial Na^+ channels (ENaC) and renal outer medullary K channels (ROMK) localized to the apical membrane and the Na^+-K^+-ATPase on the basolateral membrane [28]. Transepithelial sodium absorption via ENaC and Na^+-K^+-ATPase is electrogenic and generates a lumen-negative transepithelial potential difference that acts as a driving force for K^+ secretion via apical K^+ channels such as ROMK and the flow dependent maxi K^+ channels (BK) [24, 29-31]. Potassium secretion in the PC is a two step process that involves first an active uptake of K^+ across the basolateral membrane by Na^+-K^+-ATPases and then second the passive diffusion of K^+ through apical K^+ channels along the electrochemical gradient generated by ENaC and the Na^+-K^+ ATPase (figure 4) [22]. Aldosterone stimulates K^+ secretion by activation of the Na^+-K^+-ATPase, ENaC, and perhaps also the apical K^+ channels. Aldosterone sensitivity is conferred to the ASDN by the expression of the MR and the 11β-HSD2 in the ASDN [28, 32]. Potassium absorption by intercalated cells occurs by an active transport of K^+ via H^+-K^+-ATPases across the apical membrane and leaving the cell across the basolateral membrane along a favourable K^+ electrochemical gradient (figure 5) [24, 33, 34].

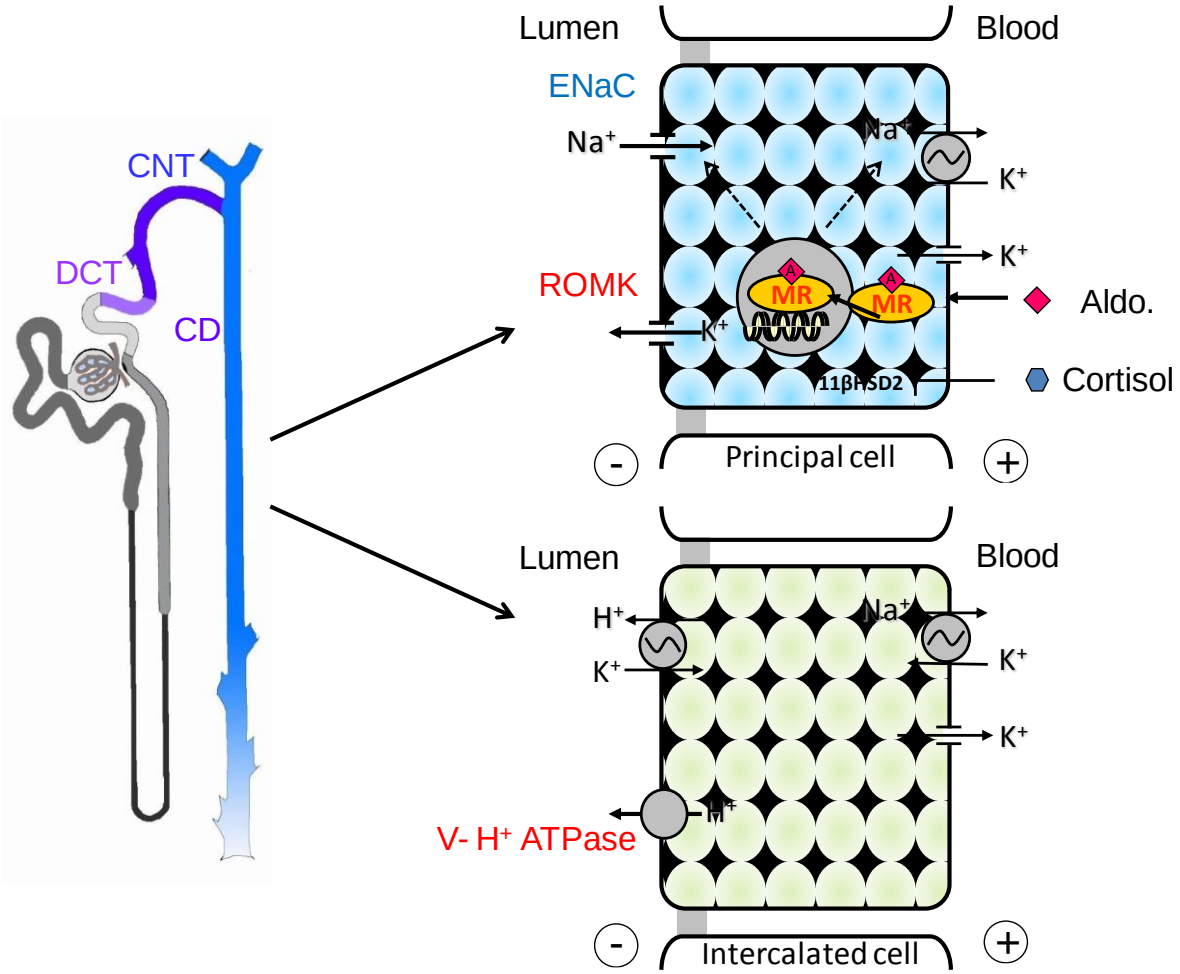

Figure 5. **Potassium secretion and absorption in the Aldosterone-sensitive distal nephron.** Principal cell show expression of the Epithelial Sodium channel (ENaC), the Renal outer medullary potassium channel (ROMK), Na^+-K^+-ATPase, and the mineralcorticoid receptor (MR). Intercalated cell shows expression of H^+-K^+-ATPase, vacuolar H^+-ATPase and Na^+-K^+- ATPase.

In addition to aldosterone, a variety of other factors including dietary K^+ intake, vasopressin (antidiuretic hormone – ADH) and tubular flow rate [22, 23, 27, 35] have been shown to stimulate either K^+ secretion of absorption along the ASDN (figure 6).

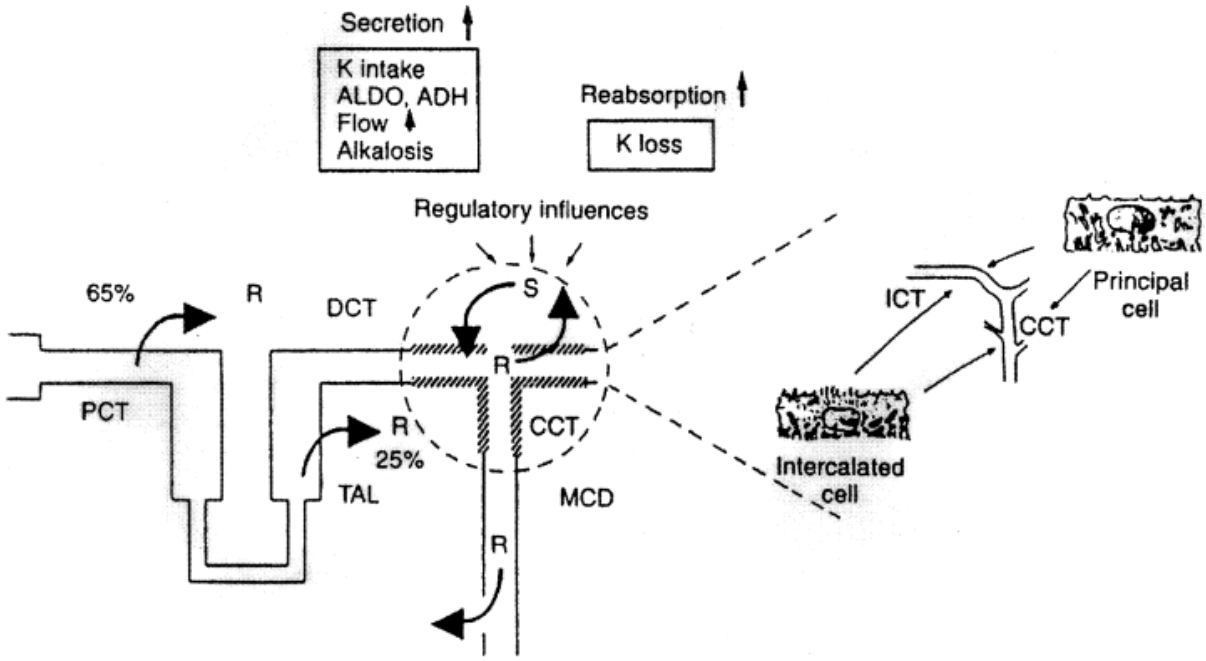

Figure 6. Regulatory factors influencing K^+ secretion or absorption in the ASDN (adapted from [23].)

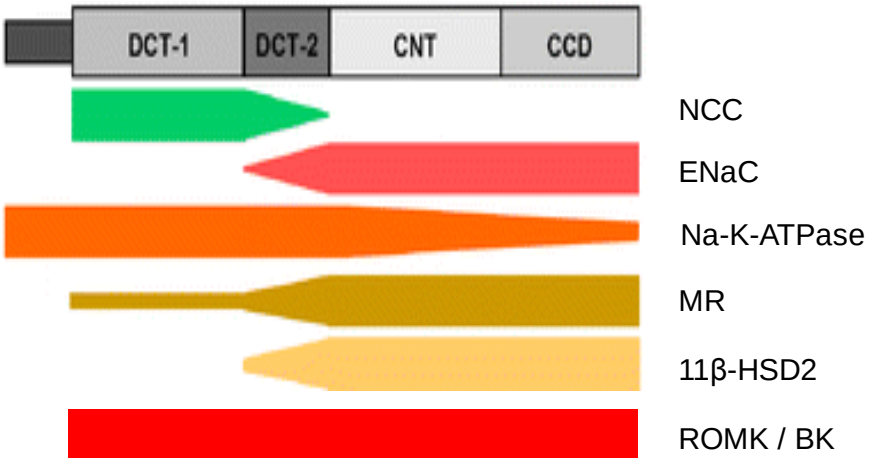

Figure 7. Expression and distribution patterns of Na^+ and K^+ transport systems along the ASDN. Distribution of the MR and 11β-HSD2 and the DCT specific thiazide sensitive NCC are also indicated. (Adapted and modified from [28]).

1.1.6 Structure, function and regulation of sodium and potassium channels and transporter in the ASDN

1.1.6.1 The epithelial sodium channel (ENaC)

ENaC plays an important role in whole body Na^+, K^+ and fluid homeostasis.

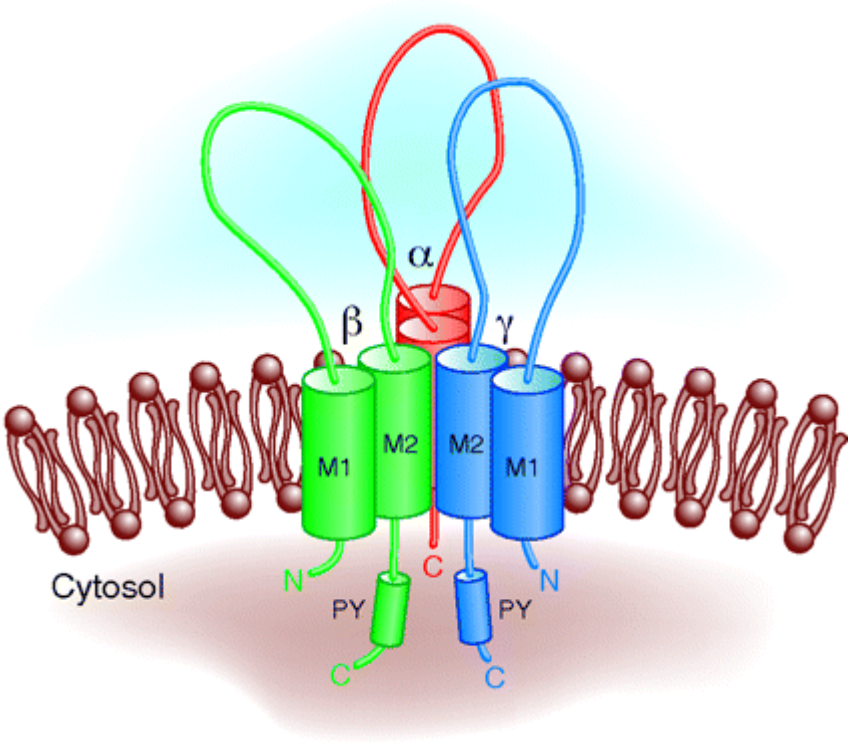

Figure 8. Structure of the ENaC channel (as predicted by Jasti et al [36]). Adapted from [37]

This is emphasised by the observations that gain of function mutations of ENaC such as in Liddle's syndrome lead to severe arterial hypertension and hypokalemia whereas loss of function mutations of ENaC such as in pseudohypoaldosteronism type 1 (PHA-I) lead to a renal salt wasting syndrome and hypotension associated with hyperkalemia [38, 39]. ENaC is a heteromultimeric channel consisting of three different homologous subunits α, β and γ (figure 8). The three subunits share 30 to 40% homology at the level of amino acid sequence [28, 40]. ENaC might be a heterotrimer as suggested by the crystal structure of related acid sensing ion channel 1 (ASIC1) [36, 41]. Each subunit of ENaC consists of two transmembrane domains (M1 and M2), a large extracellular loop and short intra-cellular amino and carboxy termini. It is thought that ENaC forms its pore with their

M2 domains [38]. Co-expression of all three ENaC subunits is necessary for full activity of the channel. Na^+ movement across the channel corresponds to the electrophysiologically measurable ion currents and can be specifically blocked by the diuretics amiloride and triamterene [38, 42].

ENaC is regulated by a variety of extrinsic and intrinsic factors. Figure 9 and table 1 shows some of these factors.

Extrinsic factors

Hormonal regulation - ENaC is known to be regulated by volume regulatory hormones such as aldosterone, arginine vasopressin (AVP), the atrial natriuretic peptide (ANP), and other hormones such as insulin and endothelin [37]. The hormones regulate ENaC via receptor mediated modulation of intracellular signalling pathways including kinase cascades. Aldosterone regulates ENaC - by stimulation of the serum and glucocorticoid-regulated kinase (Sgk1) or inhibition of the extracellular signal-regulated kinase (ERK) [43, 44]. AVP and ANP, insulin and endothelin regulate ENaC via protein kinase A (PKA), phosphatidylinositol 3-kinase-dependent signalling and SRC family kinases, respectively [45-49].

Table 1. Factors regulating ENaC

Extrinsic factors	**Intrinsic factors**
Hormonal regulation	ENaC traffiking
Mechanosensation	Phosphorylation
Proteolytic cleavage	Na^+ self inhibition and feedback inhibition
	Metabolic depletion and pH

Mechanosensation - In non-epithelial tissues, ENaCs subunits were shown to be involved in mechanosensation. The β and γ subunits may play an important role in the mechanosensitivity of neurons innervating the aortic arch and vascular smooth muscles [50, 51]. Also in isolated rabbit CCD, ENaC might become activated by laminar shear stress due to an increased tubular flow rate [52]. ENaC activation via shear forces occurs likely directly via an increased opening probability (P_o) of the channel [37, 53-55].

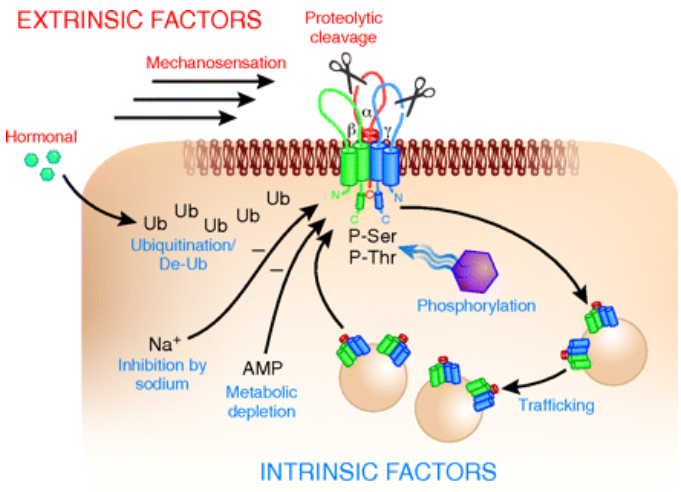

Figure 9. Summary of extrinsic and intrinsic factors regulating ENaC channel (adapted from [37]).

Proteolytic cleavage - Recent evidence indicates activation of ENaCs by proteolytic processing by intra and extracellular proteases. One such ENaC activation protease is furin. Furin is a serine protease, which is highly abundant in the trans-golgi network and likely cleaves ENaC already during the biosynthetic pathway. Furin likely cleaves the α- and the γ-ENaC subunits at two and one extracellular sites, respectively [56]. The furin-dependent cleavage of the α-ENaC subunit releases an inhibitory peptide from the extracellular loop of ENaC and thereby activates the channel [57, 58]. Another ENaC-activation protease is prostasin, which is also called "channel activating peptidase 1 (CAP-1)". Prostasin is an extracellular protease that likely cleaves γ-ENaC in the extracellular loop in close proximity to the furin cleavage site. The combined actions of prostasin and furin release then an inhibitory peptide from γ-ENaC to fully activate ENaC [59].

Intrinsic factors

ENaC trafficking - ENaC activity is also regulated by trafficking to and from the plasma membrane. The three different ENaC subunits are synthesized in the endoplasmic reticulum (ER) and modified along the biosynthetic pathway before they traffic from intracellular pools to the apical plasma membrane [60]. ENaC is endocytosed into clathrin-coated vesicles and may be recycled back to the apical plasma membrane or is shuttled to lysosomes or proteasomes for degradation [61, 62]. Several cellular and molecular mechanisms are involved in ENaC trafficking. One of the best studied regulatory proteins is the ubiquitin-protein ligase Nedd4-2.

Nedd4-2 interacts with a proline-rich PPXY (PY) motif of ENaC subunits, promotes ubiquitylation, which is followed by endocytosis and proteasomal degradation of the channel [63]. Another ENaC trafficking associated protein is AS160, a Rab protein regulator, which stabilises ENaC in an intracellular compartment preventing the channel from trafficking to the apical membrane [64].

Phosphorylation - Regulation of ENaC by kinases via direct phosphorylation of its subunits or phosphorylation of proteins interacting and regulating the channel is well known [28, 42]. One of the best studied kinases is the aldosterone induced kinase Sgk1 which stimulates cell surface activity and density of ENaC via direct phosphorylation of the α-subunit [65] and indirectly via phosphorylation of Nedd4-2 and AS160 [64, 66]. Phosphorylated Nedd4-2 or AS160 are recognised and blocked by 14-3-3 proteins, which prevents Nedd4-2-dependent endocytosis and AS160-mediated intracellular retention that eventually increases the channel density and activity at the apical plasma membrane [28, 64].

1.1.6.2 ROMK

The channel (Kir1.1) is a member of the inwardly rectifying K^+ channel family [67] with high K^+ selectivity [68].

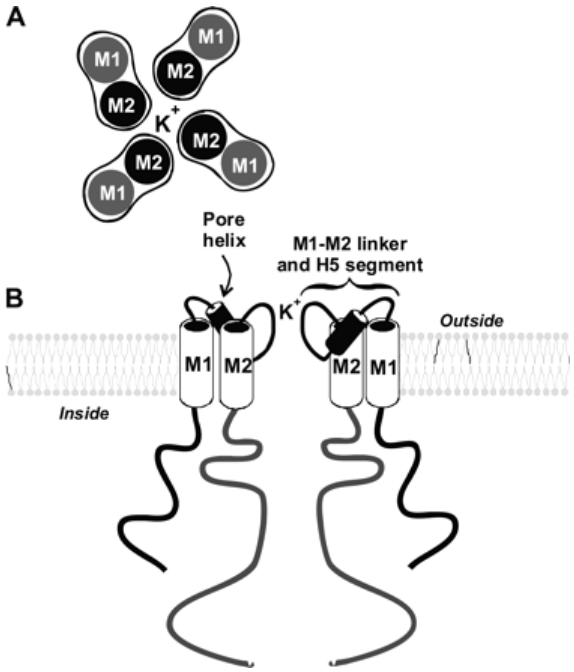

Figure 10. A schematic structural model of ROMK. A. Proposed subunit structure. B. Two of the 4 subunits illustrate the pore helices in the M1 and M2 linker (taken from [30].

ROMK is a pore forming protein expressed in the apical membrane of the TAL and PC of the ASDN [30]. X-ray crystallography of homologous K^+ channels from *Streptomyces lividans* [69], suggest that the ROMK channel is a tetrameric channel complex. Each monomer consists of two membrane spanning segments (M1 and M2) and cytoplasmic N- and C-termini with high homology to the pore-forming H5 segment of voltage-gated K^+ channels [24]. Studies on the packing structure of the M1 and M2 domains by Minor et al. suggest that the M2 segments line the pore and are surrounded by M1 segments which also participate in subunit-subunit interactions [70] (figure 10).ROMK channels are sensitive to intracellular pH. Channel activity is completely inhibited by a decrease in the cytosolic pH from 7.4 to 7.0 [71, 72]. An important property of ROMK channels is the sensitivity to intracellular ATP concentrations. High concentrations of ATP inhibit channel activity (milimolar range) whereas low concentrations of ATP (submilimolar range) are found to activate the channel [22, 73]. ROMK channels are also known to be regulated by phosphorylation. The ROMK channel has three putative PKA phosphorylation sites and stimulation of these sites increases channel activity [74, 75] either by insertion of ROMK channels into the plasma membrane [76, 77] or by augmenting the effect of phosphatidylinositol phosphates (PIP2) [78], which activates ROMK channels [79]. Moreover, Sgk1 stimulates ROMK channel activity by phosphorylation of a serine residue at the N-terminus of ROMK [80]. Protein kinase C (PKC) has both stimulatory as well as inhibitory effects on ROMK channels as phosphorylation induces export of channels to the cell membrane but decreases the sensitivity of channels to PIP2 [81, 82]. The ROMK1 channel variant is also regulated by PTK which increases endocytosis of channels in the CCD by tyrosine phosphorylation [24].

1.1.6.3 BK or Maxi K channels

A large conductance Ca^+ activated K^+ channel (also called BK or Maxi K) is reported to be expressed in various nephron segments such as the medullary and cortical TAL, DCT, CNT, CCD and medullary collecting duct. The functional BK channel consist of a pore forming α subunit (*Slo* 1) with six transmembrane segments and one of the four accessory β subunits (β1, β2, β3, and β4). The β1 subunit is reported to be expressed exclusively in the CNT mostly in the PCs in mouse whereas other

subunits β2-β4 are thought to be expressed in the CCD. BK β2 and β3 are found to be expressed in either IC or PC of the CCD and β4 is expressed in IC of the CNT and CCD [24, 83]. It has been shown that BK channels are also sensitive to cellular pH and ATP at physiological Ca^{2+} levels [84, 85]. BK channels may have a role in flow induced K^+ secretion along CNT and the CCD [86, 87]. This function of BK channels was further emphasised by the failure of increasing flow induced K^+ secretion in BK-α subunit knockout mice. Interestingly, net K^+ excretion in response to high K^+ diet was normal in the knockout mice indicating that K^+-diet induced ROMK channels may compensate for non-functional BK channels [88]. Similarly, BK channels appear to contribute to urinary K^+ excretion in ROMK-deficient mice, suggesting that ROMK and BK channels are somehow redundant in function and can partially compensate for each other [89].

1.1.6.4 NCC

As shown in figure 7, the ASDN begins within the distal convoluted tubule (DCT). In the DCT, sodium transport depends on the thiazide-sensitive sodium-chloride co-transporter (NCC), which is co-expressed with ENaC in the late DCT (DCT2).

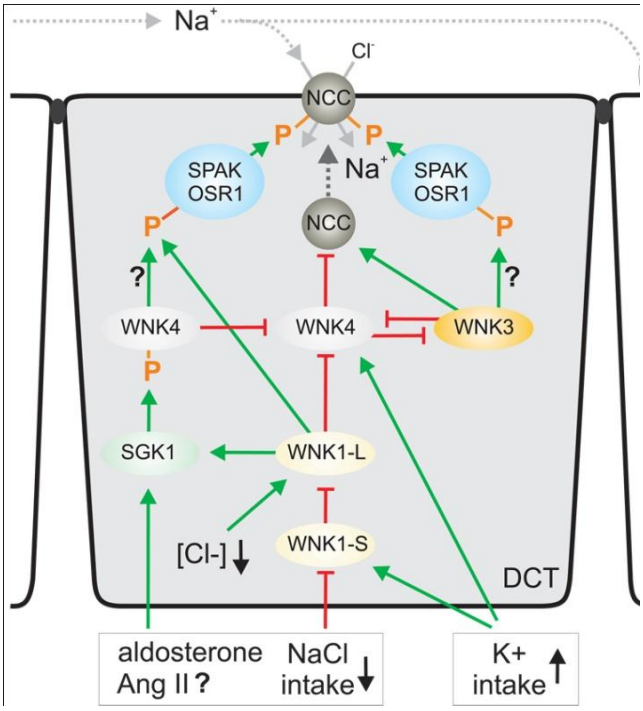

Figure 11. Phosphorylation and activation of NCC (adapted and modified from [91])

NCC, encoded by the *Slc12a3* gene, is a member of the cation-chloride cotransporter family which also includes the Na^+-K^+-$2Cl^-$ cortransporters NKCC2 and NKCC1 [90]. In the distal tubule NCC plays a critical role in NaCl reabsorption and, indirectly in, K^+ homeostasis [91].A recent study has shown a decrease in the amount of total and surface NCC due to dietary K^+ intake indicating a role of NCC in K+ homeostasis [92] NCC and two other members of the family, NKCC2 and NKCC1, are known to be activated by phosphorylation at their amino termini in response to low chloride concentrations. Recently it has been shown that mammalian sterile 20 (STE20)-like kinases STE20/SPS1-related proline/alanine-rich kinase (SPAK) and oxidative stress-responsive kinase 1 (OSR1) phosphorylate NCC at three specific residues: Thr46, Thr55 and Thr60 in human NCC. The regulation of NCC by complex interactions of different kinases is shown in figure 11. The SPAK and OSR1 enzymes are further phosphorylated and activated by another set of kinases, With-No-Lysine Kinase 1 and 4 (WNK1 and WNK4). Recently, it has been shown that WNK3 also stimulates NCC activity by inhibiting WNK4.

All WNK kinases 1, 2 and 3 are expressed in the DCT. A shorter transcript of WNK1 lacking its kinase domain is expressed only in the kidney (Ks-WNK1) stimulates NCC activity by blocking the inhibitory effect of WNK-1L on WNK4. Aldosterone has been shown to activate NCC through Sgk1 dependent phosphorylation of WNK4 kinase thus possibly blocking the inhibitory effect of WNK4 on NCC [91, 93].

The critical role of NCC for Na^+ and K^+ homeostasis is evidenced by genetic diseases that over-activate or block NCC function. In Familial Hyperkalemic Hypertension, also known as Gordon's syndrome or Pseudohypoaldosteronism type II (PHAII), mutations in WNK kinases causes an abnormal high activity of NCC leading to hypertension, hyperkalemia and metabolic acidosis [94]. In contrast, loss-of-function mutations within NCC cause Gitelman-syndrome characterized by renal Na^+ wasting, hypokalemia and metabolic alkalosis [95]. Interestingly, some of the patients with Gitelman-syndrome have mutations at position 60 confirming the critical relevance of the serine residue at this site for the activation of NCC via phosphorylation [96].

1.1.7 Potassium handling by the colon

The colon does also participate in the control of K^+ homeostasis. Although under standard conditions, only 10% of the ingested K^+ is excreted via the colon, colonic K^+ excretion may dramatically rise and become crucial in chronic renal insufficiency [97]. On the other hand, intestinal K^+ loss during diarrhoea can lead to extreme forms of acute hypokalemia [98]. The colon can participate in active K^+ absorption and secretion [99, 100]. Under normal conditions, the proximal colon secretes K^+ while the distal colon contributes to net K^+ absorption via the non-gastric H^+/K^+-ATPase ($HK_{\alpha 2}$) present in the apical membrane of the surface cells [97]. On a high K diet, both proximal and distal colon secretes K^+ via trans- and paracellular pathways [101, 102].

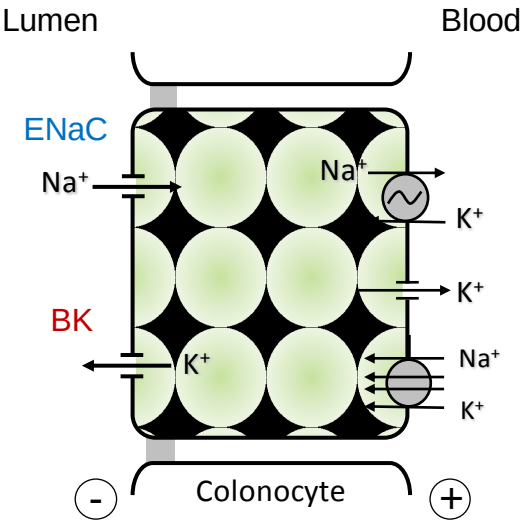

Figure 12. Colonocyte: showing different channels and transporters in the apical and basolateral membranes.

The transcellular pathway involves active transport of K^+ into the cell via the basolateral Na^+/K^+ pump and the co-transporter NKCC1. K^+ is then secreted through apical K^+ channels [103, 104] that is in the colon the BK channel [97, 105]. In addition, to transcellular K^+ secretion, paracellular K^+ fluxes have been described [103]. Both the transcellular and the paracellular pathway for net K^+ secretion depend on the lumen negative transepithelial voltage [106, 107], which is like in the kidney generated by transepithelial sodium reabsorption via ENaC (figure 12) [97]. Moreover, like the ASDN, the distal colon is aldosterone-sensitive and aldosterone plays an important role in the regulation of K^+ transport in the colon as well [108].

1.2 Project 2. Role of aldosterone in pregnancy

1.2.1 Pregnancy specific disorder- Pre-eclampsia

Pregnancy is characterized by a profound volume expansion due to high aldosterone levels meant to support fetal well-being [6]. Pre-eclampsia is a clinical syndrome in pregnant women defined as the new onset of hypertension and proteinuria after 20 weeks of gestation. It affects 3-5% of all pregnancies and is the leading cause of maternal and fetal morbidity and mortality. The criteria to define hypertension are a systolic blood pressure level ≥140 mmHg or a diastolic level ≥90 mmHg on two or more occasions at least 4 to 6 hr apart. Proteinuria is defined as the urinary excretion of more than 0.3 g protein in 24 hr urine samples, or a protein concentration of more than 0.3 g/l protein or ≥1+ on dipstick test strips when two random urine samples are taken 4-6 hr apart. The etiology of pre-eclampsia is unknown but is likely to be multifactorial [109]. Risk factors include a previous history of pre-eclampsia, multiple pregnancies, nulliparity, high body mass index before pregnancy, maternal age older than 40 years, very young maternal age, diabetes mellitus, renal disease, chronic hypertension, metabolic syndrome, hypercoagulable states, and more than 10 years since the last pregnancy [109, 110].

1.2.2 Pregnancy specific disorder- IUGR

Another pregnancy specific disorder is intrauterine growth restriction or retardation (IUGR). IUGR is the impairment of fetal growth due to anatomical and/or functional disorders and diseases of the feto-placental-maternal unit [111]. IUGR is usually defined as less than 10% of the predicted fetal weight for gestational age and, if not diagnosed properly, may result in significant fetal morbidity and mortality [67]. IUGR is further subdivided into symmetrical and asymmetrical IUGR. Symmetrical IUGR consists of low weight, length and head circumference and is usually indicative of processes originating early in pregnancy. In contrast asymmetrical IUGR consists of sparing of fetal head circumference and length (relatively large head with undergrown trunk and extremities) indicative of processes occurring in the later stages of gestation. Symmetrical IUGR is caused by several diseases including genetic disorders (trisomies, other chromosomal disorders and constitutional), dwarf syndromes, congenital viral infections, some inborn errors of metabolism and intrauterine drug exposures. Asymmetrical IUGR is mostly due to impaired utero-

placental function or nutrient deficiency. There are many different risk factors for IUGR, among them placental insufficiency and pre-eclampsia are included [112].

1.2.3 Abnormal placental implantation - common to pre-eclampsia and IUGR

During normal pregnancy, maternal uetroplacental blood flow increases drastically to support the growth of the fetus (figure 13). The uteroplacental arteries, also called spiral arteries, undergo a series of pregnancy specific changes that include 1) endovascular invasion of trophoblast and apparent replacement of endothelium and media smooth muscle cells, 2) loss of elasticity of the arteries, 3) dilation of arteries to wide and in-contractile tubes, 4) and finally loss of vasomotor control.

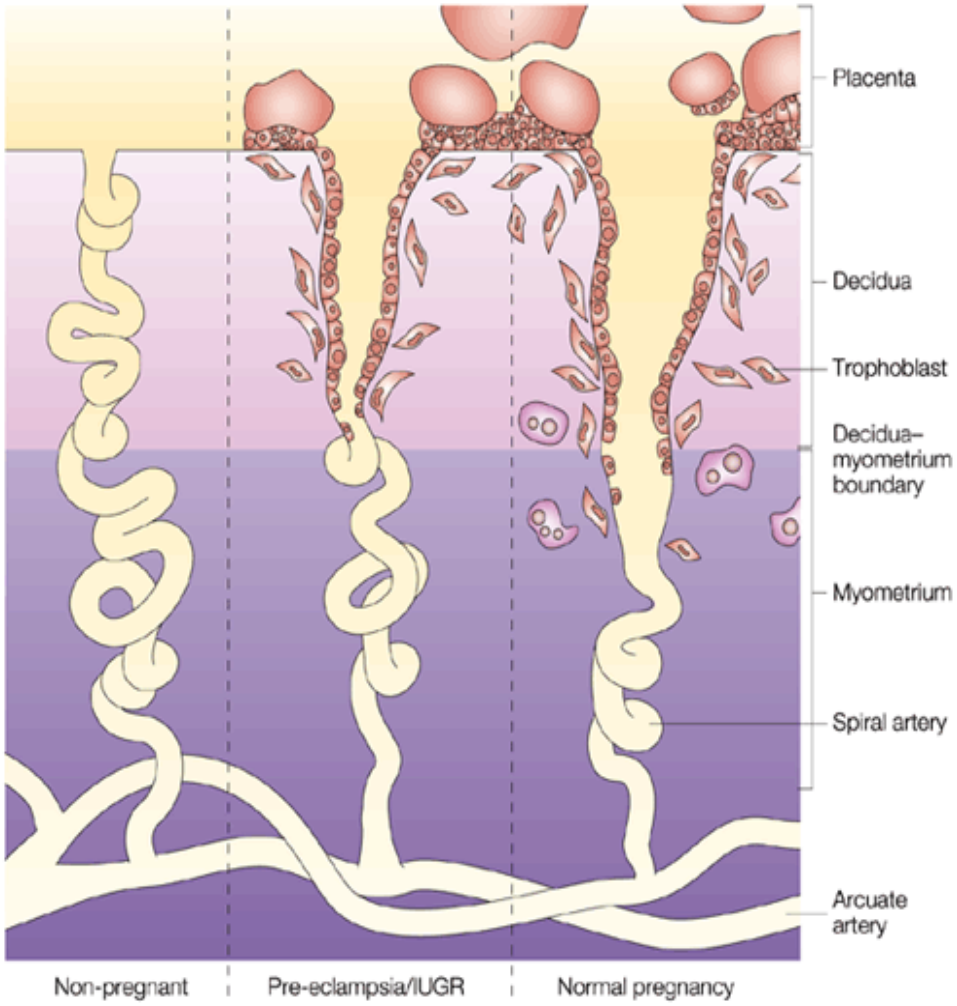

Figure 13. Modulation of spiral arteries. Comparison in non-pregnant, normal pregnancy and pregnancy associated with IUGR or preeclampsia (adapted from [113]).

The remodelling of the spiral artery increases uteroplacental perfusion and reduces maternal vascular blood flow resistance to meet the requirement of the fetus. Moreover, vasodilation and loss of vasomotor control guarantee sufficient blood supply to the placenta irrespective of altered regulation of vascular resistance and blood pressure in the mother [114].

IUGR and pre-eclampsia have in common an abnormal vascular remodelling and placental implantation. Brosens and colleagues [115] demonstrated decreased trophoblast invasion and absence of pregnancy specific changes in spiral arteries in pregnancies with IUGR and preeclampsia and it is now well accepted that reduced endovascular trophoblast invasion and spiral artery remodelling are key pathogenic features of IUGR and pre-eclampsia as shown in figure 9. Basic research and clinical data indicate that the inadequate invasion of uteroplacental arteries results from the concerted action of intrinsic fetal factors (abnormal biology of extravillous trophoblasts) and extrinsic maternal uterine factors including impaired decidual remodeling, impaired function of uterine natural killer (NK) cells and expression of endothelial adhesion molecules [110, 113]. Hypoxia is considered to be a central feature of both IUGR and pre-eclampsia [116-118]. Hypoxia driven dysregulation of placental angiogenesis via hypoxia inducible factor (HIF) may be a key to the altered trophoblast maturation associated with IUGR or pre-eclampsia. Pro-inflammatory cytokines can influence HIF which in turn can alter the expression of cytokines and therefore modify trophoblast invasion [118-123]. Low oxygen tension has been demonstrated to inhibit the normally invasive phenotype of cytotrophoblasts needed for deep placental implantation [124]. Several animal models showing pre-eclampsia like syndromes have been constructed by disruption of uterine, placental, or renal blood flow and indicated that prepregnancy endothelial dysfunction underlies hypoxia induced shallow placentation [125, 126].

1.2.4 IUGR and pre-eclampsia may have different pathophysiologies

Although endothelial dysfunction appears to be a common predisposing factor for both IUGR and pre-eclampsia, the clinical outcome and the consequences for the mother might be completely different. Therefore some authors suggest that IUGR and pre-eclampsia may represent pathophysiologically separate entities [127]. However, other authors suggest that depending on the presence of other co-

morbidities such as obesity, metabolic syndrome, coagulopathies, and maternal inflammation, predisposed pregnant women may either develop IUGR only or the full-blown phenotype of pre-eclampsia (figure 14) [118].

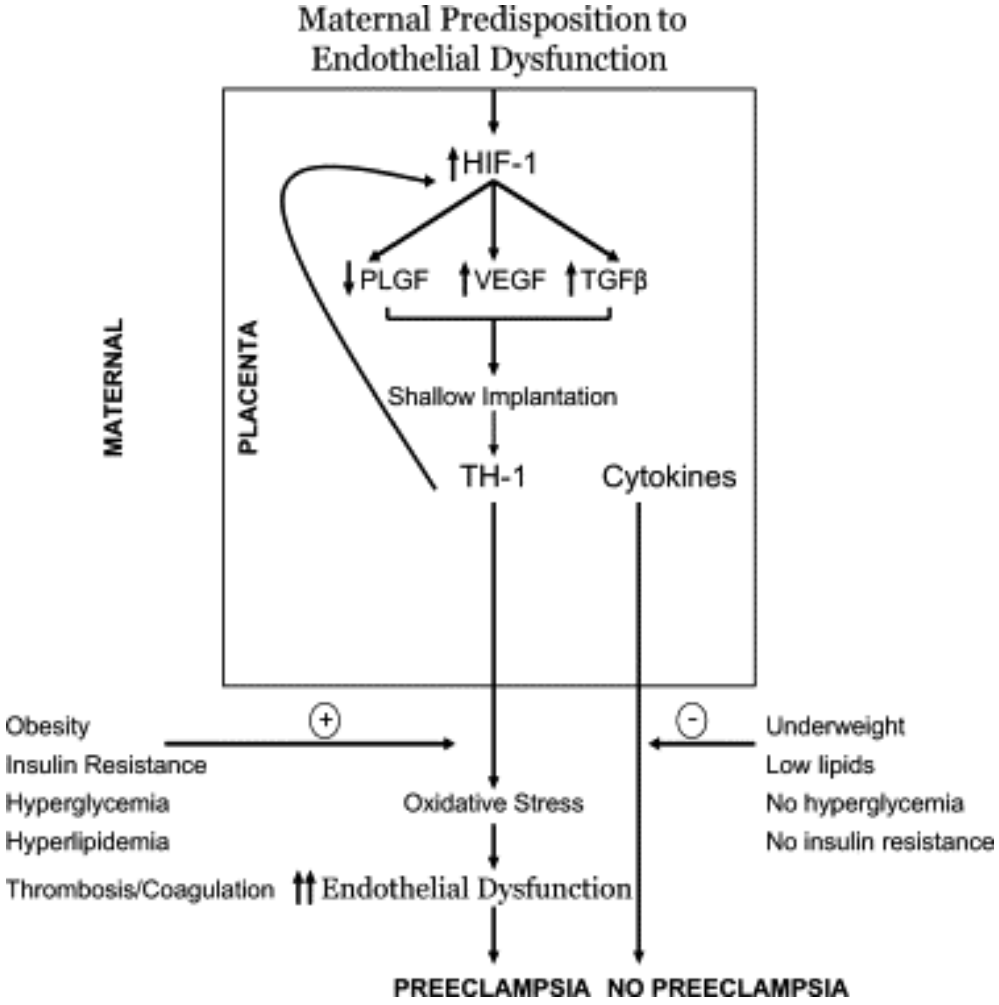

Figure 14. Proposed pathogenesis of IUGR and Pre-eclampsia (adapted from [118].

In fact, tobacco smoking causes marked endothelial dysfunction and cytokine elevation [128], but it is strongly associated with IUGR only and surprisingly inversely correlated with pre-eclampsia [129, 130]. Tobacco smokers tend to be lean and so probably are protected from metabolic syndrome and thus from development of pre-eclampsia whereas the relatively rare group of smokers with concomitant metabolic syndrome may have elevated risk for developing fulminant pre-eclampsia [118].

1.2.5 Placental efficiency- an important factor for fetal growth

Size and growth of the fetus at birth are important for determining the morbidity and mortality immediately after birth and during later life. Children small or large for

gestational age or with IUGR are more prone for developing adult-onset degenerative diseases, such as type 2 diabetes and glucose intolerance [131]. An important factor or process for fetal growth is placental efficiency [132]. The most simple definition of placental efficiency is the gram of fetus produced per gram of placenta [133]. It can also be measured as grams of fetus produced per unit area of placental exchange surface but this definition is used very rarely due to the difficulty to measure the exchange area in every placenta [134]. Indeed, in many species, a positive correlation has been shown between fetal weights near term to placental weight as a proxy measurement of surface area for transport of nutrients [134, 135]. In turn, size of the placenta, morphology, blood flow and abundance of transporters determine the nutrient transfer capacity of the placenta [136]. In addition, synthesis and metabolism of nutrients and hormones by uteroplacental tissue influence the rate of fetal growth [137]. Therefore, intrauterine growth can be affected by changes in any of the above mentioned placental factors [136, 138].

1.2.6 Role of angiogenic and antiangiogenic, and vasoactive factors in the development of pre-eclampsia

The improper opening of the spiral arteries with subsequent placental hypoxia is thought to trigger the release of vasoactive factors from the placenta into the maternal circulation that finally causes systemic endothelial dysfunction and the full blown syndrome of pre-eclampsia (figure 15). Among other factors, soluble fms like tyrosine kinase 1(sFlt1) [139-141] appears to play a crucial role in the pathogenesis of pre-eclampsia. The Fms like tyrosine kinase receptor (Flt1) is highly expressed in the developing placenta and mediates the angiogenic effects of the vascular endothelial growth factor (VEGF) and the placental growth factor (PlGF) during invasion of the trophoblasts. Most of the Flt produced in the placenta during the later stages of normal gestation is a soluble form (sFlt), which is generated by alternative splicing of the Flt mRNA. The sFlt lacks the transmembrane and cytoplasmic domains of Flt1 and is released in large amounts into blood where it reduces the level of free VEGF and PlGF via soluble antagonism. In pre-eclampsia, sFlt is produced in large amounts already during early pregnancy.

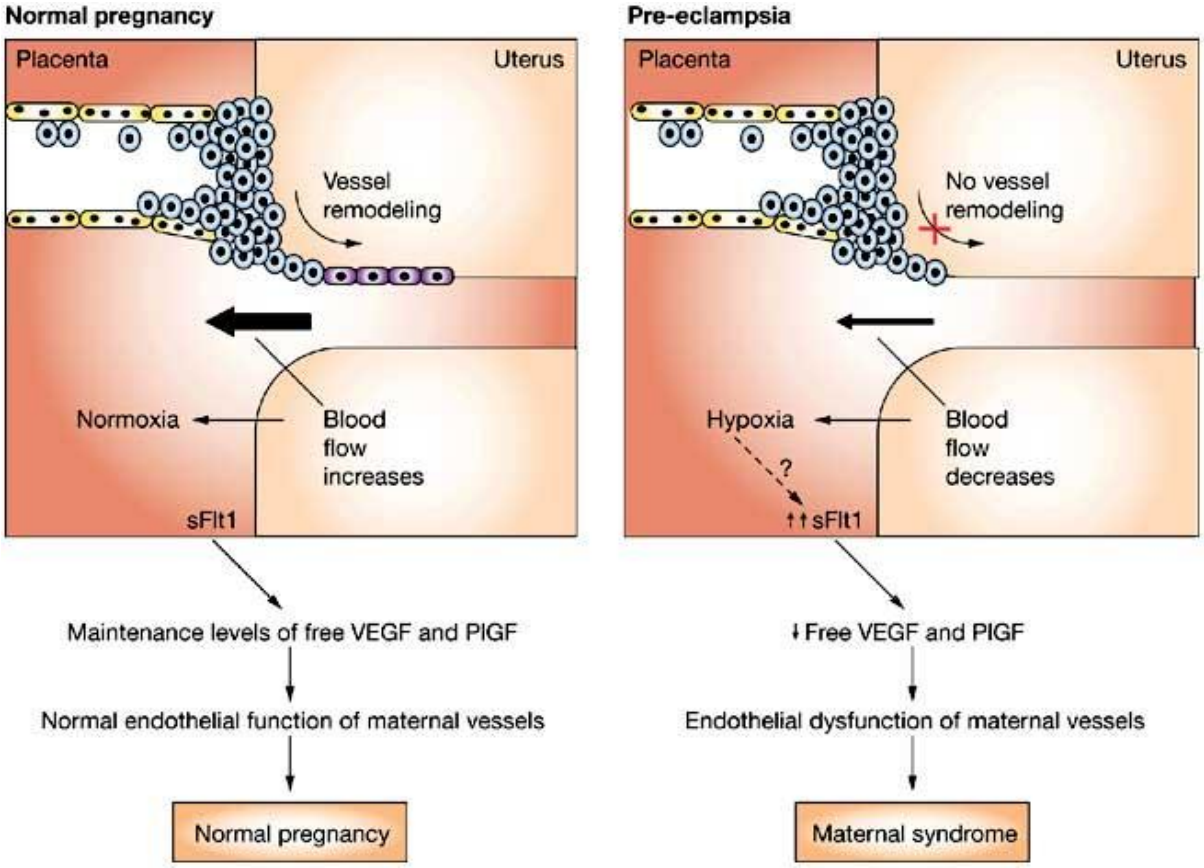

Figure 15. Role of the antiangiogenic factor sFlt 1 in the maternal syndrome of pre-eclampsia (adapted from [110]).

This premature production of sFlt leads to an inappropriate decrease of VEGF and PlGF levels in the maternal circulation causing endothelial dysfunction of maternal vessels and the maternal pre-eclamptic syndrome [110]. Consecutively, blood pressure (BP) increases and the pre-eclamptic phenotype will develop damaging maternal organs such as kidneys, liver and brain [109, 110, 139-141].

In addition to VEGF signaling, also transforming growth factor (TGF) signaling appears to be affected in the vasculature of pre-eclamptic women. Clinical studies demonstrated that the soluble Endoglin (Eng) is elevated in the sera of pre-eclamptic individuals. Membrane bound Eng is a cell-surface coreceptor for transforming growth factor (TGF)- β 1 and TGF- β 3 that modulate the actions of TGF-β1 and TGF-β3 in endothelial cells and the syncytiotrophoblast. Soluble Eng neutralizes circulating TGF- β1 before binding to its receptors and hence impairs TGF-β signaling in the vasculature [141] leading to activation of eNOS and vasodilation.

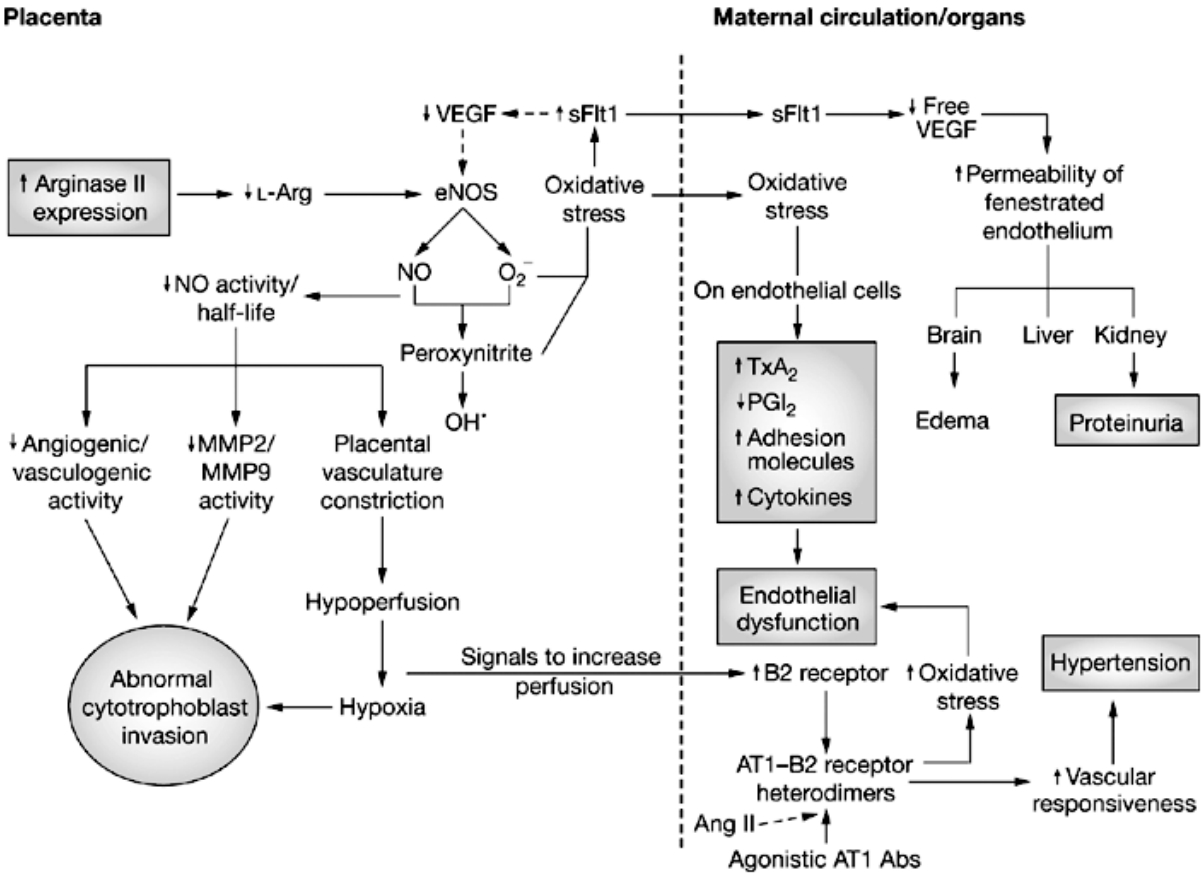

Figure 16. Hypothesis of pre-eclampsia pathophysiology (adapted from [110])

Arterial hypertension in pre-eclampsia might be also explained, at least in part, by the observed increased plasma concentrations of vasoconstrictory substances (e.g. endothelin, thromboxane) and decreased plasma concentrations of vasodilatory mediators (e.g. prostacyclin, NO) in pre-eclamptic women [110]. Several lines of evidence have implicated the role of the renin–angiotensin system in the pathogenesis of pre-eclampsia. During normal pregnancy, plasma renin concentration, renin activity and angiotensin II levels are increased. However, pregnant women remain normotensive which is likely related to a reduced vascular responsiveness to angiotensin II [142]. In pre-eclampsia, the levels of plasma renin activity, the concentration of angiotensin II and aldosterone are decreased, but the pre-eclamptic patients manifest an exaggerated pressor response to angiotensin II [142, 143].

Thus, the pathophysiology of proteinuria and hypertension in pre-eclampsia may involve the imbalanced expression of a variety of vasoactive substances

including VEGF, prostaglandins, thromboxane and angiotensin II. The schematic figure 16 summaries a unifying hypothesis of pre-eclampsia pathophysiology.

1.2.7 Possible role of aldosterone in the development of the pre-eclamapsia

Normal pregnancy is characterized by a marked expansion of plasma and extracellular volume associated with changes in renal hemodynamics as well as in the circulating level of adrenal steroid hormones [144, 145], which likely help to adapt the maternal circulation to the increasing blood and substrate requirements of the growing placenta and fetus. Consistently, plasma aldosterone concentrations increase during normal pregnancy coinciding with plasma volume expansion [146, 147]. In pregnancies later destined for pre-eclampsia, a reduced plasma volume precedes the onset of the disease [147-149] while plasma aldosterone concentration and renin activity are paradoxically suppressed [150]. This observation suggested pre-eclampsia to be caused or aggravated by an inadequate balance of extracellular volume and the activity of the renin-angiotensin-aldosterone system. As a substantial group of pre-eclamptic women show reduced aldosterone synthase enzyme (*Cyp11b2* gene) activity [151], aldosterone deficiency was implicated to play an important role in the pathogenesis of pre-eclampsia. Aldosterone deficiency may lower extracellular volume and increase thereby the risk of placental hypoperfusion [151] with subsequent release of vasoactive factors leading to pre-eclampsia. The possible role of aldosterone was further evidenced by the finding that loss- and gain-of function due to distinct gene variants of the *Cyp11b2* may predispose for and protect from pre-eclampsia, respectively. In fact, the V386A variant of *Cyp11b2* gene, which causes a deficiency in the rate-limiting step of aldosterone synthesis, namely the 18-hydroxycorticosterone methyl oxidase activity [152], was observed solely in a subgroup of pre-eclamptic women, but never in normal pregnant women [151]. In contrast, the gain of function variants of the *Cyp11b2* gene, SF-1 and Int2 (C), which have been shown to be associated with hypertension in non-pregnant women [153], apparently reduce the risk of developing pre-eclampsia [154]. Recently, observations by Gennari-Moser et al. [5] suggest a role of aldosterone for fetal perfusion and also for placental growth. Taken together, these studies propose a role of aldosterone availability for placental size, fetal perfusion and also the development of pre-eclampsia.

1.2.8 Different components of aldosterone effector mechanism expressed in placenta

The following figures 17 gives an overview on the different placental cell types involved in the development of the placenta.

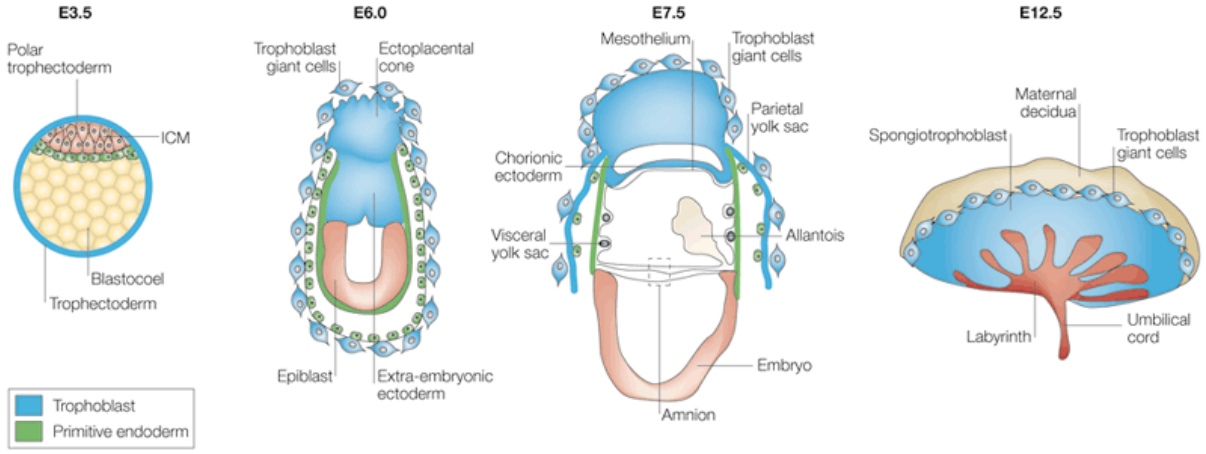

Figure 17. Development of the placenta from the embryonic day E 3.5 to E 12.5 (adapted from [155]).

The syncytiotrophoblast acts as a transporting barrier that regulates the transfer of nutrients, solutes and water between maternal and fetal blood. In the human trophoblast, expression of the mineralocorticoid receptor (MR) and 11β-HSD2 mRNA have been detected [156]. In addition, MR protein was immunolocalized to human syncytiotrophoblast and cytotrophoblast cells, and 11β-HSD2 was found in the syncytiotrophoblast [20]. Driver et al. [157] demonstrated that primary cytotrophoblast cell cultures express the Na^+/K^+-ATPase (α1 and β1 subunits), α- and γ-subunits of ENaC and the Sgk1. Sgk1 was strongly and rapidly induced by corticosteroids (aldosterone and dexamethasone). Aldosterone induced Sgk1 activation was not inhibited by a GR antagonist indicating the presence of functional MR receptors in the placental trophoblast cells. Placental 11β-HSD2 may protect the MR in a fashion analogous to classical mineralocorticoid target tissues to modulate trophoblast sodium transport [156]. Significantly decreased 11β-HSD2 mRNA expression levels were observed in placentas of patients with pre-eclampsia [158].

In syncytiotrophoblasts from normal placenta, ENaC was present on the apical membrane but not detected in pre-eclamptic placenta on mRNA and protein

level. In the BeWo cell line, a model of human syncytiotrophoblasts, ENaC was found and its expression is regulated by aldosterone, vasopressin, progesterone and estradiol [159]. Some evidence exists supporting the hypothesis that ENaC channels are required for the migration of BeWo cells [160]. Recently the role of ENaC proteins in the migration of vascular smooth muscle cells (VSMC) has been demonstrated in cell culture [161]. In sheep low aldosterone levels resulted in reduced placental weight, adverse fetal outcome and up-regulation of VEGF in placenta [162]. VEGF stimulates aldosterone production in cultured adrenal and endothelial cells (unpublished data from Markus Mohaupt). In vitro studies suggest that aldosterone stimulates trophoblast proliferation [5]. These experiments suggest that VEGF stimulates aldosterone production via the adrenal gland and aldosterone may have a role in trophoblast proliferation/migration and in placental development.

1.2.9 High salt diet during pregnancy may affect blood pressure and pregnancy outcome

Aldosterone is closely linked to salt reabsorption. Of interest, an old clinical study forwards the observation of a reduced number of pre-eclampsia and fetal death on a high salt diet [163]. In addition, in a hypertensive woman homozygous for the V386A mutant of *Cyp11b2* and low aldosterone availability, salt supplementation lowered BP throughout pregnancy [164]. In contrast, in pre-eclampsia, the benefits of salt supplementation are still controversial and a recent meta-analysis did not show any beneficial impact [165].

2 AIMS OF THE STUDY

2.1 Role of aldosterone in renal potassium excretion

Previous observation by Muto et al. [166] on isolated perfused CCD of adrenalectomized rabbits suggested an aldosterone-independent mechanism of K^+ secretion on high K^+ diet. In this study, increased apical Na^+ and K^+ channels currents were observed on high K^+ diet in adrenalectomized rabbits. Another studies in adrenalectomized rats on high K^+ diet also showed an increased number of conducting Na^+ channels suggesting that there are factors other than aldosterone that regulate ROMK-like SK channel, Na^+ channels and Na^+/K^+ pumps on high K diet [167]. Moreover, the presence of a local renal aldosterone system and its regulation by salt has been suggested [168, 169]. Obviously the presence of a local renal aldosterone system was not considered in previous studies. Therefore, to further address the role of aldosterone for the renal and colonic control of K^+ homeostasis, we used the aldosterone synthase knockout ($AS^{-/-}$) mice as an in vivo model without any endogenous aldosterone production.

2.2 Role of aldosterone in pregnancy

Available literature suggests that aldosterone plays an important role in pregnancy. However, it is not clear whether aldosterone deficiency alone can lead to compromised pregnancy, IUGR, or preeclampsia and whether aldosterone deficiency can be counterbalanced by a high salt diet. To address these questions we used aldosterone synthase deficient knockout mice ($AS^{-/-}$) [9]. Monitoring of pregnancy in $AS^{-/-}$ mice for systolic BP, proteinuria, and pregnancy outcome was performed to assess the effects of aldosterone in murine pregnancy. Detailed analysis of placentas and pups also examined the role of aldosterone in the development of IUGR and placental efficiency.

3 MATERIAL AND METHODS

3.1 Role of aldosterone in renal potassium excretion

3.1.1 Animal model

All experiments were performed on aldosterone synthase wild type (*Cyp11b2*, $AS^{+/+}$) and aldosterone synthase-deficient ($AS^{-/-}$) mice with a inbred129Sv genetic background [170]. This mouse model was generously provided by Prof. Oliver Smithies, University of North Carolina, Chapel Hill, NC, USA [9]. Age-matched male $AS^{+/+}$ and $AS^{-/-}$ mice (8 to 14 weeks) were used for all experiments. All experiments were performed according to Swiss Animal Welfare laws and approved by the local veterinary authority (Veterinäramt Zürich). All animals received standard rodent chow GLP 3433 (PROVIMI KLIBA, Kaiseraugst, Switzerland).

3.1.2 Metabolic cage experiments

To analyze adaptive physiological changes in mice, animals were kept individually in metabolic cages (Tecniplast, Buguggiate, (VA) Italy). This type of cages allows an exact monitoring of individual food and water consumption as well as urine and faeces collection. Mice were adapted to metabolic cages for 3 days before the actual measurements. During the experiment bodyweight, consumption of food and water as well as urine volumes and faeces were monitored and collected daily. 24 hour urine was collected under mineral oil to avoid evaporation. At the end of the experiments urinary electrolytes (Na^+, K^+, Ca^{2+},Mg^{2+},Cl^-,SO^{4-}) were measured by ion chromatography (Metrohm ion chromatograph, Herisau, Switzerland) and urine creatinine was measured by the Jaffe method [171].

3.1.3 Experimental protocol for dietary potassium loading

Four different potassium (K^+) diets were used in this study. Control diet (0.8% K; standard powder food), 2% K^+ diet (2.2 g of KCl + 97.8 g standard powder food), 3% K^+ diet (4.2 g KCl + 95.8 g standard powder food) and 5% K^+ diet (8 g of KCl + 92 g standard powder food). Powdered food with the appropriate amount of KCl was mixed with milliQ water in 1:1 proportion (50 g food + 50 ml water) to prepare wet diets. $AS^{+/+}$ and $AS^{-/-}$ mice were divided into four different groups: Control group

(Control diet, n = 5), 2% K^+ diet group (n = 7), 3% K^+ diet group (n = 7) and 5% K^+ diet group (n = 5). After an adaptation phase in the metabolic cage for 3 days all mice were fed for one day with control diet (time point 0) followed by two days on the experimental diets varying in their K^+ contents. At the end of the experiment, mice were anesthetized with ketamine/xylazine (Narketan (Vétoquinol, CH): 65 mg/kg BW; Xylazin (Streuli, CH): 13 mg/kg BW), and heparinized venous blood from the abdominal vein was collected and analyzed immediately for pH, blood gases, and electrolytes on a Radiometer ABL 505 (Radiometer, Copenhagen, Denmark) blood gas analyzer. Serum was collected and frozen until further analysis. Kidneys were harvested, immediately frozen in liquid nitrogen, and stored at -80^{o}C until mRNA and/or protein extraction.

3.1.4 Changes in tubular workload

To assess the functional activity of ENaC and NCC in the kidney *in vivo*, $AS^{+/+}$ and $AS^{-/-}$ mice were treated with the diuretics amiloride and thiazide, respectively. Mice were kept in metabolic cages and fed one day with control diet and 2 days with 2% K^+ diet to get the control physiological values. After these three days, mice were divided into control groups and treatment group (injection of diuretics). At the end of the experiment, the urinary bladder was emptied by massage, and mice from control groups were treated with vehicles (0.9% saline i.p., $AS^{+/+}$ n = 9, $AS^{-/-}$ n = 8 or dimethyl sulfoxide (DMSO) i.p., $AS^{+/+}$ n = 8, $AS^{-/-}$ n = 9; Control-group), and mice from the treatment groups were injected with either amiloride (5 µg amiloride/g body weight in 200 µl of 0.9% saline solution i.p.; Amiloride group; $AS^{+/+}$ n = 11, $AS^{-/-}$ n = 9) or with hydrochorthiazide (50 µg hydrochlorothiazide/g body weight in 200 µl DMSO; Thiazide group; $AS^{+/+}$ n = 9, $AS^{-/-}$ n = 9). After 4 hours, urine was collected from urine collector and by emptying urinary bladder by massage. Urine was analyzed for electrolytes including Na^+ and K^+.

3.1.5 Role of angiotensin II in renal adaptation to high potassium diet

To assess the role of angiotensin II in compensating the lack of aldosterone, mice were given the AT1 receptor blocker losartan. $AS^{+/+}$ and $AS^{-/-}$ mice were individually kept in metabolic cages. After 3 days of adaptation on control diet and one and half days on 2 % K^+ diet, mice were divided in two groups and received in the evening

either a s.c. injection of vehicle (milliQ water; Control group; n = 4) or losartan (10 mg/kg body weight in 50µl milliQ; losartan group; n = 5). At the end of the experiment, mice were anesthetized and heparinized venous blood was collected from the abdominal vein and analyzed immediately for electrolytes. Urine was collected under mineral oil and analyzed for creatinine, and electrolytes including Na^+ and K^+.

3.1.6 Analysis of the urinary concentration capability of $AS^{+/+}$ and $AS^{-/-}$ mice

To examine the urinary concentrating mechanism, mice were kept in metabolic cages for 5 days. To have the same water intake in both groups, a special agar diet was prepared that comprised the same volume of water but an amount of food that matched the one recorded before to be eaten daily by the $AS^{+/+}$ and $AS^{-/-}$ mice (40 mg of agar and 4 ml of water per 1 g and 1.33 g of standard powdered food for $AS^{+/+}$ mice and $AS^{-/-}$ mice, respectively). After 3 days of adaptation to the 0.8% K^+ agar diet, mice were given 2% K^+ in the agar diet. After two days, the urinary bladder was emptied by massage and mice were divided into two groups and injected s.c. with either vehicle (0.9% saline; control group; n = 5) or with the modified form of vasopressin called as desmopressin (DDAVP) (Sigma) (1 ng/g of body weight in 100 µl of 0.9% saline solution; DDAVP group; n = 5). Urine was collected before injection and 4 hr after the treatment by emptying the urinary bladder by massage. Urine osmolarity was measured by freezing point depression (Osmometer, Roebling). At the end of the experiment, mice were anesthetized and heparinized venous blood was collected and analyzed immediately on a Radiometer ABL 505 (Radiometer, Copenhagen, Denmark) blood gas analyzer for plasma Na^+ and K^+ concentration.

3.1.7 RNA extraction from the kidney

Snap frozen kidneys (5 kidneys per group) were homogenized in RLT Buffer (Qiagen) supplemented with 2-mercaptoethanol to a final concentration of 1%. Total RNA was extracted from 200 µl aliquots of each homogenized sample using RNeasy Mini Kit (Qiagen) according to the manufacturer's instructions. Quality and concentration of the isolated RNA preparations were measured by ND-1000 spectrophotometer (NanoDrop Technologies). Total RNA samples were stored at -80^{o}C until further use.

3.1.8 Quantitative Real-time PCR

Each RNA sample was diluted to 100 ng/µl and 3 µl was used as a template for reverse transcription using the TaqMan Reverse Transcription Kit (Applied Biosystems, Forster City, CA). Quantitative real time (qRT-PCR) was performed on the ABIPRISM 7500 Sequence Detection System (Applied Biosystem). Primers for the NCC (*Slc12a3)* were designed using online Primer 3 software. Sequences of primers and probes are as follows: NCC forward 5'-TAG ACC CCA TCA ATG ACA TCC-3' and reverse 5'-AGG TAG TTG GCA AAG GAG ACC-3' (accession number: NM_001205311); BK β1 forward 5'-CCA GCG GAG ACC CAG AGA-3', reverse 5'-GGG CCA TCA CCA GCT TCT T-3'and probe 5'-CTA AAT GAC TGT TGC CTC CAG TGG CCA-3' (accession number: NM_031169); BK β2 forward 5'-GCT GCG CTC CTA CAT GCA-3', reverse 5'-GCC CAC AGC TGA AGG AAC AG-3' and probe 5'-AGC GTG TGG ACA GAA GAA GCC CAG TGT-3' (accession number: NM_028231); BK β4 forward 5'-AAC TCC AGG GCG CTG CTA-3', reverse 5'-CTC TTA CAG GGC GGG ATA TAG GA-3' and probe 5'-ACA GCG ACC AGC ACC AGC TCC TG-3' (accession number: NM_021452). Primers for hypoxanthine guanine phosphoribosyl transferase (HPRT) as a housekeeping gene were designed using Primer Express software from Applied Biosystem. Primer sequences for HPRT were forward 5'-TTA TCA GAC TGA AGA GCT ACT GTA AGA TC-3 and reverse 5'-TTA CCA GTG TCA ATT ATA TCT TCA ACA ATC-3' (accession number: NM_013556) as described previously [172]. Specificity of the primers was - tested in a standard PCR and always resulted in a single product of the expected size on 2% agarose gel. Real time PCR reactions were performed for NCC using the iQ SYBR Green Supermix (Bio-rad). ROX Passive reference Dye (Bio-rad) 3.3 µl/1.25 ml of iQ SYBR Green Supermix was added. Briefly, 3 µl cDNA, 0.8 µl of each primer (10 µM), 5.4 µl RNase free water, 10 µl iQ SYBR Green Supermix reached 20 µl final reaction volume. Real time PCR reactions were performed for BKβ1, BKβ2 and BKβ4 using TaqMan Universal PCR Mastermix (Applied Biosystem). Briefly, 3 µl cDNA, 0.8 µl of each primer (25 µM), 0.4 µl of labeled probe, 6 µl of RNAse free water and 10 µl of TaqMan Universal PCR master mix reached total volume of 20 µl of final reaction volume. Reaction conditions were: denaturation at 95^{o}C for 10 min followed by 40 cycles of denaturation at 95^{o}C for 15 s and annealing/elongation at 60^{o}C for 60 s with auto ramp time. For PCR reactions using the iQ SYBR Green Supermix last

step is followed by dissociation stage (95^{o}C for 15 s, 60^{o}C for 15 s followed by slow ramp to 95^{o}C). All reactions were run in duplicate. The expression of gene of interest was calculated in relation to HPRT. Relative expression ratios were calculated as R = $2^{[Ct(HPRT/\_-actin)\_Ct(test\ gene)]}$.

3.1.9 Membrane preparation and western blot analysis

Total membrane proteins were prepared as described previously [173]. After measurement of the protein concentration (Bio-rad D_c Protein Assay, Bio-rad, Hercules, CA, USA), 50 µg of crude membrane proteins were solubilized in Laemmli sample buffer, and SDS-PAGE was performed on 8% polyacrylamide gels. For immunoblotting, the proteins were transferred electrophoretically to nitrocellulose transfer membrane (PROTRAN 0.2 µM, Whatman GmbH, Dassel, Germany). After incubation with Odyssey blocking buffer, (Li-COR) for 60 min, the blots were incubated with the respective primary antibodies diluted in Odyssey blocking buffer overnight at 4^{o}C.The primary antibodies used are listed in Table 1.

Table 2. Antibodies used for immunohistochemistry and western blotting

		Dilution		
Antibody	Host	WB	IF	Source
ROMK1	Rabbit	1:800	1:4,000	Alomone
αENAC	Rabbit	1:5000	1: 5,000	J.Loffing
βENaC	Rabbit	1:10,000	1:40,000	J.Loffing
γENaC	Rabbit	1:10,000	1:40,000	J.Loffing
NCC	Rabbit	1:8000	1:10,000	J.Loffing
pNCCT53	Rabbit	1:1000	1:15,000	R. Fenton
pNCCT58	Rabbit	1:2000		R.Fenton
pNCCs89	Rabbit	1:4000		J.Loffing
AQP2	Rabbit	1:10,000		J.Loffing
β actin	Rabbit	1:10,000		Sigma
Calbindine D28k	Mouse		1:10,000	Swant (CH)
BK	Mouse	1:10,000		NeuroMab

After overnight incubation, the membranes were washed three times with phosphate buffer saline containing 0.1% Tween 20, and incubated with the fluorescent secondary antibody (goat anti-rabbit IRdye 800 1:10,000, or goat anti mouse IRDye 680, 1:20,000, Li-COR, Nebraska, USA or from Rockland, Gilbertsville, PA) for 1 h at room temperature. After washing the membranes three times, the protein signal was detected by scanning the membrane with the Odyssey Infrared Imaging System (Li-COR Biosciences). All images were analyzed using analysis software provided with the system to calculate the protein of interest/actin ratio.

3.1.10 Immunohistochemistry

For immunohistochemistry, $AS^{+/+}$ and $AS^{-/-}$ mice of the different experimental groups (n = 5 each) were anesthetized with ketamine/xylazine (Narketan (Vétoquinol, CH): 65 mg/kg BW; Xylazin (Streuli, CH): 13 mg/kg BW) and the kidneys were fixed by intravascular perfusion via the abdominal aorta [174]. The fixation solution contained 3% paraformaldehyde (Sigma-Aldrich, USA) in 0.1 M phosphate buffer. After 5 min of fixation kidneys were rinsed for 5 min with 0.1 M phosphate buffer. 2 mm thick kidney slices were subsequently mounted on thin cork slices, frozen in liquid propane and stored at -80°C until further use.

For immunohistochemistry, kidneys were cut into 4 - 5 µm thin sections in a cryostat (Microm, Leica, CH), and mounted on chrome-alum/gelatin coated glass slide. After 10 min blocking of unspecific binding sites by 10% normal goat serum, sections were incubated over night with the primary antibodies diluted in 1% PBS/BSA. Overnight incubation took place at 4°C in a humidified chamber. Antibody dilutions are given in table 1. After repeated rinsing of the sections with PBS, binding sites of the primary antibodies were detected with either Cy3 conjugated goat anti rabbit antibody or FITC conjugated goat anti mouse antibody (Jackson Immuno Research Laboratories, USA). After three times rinsing, the slides were mounted in Glycergel (DAKO, USA) with 2% 1,4-Diazabicyclo[2.2.2.]octans (Sigma-Aldrich, USA) to avoid fading of the signal. Sections were studies by epifluorescence (Leica DM6000; Leica D) and analyzed by Leica AF6000 system (Leica D).

3.1.11 Ussing chamber experiments

Male mice kept on the respective K^+ containing diets were sacrificed by cervical dislocation. The distal part of the colon was isolated and rinsed in ice cold ringer solution. Only the distal 1.5 cm of the intact mouse colon was then mounted in an Ussing Chamber. The two halves of the chamber were continuously perfused by a bubble lift system. The solutions on the two sides were symmetrical and with the following composition (in mM): NaCl 120; $NaHCO_3$ 25; K_2HPO_4 1.6; KH_2PO_4 0.4; Ca-gluconate 1.3; $MgCl_2$ 1; D-glucose 5, indomethacine (5 µM). The reservoirs were bubbled with carbogen (5% CO_2 and 95% O_2) and kept at 37^oC by water jackets. Initially, tetrodotoxin (TTX, 1 µM) was added to the serosal side to inhibit possible secretory activation by the enteric nervous system or other autonomous nerve cells.

Experiments were performed in a setup where the transepithelial voltage was clamped to “zero” (Physiological Instruments, USA). The apertures of the clamped chambers were 0.283 cm^2. After mounting the tissues and an equilibration period of 30 min, amiloride (100 µM) was added to the mucosal perfusate to obtain a value of amiloride-sensitive short circuit current (ΔI_{sc}(amil)), a measure of electrogenic ENaC-mediated Na^+ absorption. After additional 5 min. $BaCl_2$ (5 mM) was added also to the mucosal perfusate to obtain a value of Ba^{2+}-sensitive short circuit current (($I_{sc}(Ba^{2+})$), a measurement of electrogenic BK-mediated K^+ secretion.

3.1.12 Statistical analysis

Results are expressed as mean ± SEM. All data were tested for significance using unpaired and paired Student’s test where appropriate. Only values with $p < 0.05$ were considered as significant.

3.2. Role of aldosterone in pregnancy

3.2.1 Animals

All experiments were performed on inbred 129 SvEv genetic background aldosterone synthase wild type ($AS^{+/+}$) and aldosterone synthase-deficient ($AS^{-/-}$) female mice. Mice were bred in our own animal facility. All experiments were performed according to Swiss Animal Welfare laws and approved by the local veterinary authority (Kantonales Veterinäramt, Zürich). Unless indicated otherwise, animals were fed standard rodent chow (3430, KLIBA NAFAG, Kaiseraugst, Switzerland) with free access to normal tap water.

3.2.2 Study design and treatment

Age matched female $AS^{+/+}$ and $AS^{-/-}$ mice, between 3.5 to 6.5 months old, were used for experiments. Animals were divided into two groups, a control group and an experimental group. In the control group, $AS^{-/-}$ male were mated with $AS^{+/+}$ female mice, whereas in the experimental group, $AS^{+/+}$ male mice were mated with $AS^{-/-}$ females to generate only heterozygous pups to have the same genotype for all pups. Both groups were fed with either the standard rodent chow powder, (3433 KLIBA NAFAG, Kaiseraugst, Switzerland) containing 0.20% Na^+ and 0.36% Cl^- ($AS^{+/+}$ n = 9 and $AS^{-/-}$ mice n = 9) or with standard diet supplemented with NaCl (high salt diet, 5% NaCl) ($AS^{+/+}$ n = 6-8 and $AS^{-/-}$ mice n = 8-10). To feed the mice with high salt diet, 100 g of standard rodent chow powder was mixed with 5 g NaCl and then mixed with an equal volume of deionised water to moisten the food for feeding. Male and female mice were kept together in individual cages for breeding and female mice were controlled daily in the early morning for the presence of copulation plugs and the following day was considered as gestational day 1. Systolic blood pressure (SBP) was measured in female mice using the tail cuff method (see below). In second set of experiments mice were fed either the control diet ($AS^{+/+}$ n = 8, $AS^{-/-}$ n = 15) or high salt diet (5% NaCl) ($AS^{+/+}$ n = 6, $AS^{-/-}$ n = 9) and sacrificed on day 18 of pregnancy by cervical dislocation. The number and weight of the pups and the placentas were measured, and tissues collected for further analysis. Placentas were collected and rapidly frozen in liquid nitrogen and stored at -80^{o}C for RNA extraction. Some placentas were fixed in 4% paraformaldehyde for further histological analysis.

3.2.3 Tail cuff blood pressure measurements

SBP was measured by a non-invasive computerized tail cuff method (BP2000, Visitech Systems, Apex, NC, USA) as described previously [175]. Mice were adapted for 5 days before the start of the study. Blood pressure was measured daily between 1 pm to 5 pm. Averages of systolic BP with a standard deviation of less than 10 mmHg were considered to be stable measurements and were used for further analysis. SBP from female mice on control diet was measured on control conditions 2 to 3 days before pregnancy and from day 1 of pregnancy until the end of pregnancy up to 21 days. Mean SBP was calculated from each day's average SBP measurements. SBP of animals in the high salt diet experiments was measured first on control diet, then from day 4 to 6 of high salt diet. Thereafter, female mice were kept together with male mice for mating and SBP was measured at gestational days 5 to 7 and days 15 to 17. Mean SBP was calculated from 3 days of average SBP measurements.

3.2.4 Urinary protein concentration measurement

Spot urines were collected from female mice during pregnancy daily by gentle massage of the urinary bladder. Total urinary protein concentration was measured with a standard protein assay kit (Bio-rad D_c Protein Assay, Bio-rad, Hercules, CA, USA). Urinary creatinine concentration was measured by the Jaffe method [171].

3.2.5 RNA extraction

Snap frozen placentas (5 placentas per group) were homogenized in RLT buffer (Qiagen, Hilden, Germany) supplemented with 2-mercaptoethanol to a final concentration of 1%. Total RNA was extracted from 200 µl aliquots of each homogenized sample using RNeasy Mini Kit (Qiagen, Hilden, Germany) according to the manufacturer's instructions. Quality and concentration of the isolated RNA preparations were measured on a ND-1000 spectrophotometer (Thermo Fischer Scientific Inc., Wilmington, DE, USA). Total RNA samples were stored at -80^{o}C until further use.

3.2.6 Semi-quantitative Real-time PCR

Each RNA sample was diluted to 100 ng/µl and 3 µl was used as a template for reverse transcription using the TaqMan Reverse Transcription Kit (Applied Biosystems, Forster City, CA). Quantitative real time (qRT-PCR) was performed on the ABIPRISM 7500 Sequence Detection System (Applied Biosystem, Foster City, CA, USA). Primers for vascular endothelial growth factor (VEGF), soluble fms-like tyrosine kinase-1 (sFlt-1), and the hypoxia inducible factor 1α (HIF1α) were designed using Primer 3 online software, whereas primers for hypoxanthine guanine phosphoribosyl transferase (HPRT) as housekeeping gene were designed using Primer Express software from Applied Biosystem. The primers and probes used from Applied Biosystem are monocyte chemo-attractant protein 1 MCP-1 (Mm00441242) and Tumor Necrosis Factor 1alpha TNFα (Mm99999068). Sequences of primers designed by ourselves are as follows: VEGF forward 5'-CAG GCT GCT GTA ACG ATG AA-3' and reverse 5'-GCA TTC ACA TCT GCT GTG CT-3' (accession number: NM_009505.4); sFlt forward 5'-GGG AAG ACA TCC TTC GGA AGA-3' and reverse 5'-TGT GGT ACA ATC ATT CCT CCT G-3' (accession number: D88690); HIF1α forward 5'-ATC TCG GCG AAG CAA AGA G and reverse 5'-CTG TCT AGA CCA CCG GCA TC-3' (accession number: NM_010431); HPRT forward 5'-TTA TCA GAC TGA AGA GCT ACT GTA AGA TC-3 and reverse 5'-TTA CCA GTG TCA ATT ATA TCT TCA ACA ATC-3' (accession number: NM_013556). The specificity of the primers was first tested in a standard PCR that resulted in a single PCR product of the expected size on 2% agarose gels. Real time PCR reactions were performed using the iQ SYBR Green Supermix (Bio-rad, Hercules, CA, USA). ROX Passive reference Dye (Bio-rad, Hercules, CA, USA) 3.3 µl/ 1.25 ml of iQ SYBR Green Supermix was added. Briefly, 3 µl cDNA, 0.8 µl of each primer (10 µM), 5.4 µl RNase free water, 10 µl iQ SYBR Green Supermix were mixed to 20 µl final reaction volume. Reaction conditions were: denaturation at 95^{o}C for 10 min followed by 40 cycles of denaturation at 95^{o}C for 15 s and annealing/elongation at 60^{o}C for 60 s followed by dissociation stage (95^{o}C for 15 s, 60^{o}C for 15 s followed by a slow ramp to 95^{o}C). All reactions were run in duplicate. The expression of gene of interest was calculated in relation to HPRT. Relative expression ratios were calculated as $R = 2^{[Ct(HPRT/-actin)\_Ct(test\ gene)]}$.

3.2.7 Histology

Placentas were fixed by immersion in 4% paraformaldehyde (Applichem, Darmstadt, Germany). After tissue processing and embedding in paraffin, 5 µm sections were prepared. Paraffin sections were stained with hematoxylin-eosin (H&E) and scanned with the Mirax Midi Slide Scanner microscope (Zeiss, Jena, Germany).

3.2.8 Immunoblotting

Placentas, stored at -80°C, were homogenised in ice cold homogenisation buffer (0.27 M sucrose, 2 mM EDTA, 0.5% NP40 prepared in 1x buffer A supplemented with protease and phosphatase inhibitor cocktails (Roche, Mannheim, Germany) (buffer A: 0.6 M KCl, 150 mM NaCl, 150 mM HEPES, pH 7.5,). Homogenates were overlaid on a sucrose cushion (30% w/v sucrose, 2 mM EDTA, pH 8 prepared in 1x buffer A) and centrifuged at 3,000 rpm for 10 mins at 4°C. After centrifugation, supernatant obtained were stored as a cytoplasmic fraction, and pellets of nuclei were resuspended in 1x nuclei extraction buffer (20 mM HEPES, pH 7.5, 400 mM NaCl, 1 mM EDTA, pH 8) and incubated for 15 minutes on ice with intermittent vortexing. Solubilised nucleated pellet fractions were centrifuged again at 15,000 rpm for 5 min at 4°C and supernatant collected as nuclear protein fraction. Protein concentration was measured with a protein assay kit (Bio-rad protein assay, Munich, Germany). 60 to 80 µg of proteins were solubilised in 5X Laemmli sample buffer and run on 8% polyacrylamide gels. Briefly, protein was separated by SDS-PAGE, transferred on nitrocellulose membrane by the wet transfer method and incubated overnight with the following primary antibodies: rabbit polyclonal anti-HIF1α (1:1000, Novus Biologicals) and mouse monoclonal β-actin (1:10,000, Sigma). After washing, nitrocellulose membranes were incubated with anti-rabbit secondary fluorescent antibody (goat anti-rabbit IRdye 800 1:10,000, or goat anti mouse IRDye 680, 1:20,000, Li-COR, Nebraska, USA). After washing the membranes three times, the protein signal was detected by scanning the membrane with the Odyssey Infrared Imaging System (Li-COR Biosciences). All images were analyzed using analysis software provided with the system to calculate the protein of interest/actin ratio.

3.2.9 Statistical analysis

Results are expressed as mean ± SEM. All data were tested for significance using paired or unpaired Student's test or one way ANOVA analysis followed by Tukey's multiple comparison and Bonferroni's post test where appropriate. $P<0.05$ was considered statistically significant.

4 RESULTS

4.1 Aldosterone dependent and independent regulation of renal K^+-excretion

4.1.1 Response to high K^+ loading

To assess the tolerance of $AS^{-/-}$ mice to high K^+ load, mice were given different K^+ diets. On control (0.8% K^+) and on 2% K^+ and 3% K^+ diets, $AS^{-/-}$ mice ingested slightly, but not significantly more food than $AS^{+/+}$ mice. With 5% K^+ diet food intake significantly decreased in $AS^{-/-}$ compared to $AS^{+/+}$ mice (figure 18A). $AS^{-/-}$ mice drank significantly more water compared to $AS^{+/+}$ on control (5.1 ± 0.3 ml vs. 4.3 ± 0.2 ml, p = 0.04), 2% K^+ diet (8.0 ± 0.6 ml vs. 6.4 ± 0.4 ml, p = 0.04), and on 3% K^+ diet (8.4 ± 0.7 ml vs. 5.5 ± 0.4 ml, p = 0.002). On 5% K^+ diet, water intake was significantly decreased in $AS^{-/-}$ mice compared to $AS^{+/+}$ mice (6.3 ± 1.0 ml vs. 9.9 ± 0.8 ml, p = 0.02). As expected, in $AS^{-/-}$ mice urinary volume per 24 h was elevated already on control diet and was significantly higher on 2% K^+ and 3% K^+ diet compared to $AS^{+/+}$ mice on the corresponding diets. On 5% K^+ diet, urinary volume was significantly decreased in the $AS^{-/-}$ mice reflecting the diminished water intake (figure 18B). Plasma Na^+ concentrations revealed no difference among the genotypes on different K^+ diets. In contrast, plasma K^+ concentrations on 2% K^+ and 3% K^+ diets was slightly elevated in knockout mice and culminating to a hyperkalemic situation in $AS^{-/-}$ mice on 5% K^+ diet with significantly higher plasma K^+ levels than the corresponding $AS^{+/+}$ mice (figure 18C and 18D). To examine the ability of the kidney to adapt to changes in dietary K^+ load, 24 h urinary electrolyte concentrations was measured by ion chromatography. Urinary Na^+ excretion of $AS^{-/-}$ mice was slightly elevated on control and significantly higher on 2% K^+ diet, but there was no difference on 3% K^+. On 5% K^+ diet, $AS^{-/-}$ showed a lower Na^+ excretion than $AS^{+/+}$ mice. Urinary K^+ excretion parallels the observations seen for urinary Na^+ excretion. $AS^{-/-}$ mice were able to excrete K^+ in the urine on control diet, and even excreted significantly higher K^+ on the 2% K^+ diet compared to $AS^{+/+}$ mice. However, on 3% K^+ diet urinary K^+ excretion in $AS^{-/-}$ mice was similar as in $AS^{+/+}$ mice, and on 5% K^+ diet, K^+ excretion was significantly decreased in $AS^{-/-}$ mice indicating their inability to adapt to very high K^+ load (figure 18E and 18F).

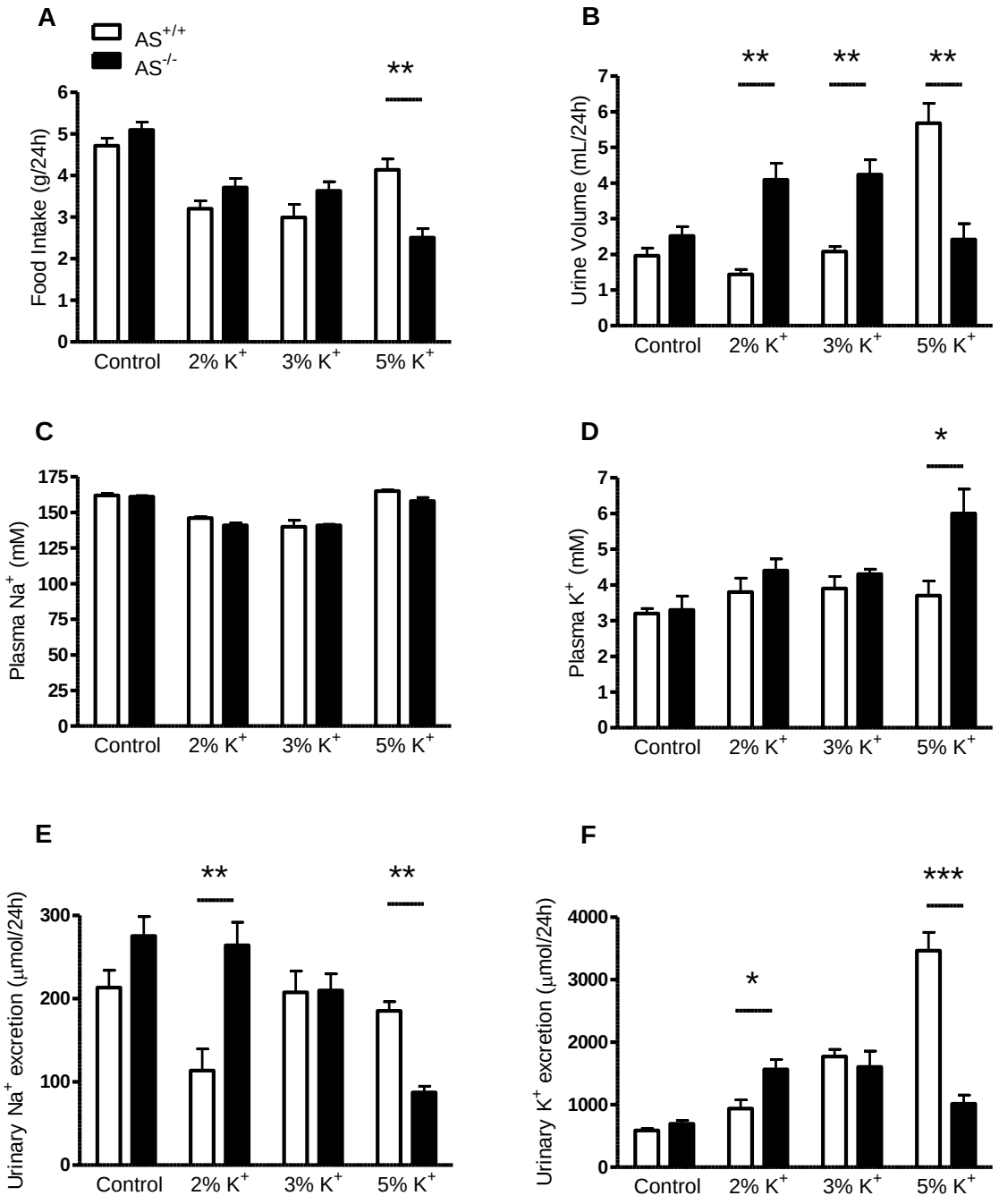

Figure 18. Response of $AS^{+/+}$, wild type mice, (open bars); and $AS^{-/-}$, aldosterone synthase-deficient mice, (filled bars) to control (0.8% K^+), 2% K^+, 3% K^+, and 5% K^+ loading. Mice were kept in metabolic cages and urine and blood electrolytes were measured. Physiological responses in relation to food intake over 24 h (A), urine excretion over 24 h (B), blood Na^+ concentration (C) and blood K^+ concentration (D) at the end of experiment after 2 days of diet, urine Na^+ excretion over 24 h (E) and urine K^+ excretion over for 24 h (F) are shown. Measurements were performed after 2 days of K^+ diet. n = 5-7 mice per group. Values are mean ± SEM. * $p \leq 0.05$, ** $p \leq 0.01$, *** $p \leq 0.001$.

4.1.2 Effect of high K^+ diet on distal nephron K^+ and Na^+ channels: Increased apical expression of ROMK and maintained ENaC cleavage in $AS^{-/-}$ mice on 2% K^+ diet

In mice on 0.8% K^+ diet, immunoblots showed significantly decreased protein abundances for the uncleaved (90kDa) band of α-ENaC in $AS^{-/-}$ mice, and no significant difference in protein abundance for β- and γ-ENaC between genotypes (figure 19).

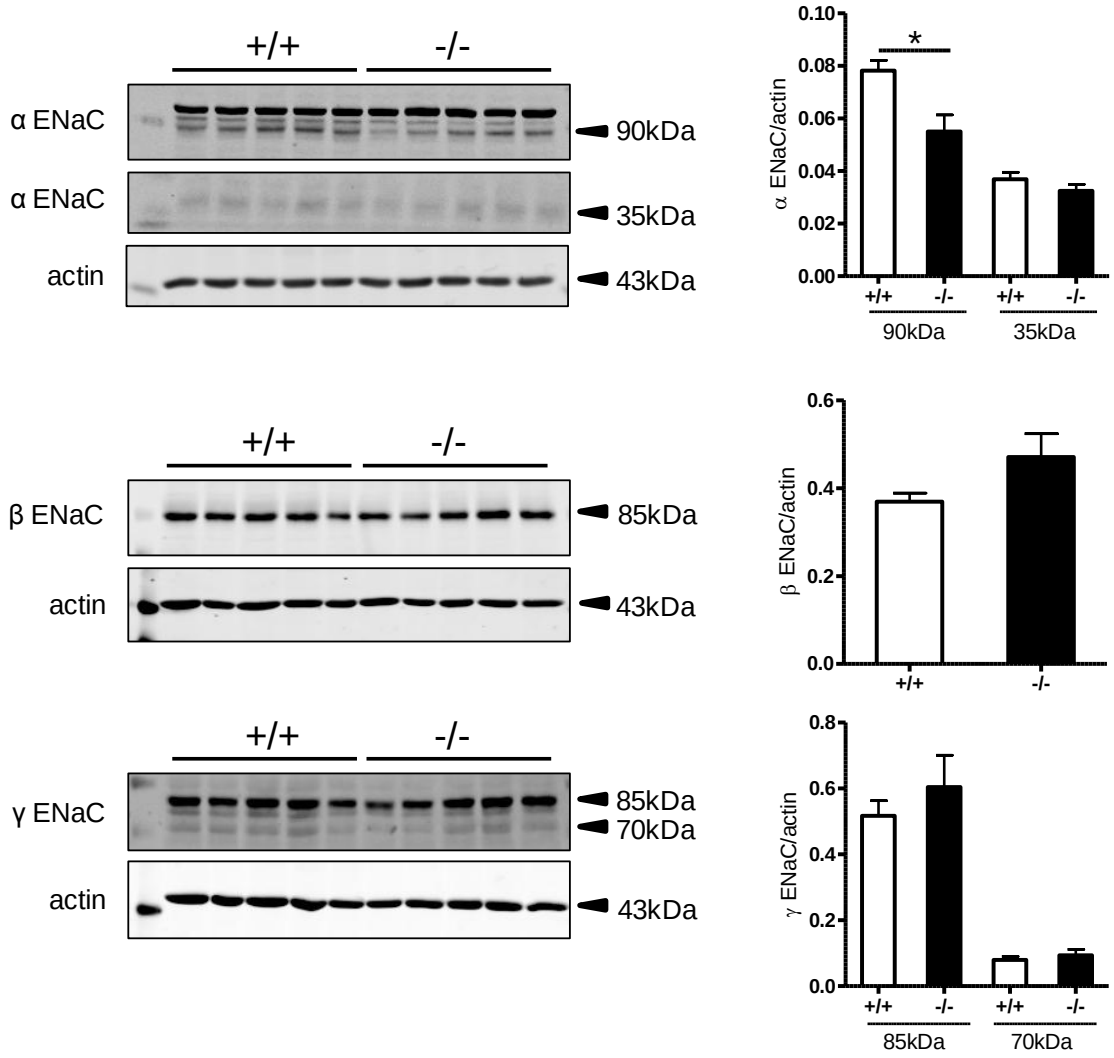

Figure 19. Protein abundance of ENaC in $AS^{+/+}$ and $AS^{-/-}$ mice on 0.8% K^+ (control) diet. Immunoblots for α-, β- and γ-ENaC subunit in total membrane fractions from mouse kidneys. All membranes were reprobed for β-actin and all data were normalized against β-actin. Bar graphs summarizing data from immunoblotting. n = 5 mice per group. +/+, wild type mice; -/-, aldosterone synthase-deficient mice. Values are mean ± SEM. * $p \leq 0.05$.

The physiological data suggested that the $AS^{-/-}$ mice are able to adapt to a moderate increases in dietary K^+ intake, but cannot stand a high dietary K^+ load (5% K^+). Therefore, we concentrated in the following experiments mainly on the 2% K^+ diet and elaborated in more detail the aldosterone-dependent and independent-mechanisms of the homeostatic adaptation of a dietary K^+ load.

First, we examined the regulation and expression of the ROMK in response to a dietary K^+ load. Immunoblotting showed no significant difference in protein abundance for the glycosylated and the non-glycosylated forms of ROMK on 2% K^+ diet. Immunostainings of kidney sections from 2% K^+ diet mice showed ROMK localized to the apical membrane in PCs of the DCT and CNT in $AS^{+/+}$ mice. Interestingly, in $AS^{-/-}$ mice, there was also apical localization of ROMK in the DCT and CNT with apparently stronger ROMK staining intensity compared to $AS^{+/+}$ mice (figure 20). We also checked for an altered expression of the BK channel at protein level by using an antibody against the α-subunit. The BK channel could be only detected in brain samples, but was not detectable in kidney samples (figure 21A). We also examined the mRNA expression of the BK channel β1, β2 and β4 subunits in kidneys from mice of both genotypes (figure 21B). All subunits were weakly expressed in the kidney and no significant differences in the mRNA expression of BK subunits were revealed between $AS^{+/+}$ and $AS^{-/-}$ mice.

To test for the protein abundance of ENaC after 2% K^+ diet loading, immunoblotting for the different ENaC subunits was done on total kidney proteins from $AS^{+/+}$ and $AS^{-/-}$ mice (figure 22A). Protein abundance for α-ENaC, both uncleaved (95 kDa) form and cleaved (30 kDa) form, was not significantly different between genotypes indicating maintained α-ENaC cleavage in $AS^{-/-}$ mice. Immunoblots for β-ENaC showed significantly increased protein abundance in $AS^{-/-}$ mice compared to $AS^{+/+}$ mice. Protein abundance for the uncleaved (85 kDa) form of γ-ENaC in $AS^{-/-}$ mice was significantly increased compared to $AS^{+/+}$ mice but did not reveal difference in protein abundance for the cleaved (70 kDa) form of γ-ENaC between the genotypes, again indicating maintained cleavage. These results suggest increased protein abundance for β- and γ- (85 kDa, uncleaved bands) ENaC and maintained α- and γ-ENaC cleavages in $AS^{-/-}$ mice.

Immunohistochemistry was used to determine whether the 2% K^+ diet altered the segmental and/or subcellular distribution of α-, β- and γ-subunits of ENaC in $AS^{-/-}$ and $AS^{+/+}$ mice (figure 22B). In the CNT, α-ENaC staining was localized to the apical membrane in $AS^{+/+}$ mice and, interestingly, also in $AS^{-/-}$ mice whereas in the CCD, α-ENaC was localized to the apical membrane in few cells in both genotypes. In $AS^{+/+}$ mice, β- and γ-ENaC staining was localized to the apical membrane in the CNT, whereas staining in the CCD was mostly cytoplasmic. Interestingly, in $AS^{-/-}$ mice, β- and γ-ENaC staining was mostly cytoplasmic in the CNT and CCD. Nevertheless, in parallel with the western blot results, the signal intensity of β- and γ-ENaC staining was stronger in $AS^{-/-}$ mice. Thus, $AS^{-/-}$ mice show an increased abundance of β- and γ-ENaC protein, but these ENaC subunits are mostly cytoplasmically localized. On 5% K^+ diet, ROMK was localized to the apical membrane both in $AS^{+/+}$ and $AS^{-/-}$ mice. In $AS^{+/+}$ mice β-ENaC was localized to the apical membrane but was mostly cytoplasmic in $AS^{-/-}$ mice (figure 24).

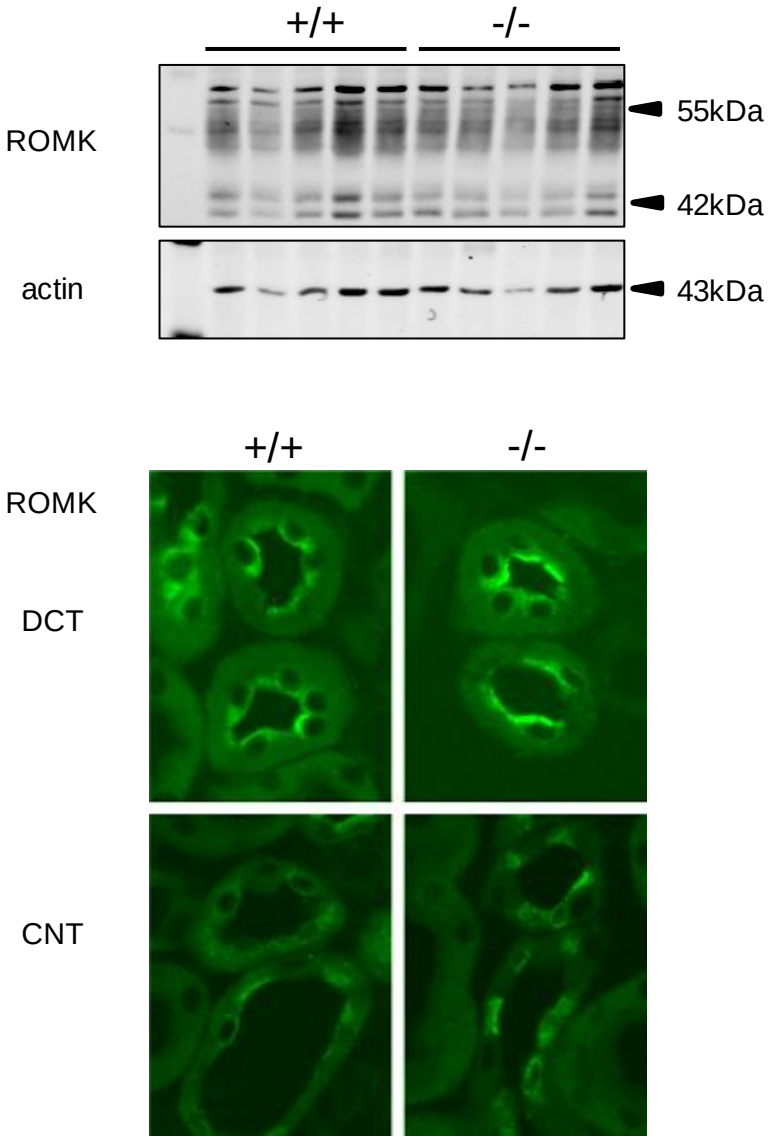

Figure 20. **Expression and subcellular distribution of the renal outer medullary potassium channel (ROMK) during 2% K^+ loading in mouse kidney.** (A) Immunoblotting for mature glycosylated (55 kDa) and core glycosylated (42 kDa) ROMK channel in total membrane fractions of kidneys. The membrane was reprobed for β-actin. n = 5 mice per group. (B) Immunolocalization of ROMK channels in distal convoluted tubule (DCT) and connecting tubule (CNT) in kidney sections. +/+, wild type mice; -/-, aldosterone synthase-deficient mice.

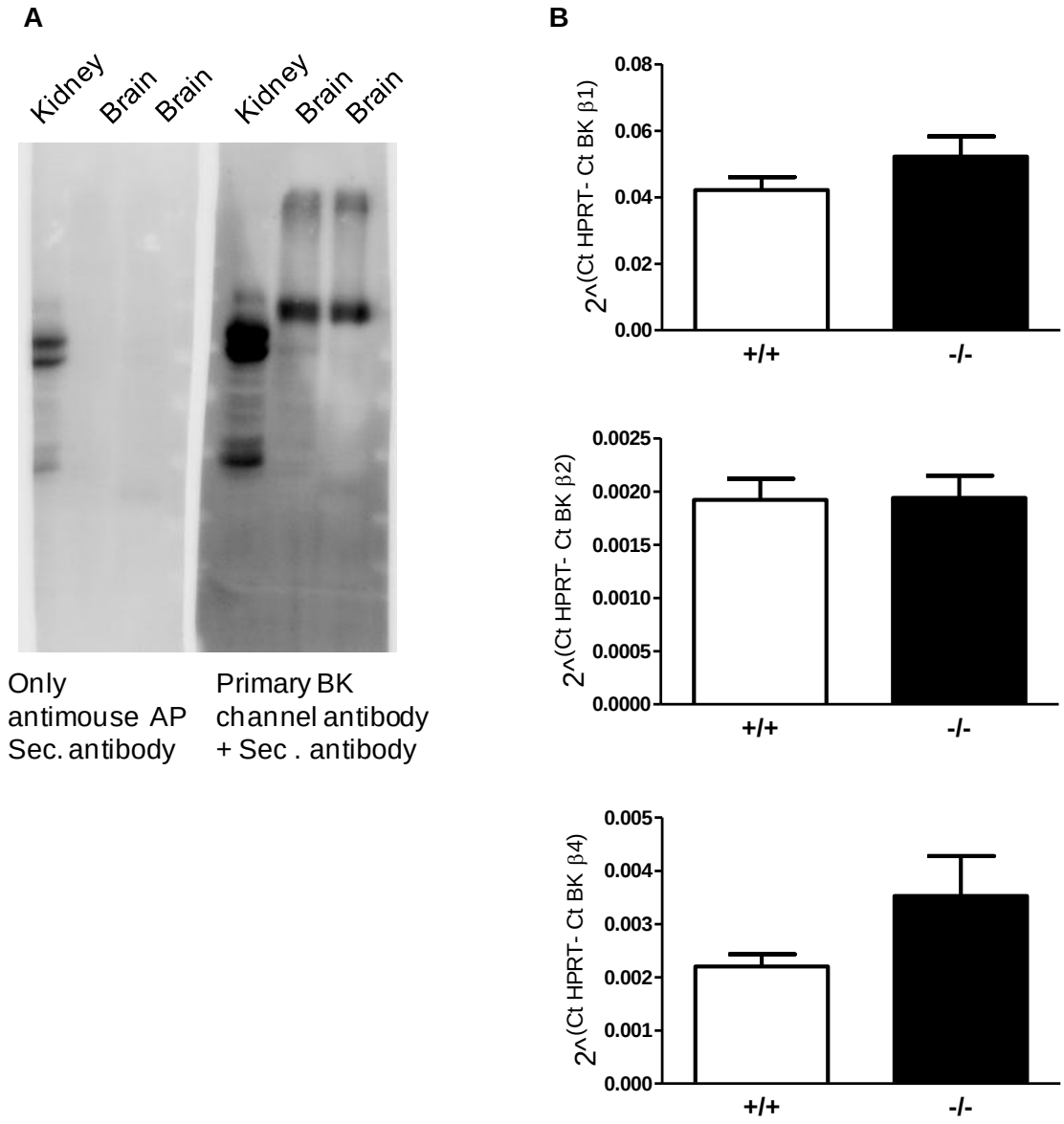

Figure 21. **Expression of Ca^+ activated large conductance K^+ channel (BK) channel during 2% K^+ loading.** (A) Immunoblotting for BK channel protein in total membrane fractions from mouse kidney and brain samples with or without primary antibody. (B) Real time PCR was used to assess the mRNA expressions of β1, β2 and β4 subunits of BK channel. n = 6 mice per group.

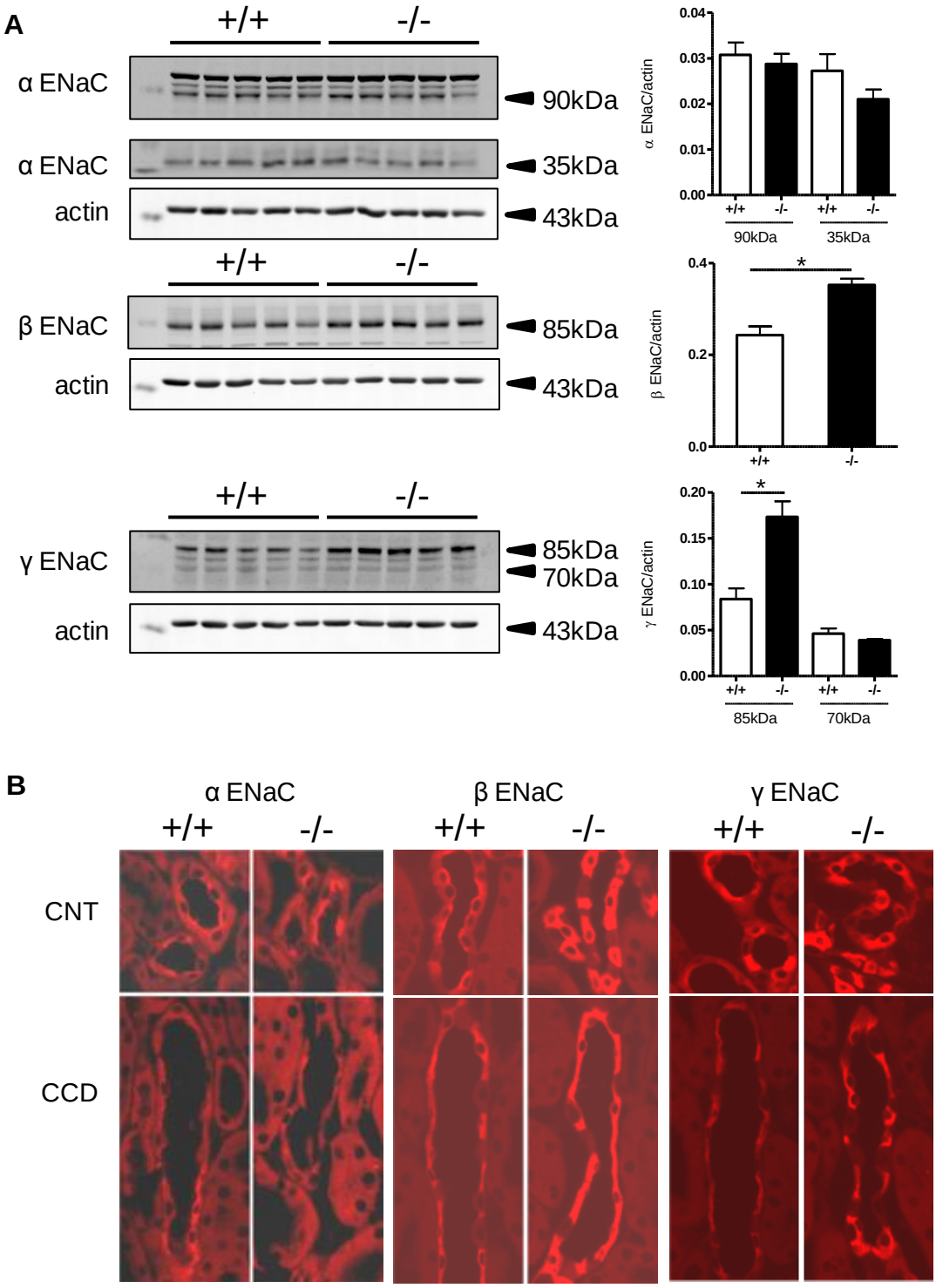

Figure 22. Expression and subcellular localization of the epithelial sodium channel (ENaC) during 2% K^+ loading in mouse kidney. (A) Immunoblotting for α-, β- and γ-ENaC subunits in total membrane fractions. All membranes were reprobed for β-actin and all data were normalized against β-actin. Bar graphs summarizing data from immunoblotting. n = 5 mice per group. (B) Immunolocalization of α-, β- and γ-ENaC subunits in the connecting tubule (CNT) and cortical collecting duct (CCD) in kidney sections. +/+, wild type mice; -/-, aldosterone synthase-deficient mice. Values are mean ± SEM. * $p \leq 0.05$.

On 5% K^+ diet (figure 23), α-ENaC protein abundance for the uncleaved (90 kDa) and cleaved (30 kDa) bands, was significantly lower in $AS^{-/-}$ than in $AS^{+/+}$ mice. No significant difference in protein abundance for the β-ENaC subunit was observed, whereas γ-ENaC protein abundance for the uncleaved (85 kDa) band was significantly increased and for the cleaved (70 kDa) band significantly decreased in $AS^{-/-}$ mice. ROMK protein abundance (glycosylated and nonglycosylated) was not different between the genotypes. These results indicate decreased ENaC cleavage in $AS^{-/-}$ after 5% K^+ loading.

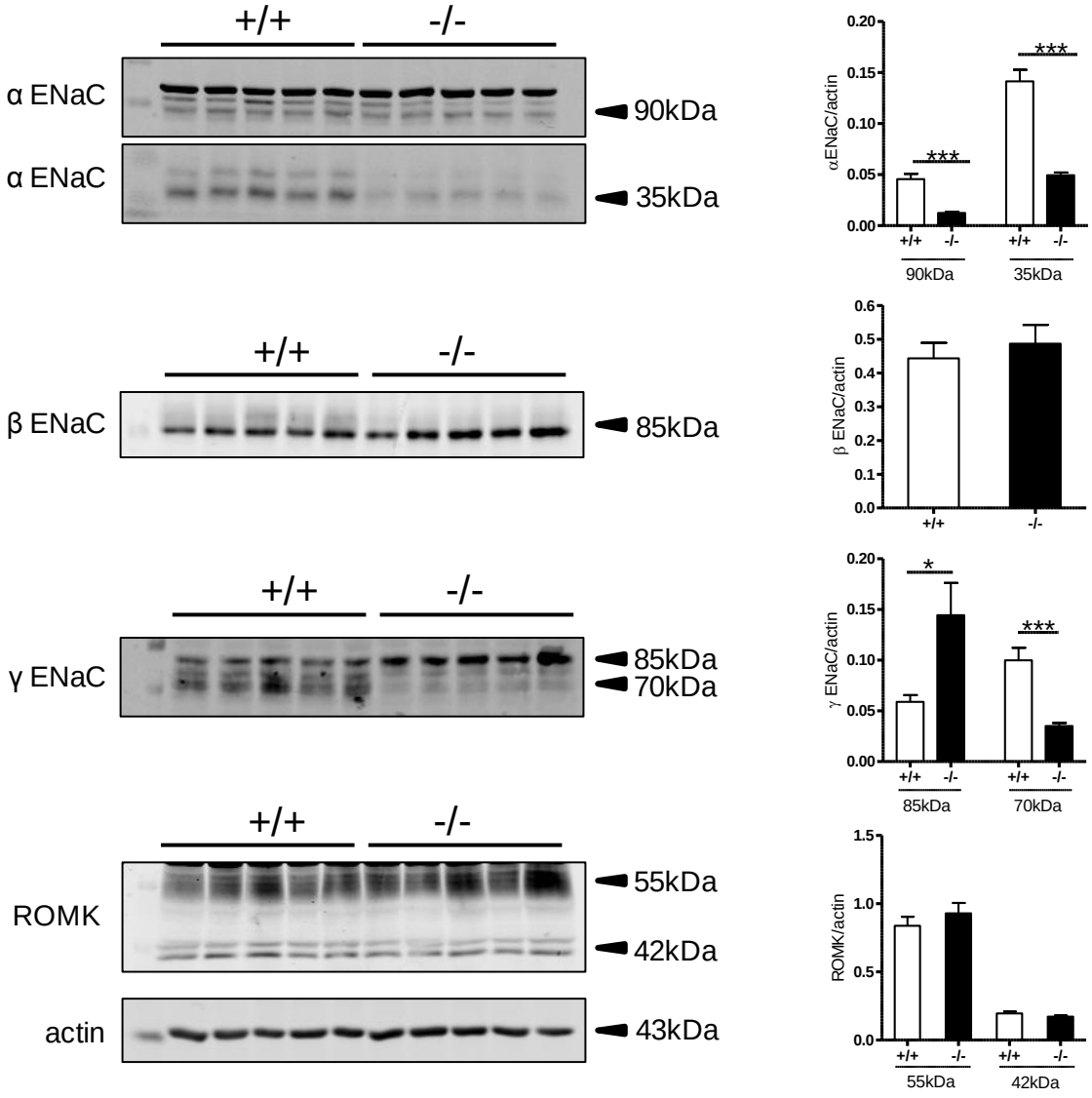

Figure 23. Expression of ENaC and ROMK in mouse kidneys during 5% K^+ loading. (A) Immunoblots for α-, β- and γ-ENaC subunits and ROMK in total membrane fractions from mouse kidneys. All membranes were reprobed for β-actin and all data were normalized against β-actin. Bar graphs summarizing data from immunoblotting. n = 5 mice per group. Values are mean ± SEM. * $p \leq 0.05$, *** $p \leq 0.001$.

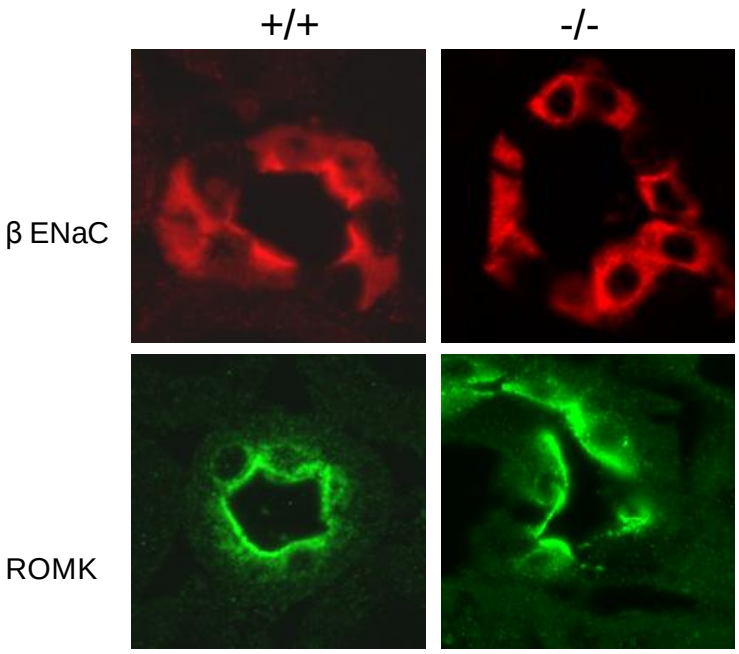

Figure 24. Subcellular distribution of ENaC and ROMK in mouse kidneys during 5% K^+ loading. Immunolocalization of β-ENaC and ROMK in mouse kidney sections. β-ENaC staining is mostly localized to apical membranes in wild type (+/+) mice whereas in aldosterone synthase-deficient mice (-/-) staining is mostly cytoplasmic. ROMK staining is localized to apical membranes in both +/+ and -/- mice.

4.1.3 Functional ENaC and apical localization of ENaC in the late DCT in $AS^{-/-}$ mice on 2% K^+ diet

To determine *in vivo* the functional activity of ENaC, mice were treated with amiloride, a specific blocker of ENaC. Urinary Na^+ excretion was significantly higher in the amiloride-treated group compared to vehicle-treated group in $AS^{+/+}$ mice as well as in $AS^{-/-}$ mice indicating active ENaC channels in both $AS^{+/+}$ and $AS^{-/-}$ mice (figure 25C). Furthermore, immunohistochemistry showed an apical localization of β- and γ-ENaC in the late DCT to but a mostly cytoplasmic localization of the channel in the CNT and CCD in $AS^{-/-}$ mice (figure 25A). These results indicate that in $AS^{-/-}$ mice, there may be functionally active ENaC channels in the kidney and they are mainly located in the late DCT. To further confirm the functional activity of ENaC in the late DCT, *ex vivo* patch clamping experiments were performed for ENaC (figure 25B) on isolated, split-open DCT2, CNT and CCD segments from $AS^{+/+}$ and $AS^{-/-}$ mice kept on 2% K^+ diet. Consistent with the results from immunohistochemistry, similar whole-cell-amiloride-sensitive-currents were observed in the early ASDN segments of $AS^{+/+}$ and $AS^{-/-}$ mice.

4.1.4 Impaired activation of colonic Na^+ and K^+ channels in $AS^{-/-}$ during 2% K^+ loading

We also examined if similar aldosterone-independent functional ENaC channels were present in distal colon. Barium-sensitive K^+ channel currents and amiloride-sensitive Na^+ channel currents (figure 26) were significantly increased in $AS^{+/+}$ mice after 4 days of 2 % K^+-loading, but absent in $AS^{-/-}$ mice. This indicates that aldosterone, unlike in the kidney, is essential for the regulation for ENaC in response to K^+-loading in the distal colon.

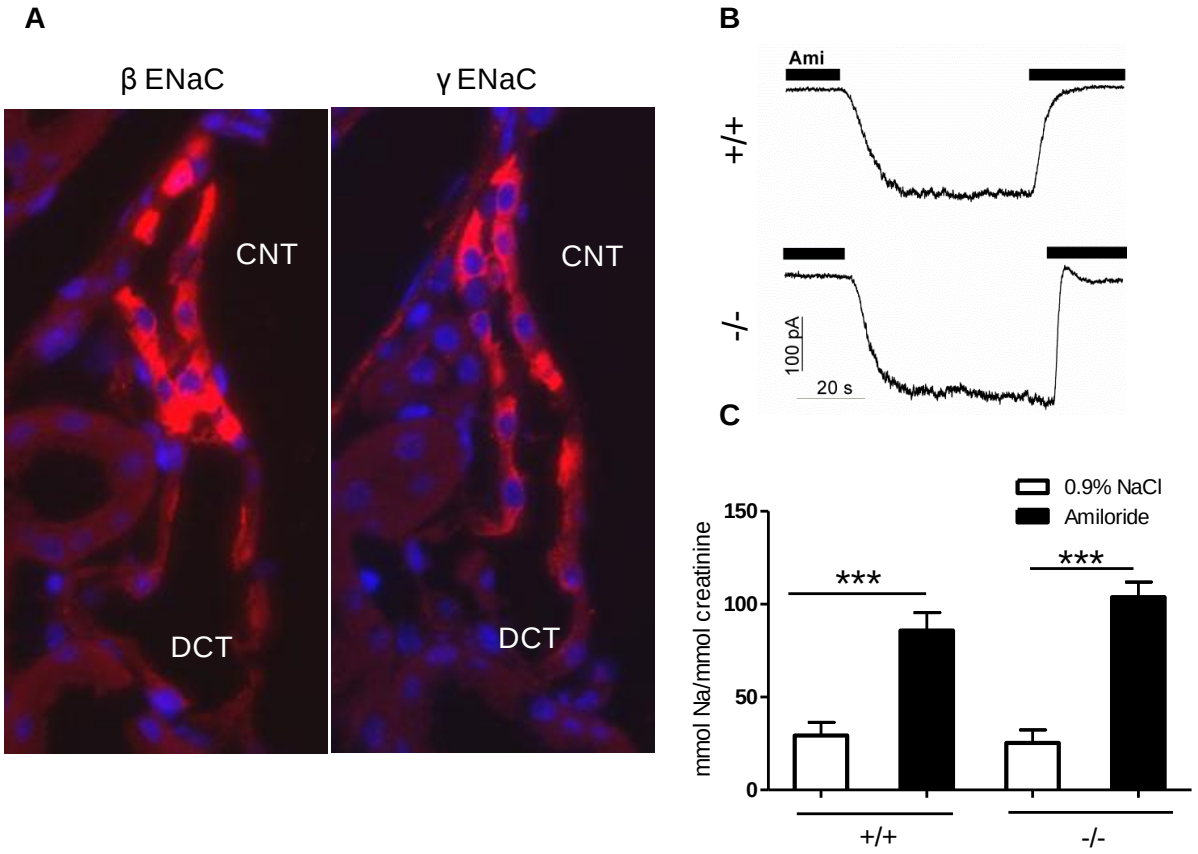

Figure 25. Functional activity and subcellular distribution of ENaC in kidney colon during 2% K^+ loading. (A) Immunolocalization of the ENaC β- and γ-subunits in the late distal convoluted tubule (DCT) and connecting tubule (CNT) in kidney sections from aldosterone synthase-deficient ($AS^{-/-}$) mice. (B) Amiloride sensitive whole cell Na^+ channel currents in the early aldosterone sensitive distal nephron (ASDN) from $AS^{+/+}$ and $AS^{-/-}$ mice on 2% K+ diet, n = 7-9 mice per group. (C) Urinary Na^+ excretion after 4 h of vehicle or amiloride injection. N = 8-11. Values are mean ± SEM. *** $p \leq 0.001$.

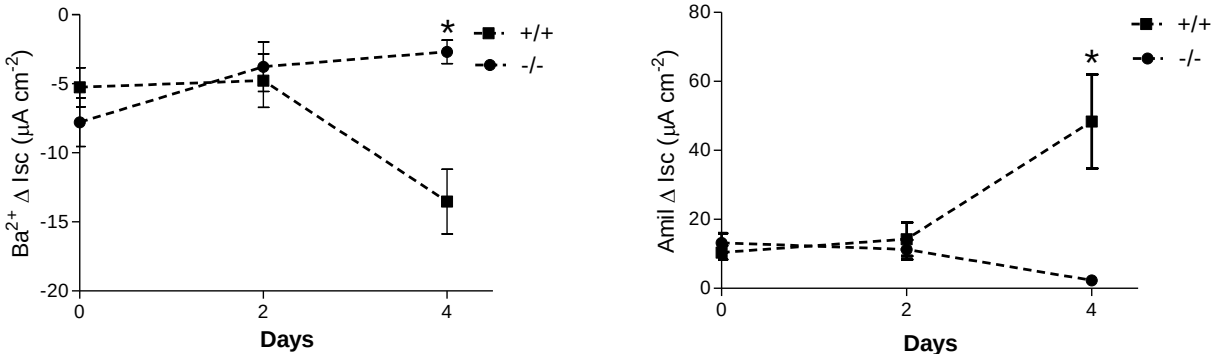

Figure 26. Functional activity of ENaC and BK channel in distal colon during 2% K^+ loading. Ussing chamber recordings of barium sensitive K+ channel and amiloride sensitive Na+ channel currents in the distal colon. N = 5-6 mice per group. Values are mean ± SEM. * $p \leq 0.05$.

4.1.5 Role of angiotensin II in $AS^{-/-}$ mice

Mice were treated with losartan, an antagonist for the angiotensin type 1 receptor (AT1R) to get insights in the role of angiotensin II for the rather compensated phenotype of $AS^{-/-}$ mice, which is evident even on a high K^+ (2% K^+) diet. Food intake was significantly decreased in losartan treated $AS^{-/-}$ mice compared to vehicle treated $AS^{-/-}$ animals (3.1 ± 0.4 g vs. 5.5 ± 0.2 g, P = 0.0015) indicating food avoidance after losartan treatment, whereas no difference in food intake was observed in losartan vs. vehicle treated $AS^{+/+}$ mice (5.5 ± 0.6 g vs. 5.3 ± 0.2 g, P = 0.8). No significant difference was seen in water intake in losartan vs. vehicle treated $AS^{-/-}$ mice (2.6 ± 0.3 ml vs. 2.2 ± 0.2 ml, P= 0.4) as well as in $AS^{+/+}$ mice (1.4 ± 0.1 ml vs. 1.0 ± 0.1 ml, P = 0.06). Urinary Na^+ excretion was significantly decreased in losartan-treated $AS^{-/-}$ mice compared to vehicle-treated animals. K^+ excretion in urine was also significantly decreased in the losartan-treated $AS^{-/-}$ mice. In contrast, no significant difference in urinary Na^+ and K^+ excretion was observed in losartan treated vs. vehicle treated $AS^{+/+}$ mice (figure 27A). Hyponatremia was seen in the losartan treated $AS^{-/-}$ mice as shown by significantly decreased plasma Na^+ concentration compared to vehicle treated mice. Interestingly, losartan treated $AS^{-/-}$ mice were hyperkalemic as shown by significantly higher plasma K^+ concentrations compared to vehicle treatment (figure 27B). Immunohistochemistry showed apical localization of βENaC in vehicle-treated mice but mostly cytoplasmic after losartan treatment in kidney sections from $AS^{-/-}$ mice (figure 27C).

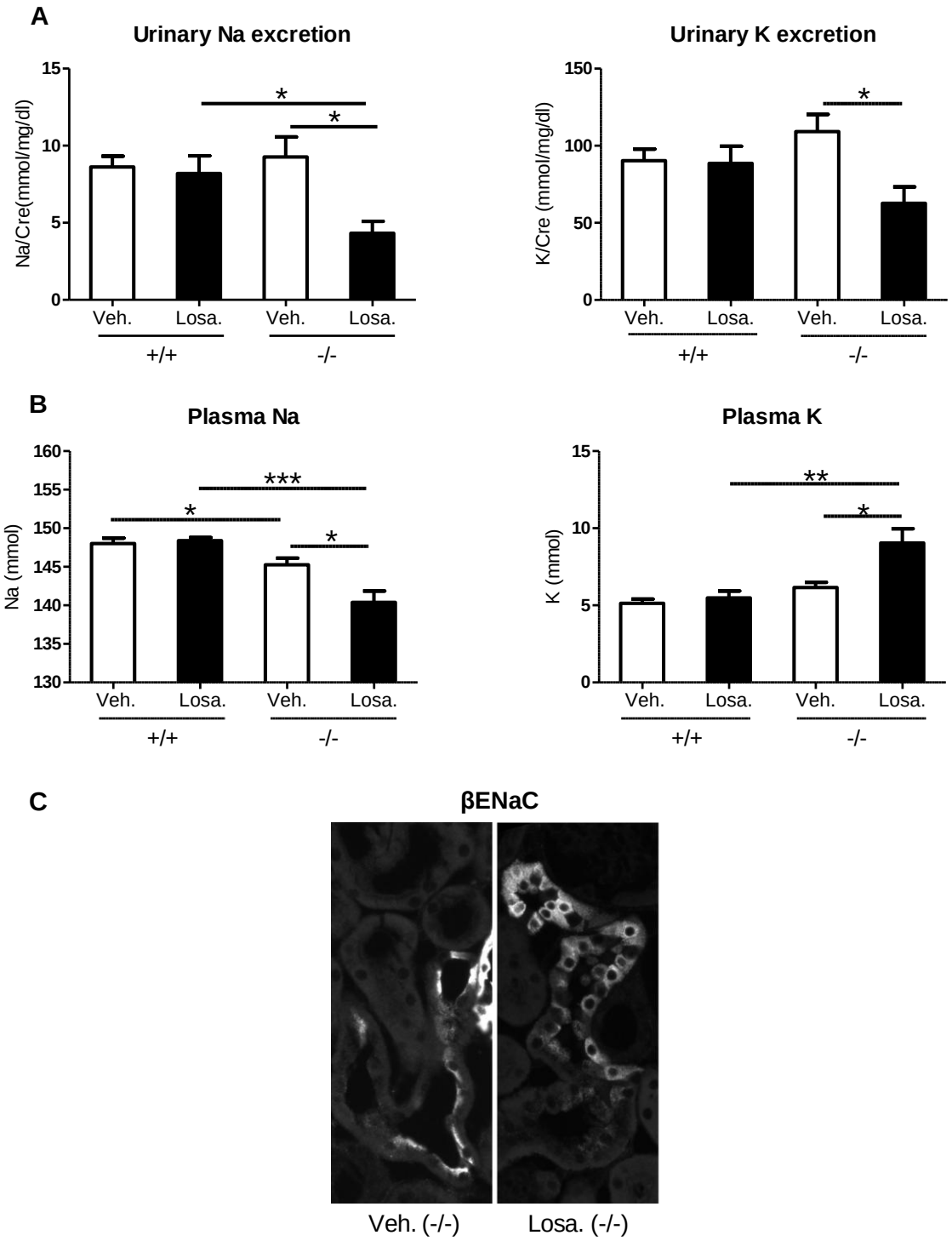

Figure 27. Effect of angiotensin type 1 receptor (AT_1R) inhibition by losartan during 2% K^+ loading on Na^+ and K^+ concentrations in blood and urine. (A) Urinary Na^+ and K^+ excretion in mice after 13 h of vehicle or losartan treatment. (B) Blood Na^+ and K^+ concentrations in mice after 13 h of vehicle or losartan treatment. n = 5, losartan group; n = 4, vehicle group. (C) Immunolocalization of the β-ENaC subunit in the early ASDN from vehicle and losartan treated mice. +/+, wild type mice; -/-, aldosterone synthase-deficient mice. Values are mean ± SEM. * $p \leq 0.05$, ** $p \leq 0.01$, *** $p \leq 0.001$.

4.1.6 Decreased sodium chloride co-transporter (NCC) protein expression and activity in $AS^{-/-}$ mice on 2% K^+ diet

Next, we tested the expression and functional activity of NCC as the Na^+ reabsorption by NCC along the DCT may affect or modulate the Na^+ and K^+ transport systems in further downstream nephron portions. The results from qPCR showed no significant difference in NCC mRNA expression between the genotypes (figure 28A). In contrast, immunoblots, for total NCC and for phospho-specific forms of NCC, namely phosphothreonine 53 (pT53), phosphothreonine 58 (pT58) and phosphoserine 89 (pS89), showed significant decreases in NCC protein abundance and phosphorylation in $AS^{-/-}$ mice compared to $AS^{+/+}$ (figure 28B).

To assess the in-vivo functional relevance of the reduced NCC abundance and phosphorylation, mice were injected either with DMSO as vehicle or with the diuretic hydrochlorothiazide to inhibit NCC. Urine was collected and analyzed for ion excretion. Urinary Na^+ excretion was significantly higher in hydrochlorothiazide treated vs. DMSO treated $AS^{+/+}$ mice as well as in $AS^{-/-}$ mice, but in line with the immunoblot results, urinary Na^+ excretion in hydrochlorothiazide-treated $AS^{-/-}$ mice was significantly lower than in hydrochlorothiazide-treated $AS^{+/+}$ mice (figure 28C).

4.1.7 Similar deoxycoticosterone levels in $AS^{-/-}$ mice on control and 2% K^+ diet

To check for the possibility that increased deoxycorticosterone levels in $AS^{-/-}$ mice might activate the MR, 11-deoxycorticosterone levels were measured in urine samples (figure 29). No significant difference in the concentration of 11-deoxycorticosterone levels was observed on control diet between $AS^{+/+}$ and $AS^{-/-}$ mice. During 2% K^+ diet 11-deoxycorticosterone levels were significantly decreased in $AS^{+/+}$ mice compared to $AS^{-/-}$ mice. The 11-deoxycorticosterone levels were not significantly different in $AS^{-/-}$ mice on control and 2% K^+ diet.

4.1.8 $AS^{-/-}$ mice can concentrate urine similar to $AS^{+/+}$ mice

$AS^{-/-}$ mice excrete more urine than $AS^{+/+}$ mice. Therefore we checked for protein abundance and subcellular localization of AQP2 in kidneys. In $AS^{+/+}$ mice, AQP2 is localized to the apical membrane whereas in $AS^{-/-}$ AQP2 is mostly cytoplasmic (figure 30A). Protein abundance for AQP2 was increased in $AS^{-/-}$ mice as seen in

immunoblots (figure 30B). Urine osmolarity was significantly increased in $AS^{+/+}$ as well as in $AS^{-/-}$ after DDAVP treatment (figure 30C). The plasma Na^{+} levels were significantly decreased in $AS^{+/+}$ and $AS^{-/-}$ mice after DDAVP treatment. In contrast, no significant change in levels of plasma K^{+} was seen in $AS^{+/+}$ and $AS^{-/-}$ mice after DDAVP treatment.

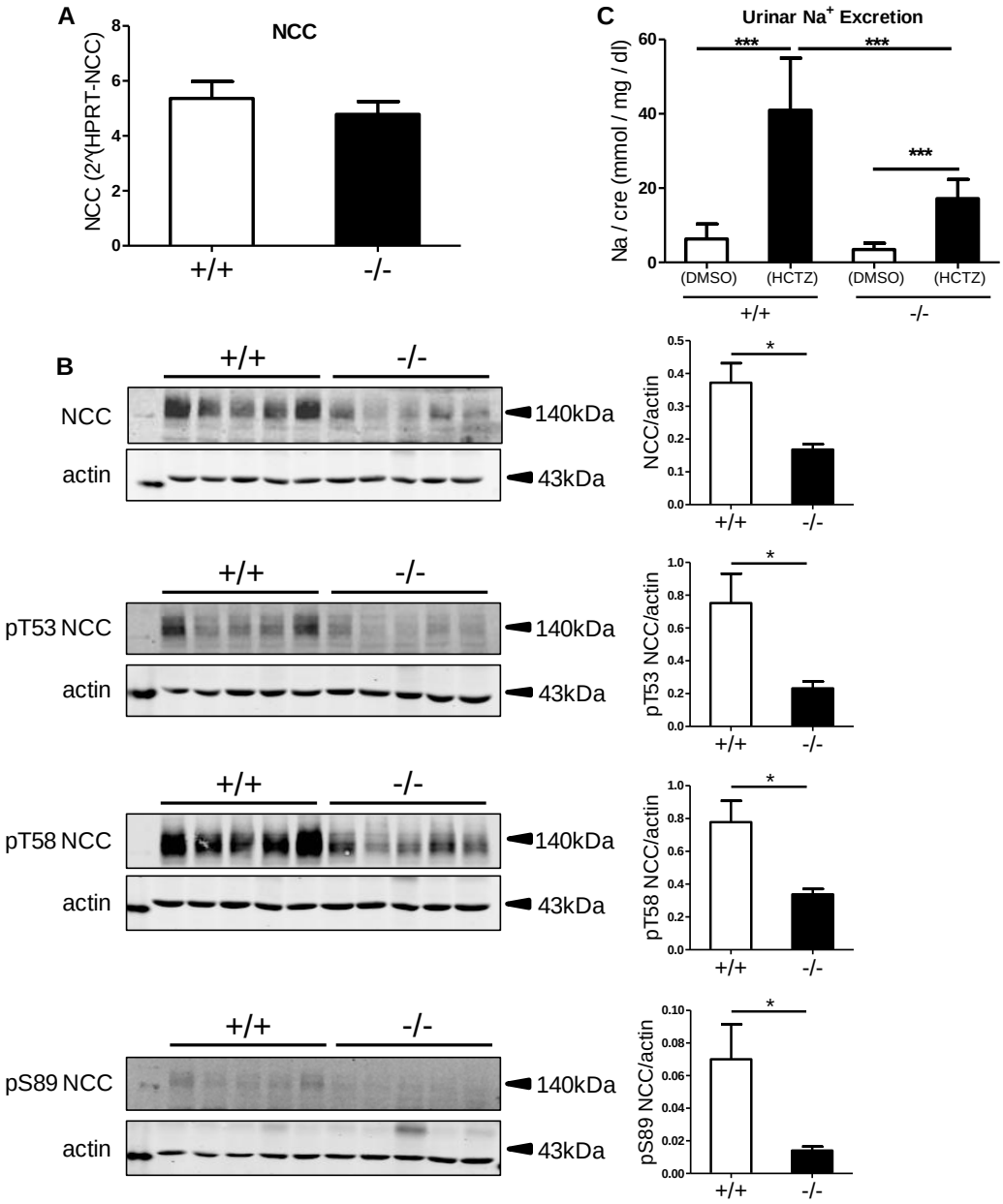

Figure 28. Expression and *in vivo* functional activity of the sodium chloride co-transporter (NCC) in mouse kidneys during 2% K^+ loading. (A) Real-time RT-PCR was used to assess NCC mRNA levels in mouse kidneys. n = 7 mice per group. (B) Immunoblotting for total NCC and phosphorylated forms of NCC at residues threonine 53 (pT53 NCC), threonine 58 (pT58 NCC) and serine 89 (pS89 NCC) normalized against β-actin in total membrane fractions from mouse kidneys. Bar graphs summarizing data from immunoblotting. n = 5 mice per group. (C) Urinary Na^+ excretion after 4 h of dimethylsulfoxide (DMSO, vehicle) or hydrochlorthiazide (HCTZ) treatment. n = 8, DMSO +/+ group; n = 9 for +/+ HCTZ, -/- DMSO and HCTZ group. Values are mean ± SEM. * $p \leq 0.05$, *** $p \leq 0.001$.

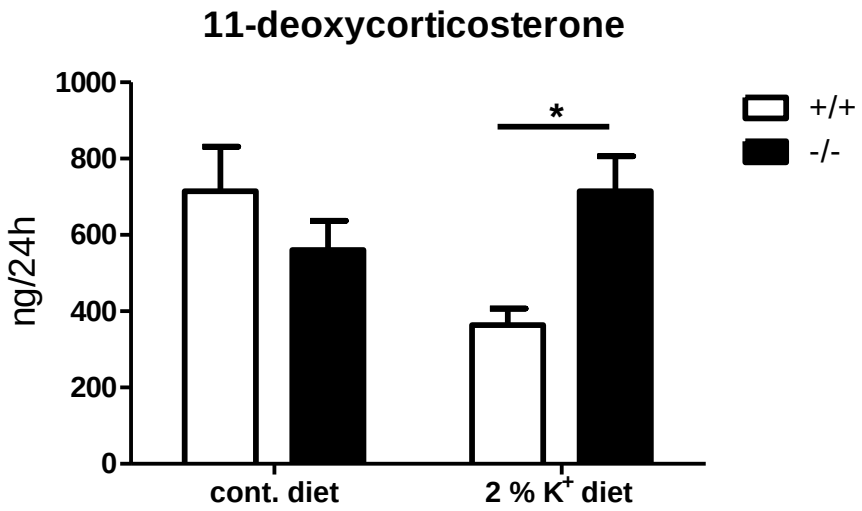

Figure 29. Concentration of 11- deoxycoticosterone in urine samples from $AS^{+/+}$ and $AS^{-/-}$ mice. Control diet n = 5 for each group; 2% K^+ diet n = 4 for $AS^{+/+}$ mice and n = 7 for $AS^{-/-}$ mice. Values are mean ± SEM. * $p \leq 0.05$.

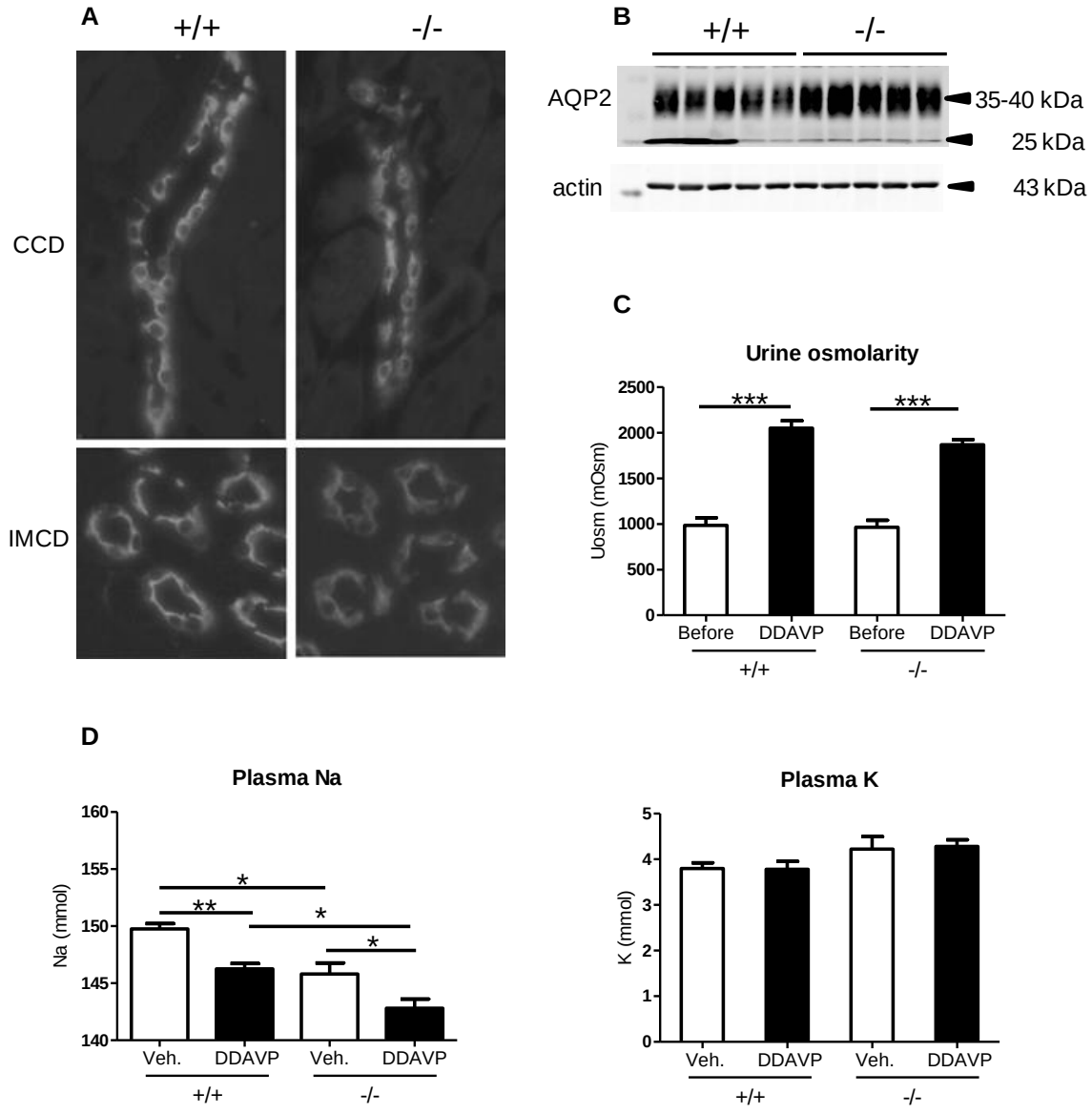

Figure 30. Expression and subcellular distribution of aquaporin 2 (AQP2) water channel and its response to desmopressin (1-deamino-8-D-arginine vasopressin (DDAVP)) treatment on 2% K^+ loading. (A) Immunolocalization of AQP2 water channel in cortical collecting duct (CCD) and inner medullary collecting duct (IMCD) in kidney sections from mice. (B) Immunoblot of AQP2 protein and β-actin as a loading control showing protein abundance in total membrane fractions from whole kidneys. (C) Urine was collected before and 4 h after DDAVP treatment from mice on 2% K diet and osmolarity was measured. Urinary osmolarity is increased in both +/+ and -/- mice after DDAVP treatment. n = 5 mice per group (D) Blood Na^+ and K^+ concentration after 4 h of vehicle or DDAVP treatment. Lower blood Na^+ concentration in DDAVP treated mice compared to vehicle group and unchanged K^+ concentration. n = 5 mice per group. Values are mean ± SEM. * $p \leq 0.05$, ** $p \leq 0.01$, *** $p \leq 0.001$.

4.2. Role of aldosterone in pregnancy

4.2.1 Absence of a maternal preeclamptic phenotype in $AS^{-/-}$ mice during pregnancy

To test the hypothesis that aldosterone deficiency during pregnancy may contribute to the pathogenesis of pre-eclampsia, we measured SBP and urinary protein excretion in $AS^{+/+}$ and $AS^{-/-}$ dams before and during pregnancy. In order to eliminate the genotype of the fetuses as confounding factor, $AS^{+/+}$ females were mated to $AS^{-/-}$ males and $AS^{-/-}$ females to $AS^{+/+}$ males producing only $AS^{+/-}$ offspring. Before and during pregnancy, SBP was significantly higher in $AS^{+/+}$ than in $AS^{-/-}$ dams (figure 31A). While blood pressure of $AS^{+/+}$ remained constant at about 110 mmHg throughout pregnancy, SBP in $AS^{-/-}$ dams decreased from about 105 mmHg at day 1 to about 90 mmHg at day 21. Importantly, there was no difference in urinary protein excretion and no increase in $AS^{+/+}$ and $AS^{-/-}$ mice during pregnancy (figure 31B). Thus, $AS^{-/-}$ dams did not become hypertensive and did not develop proteinuria during pregnancy.

4.2.2 Presence of a feto-placental phenotype in $AS^{-/-}$ mice on control diet

Mean litter size at birth was lowered in $AS^{-/-}$ dams compared to $AS^{+/+}$ mice (3.0 ± 0.55 vs. 6.22 ± 0.66, respectively; $p<0.005$) representing a strong fetal phenotype (figure 31C). To examine whether the reduced litter size at birth was due to intrauterine death of fetuses, dams were sacrificed on gestational day 18 (E18) and the number and weight of fetuses and placentas were measured. The mean litter size was again smaller in $AS^{-/-}$ compared to $AS^{+/+}$ dams (2.67 ± 0.54 vs. 7.13 ± 0.48, respectively; $p<0.0001$) (Figure 26A). The reduction of the number of pups paralleled the presence of dark and necrotic placentas in $AS^{-/-}$ mice (figures 32A and 32B). Necrotic placentas were mostly observed in series next to each other but sometimes also observed interspersed between healthy placentas. Necrotic placentas were not seen in any $AS^{+/+}$ dams on control diet.

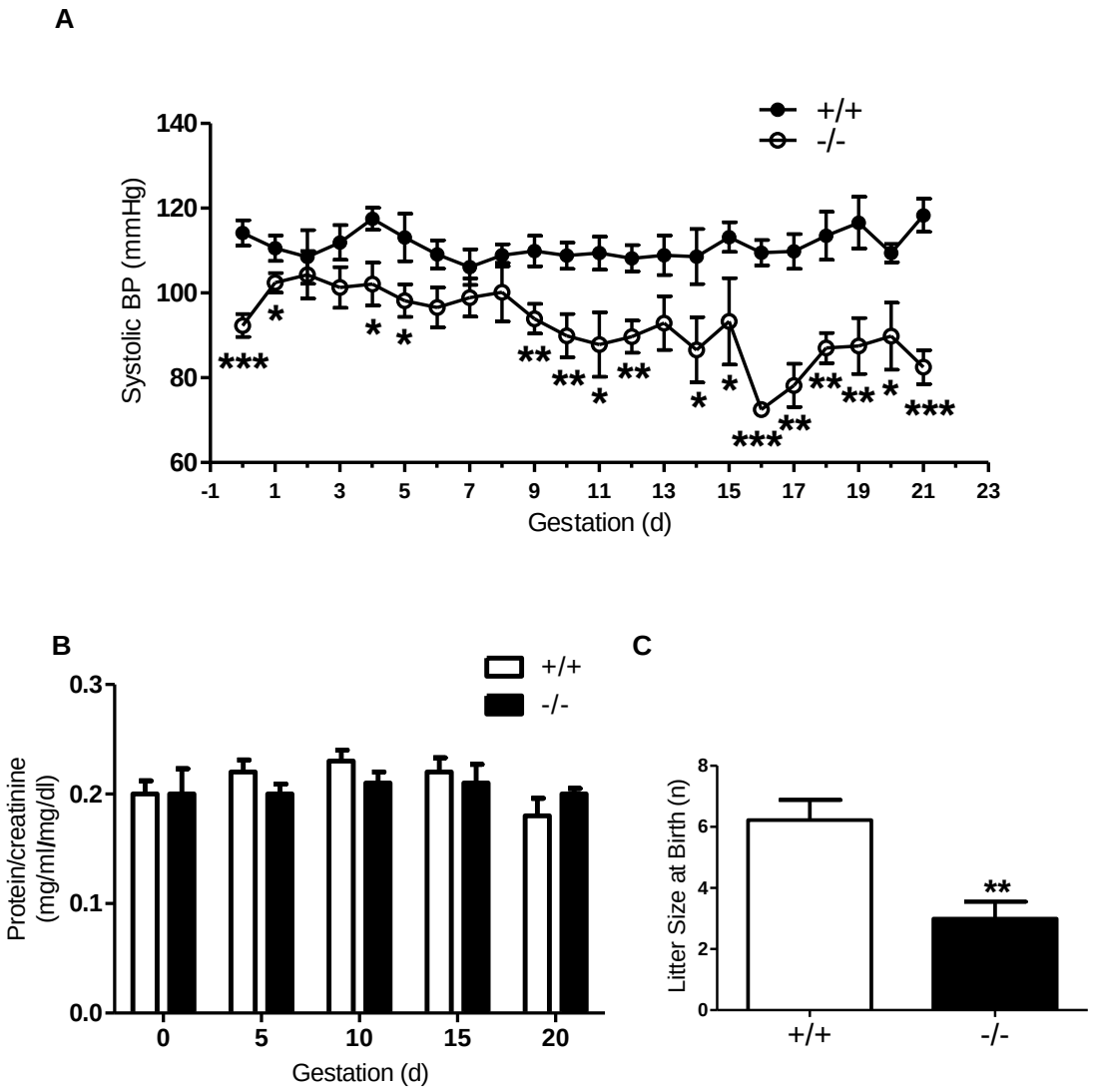

Figure 31. Systolic blood pressure, proteinuria and litter size on control diet. (A) Systolic blood pressure measured during the course of pregnancy from day 0 to day 21 in $AS^{+/+}$ (n = 6-9 animals/time point) and $AS^{-/-}$ (n = 3-9 animals/time point) dams. (B) Urine protein concentration normalized to creatinine measured from spot urine during pregnancy in $AS^{+/+}$ (n = 3) and $AS^{-/-}$ dams (n = 6). (C.) Number of pups counted on the day of delivery in $AS^{+/+}$ (n = 9) and $AS^{-/-}$ (n = 9) dams. Values are mean ± SEM. **P* < 0.05, ***P* < 0.005, ****P* < 0.001 *vs.* $AS^{+/+}$.

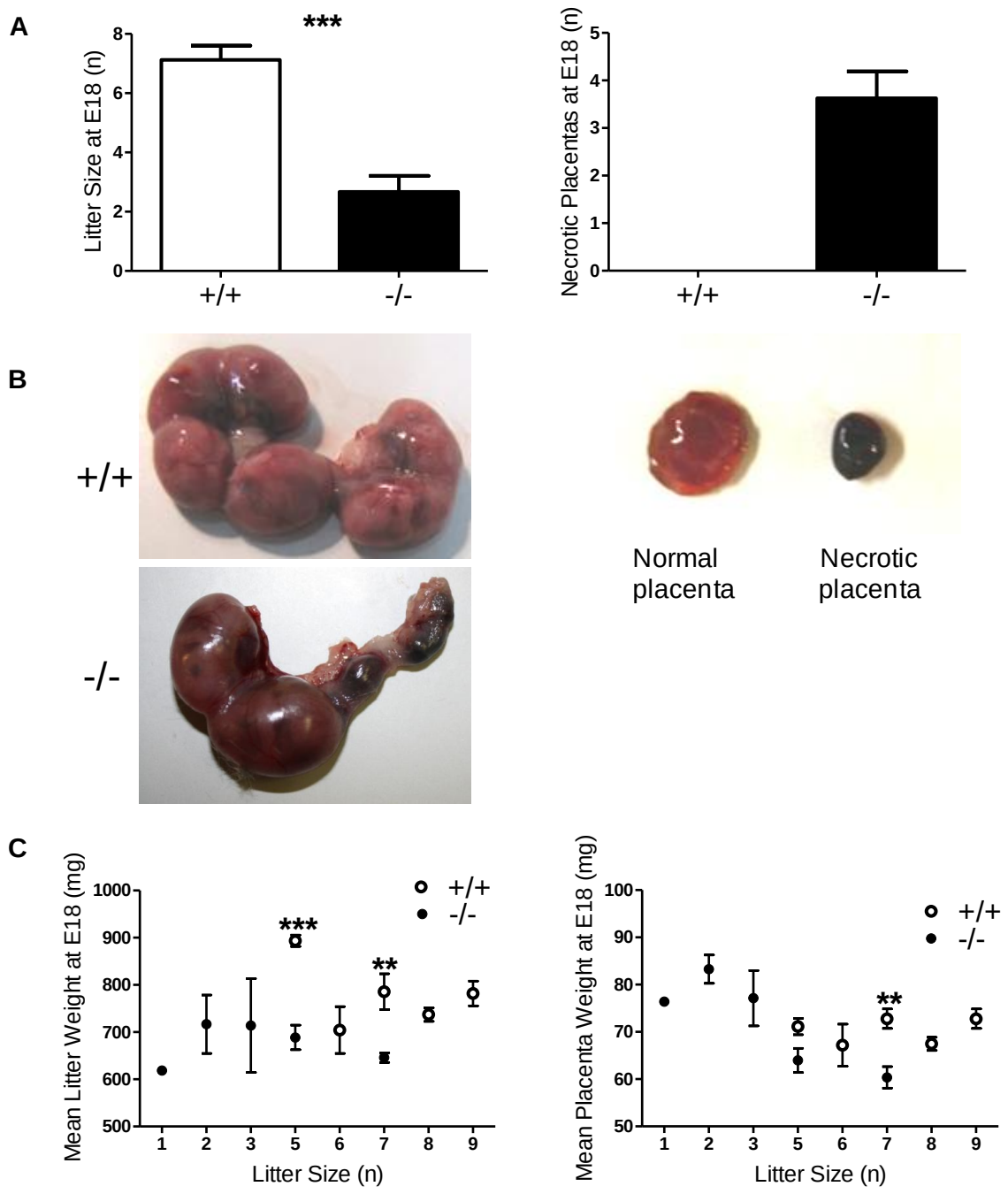

Figure 32. Litter size, litter and placenta weights, and healthy and necrotic placentas in $AS^{+/+}$ and $AS^{-/-}$ dams on day 18 of pregnancy. (A) Number of fetuses and necrotic placentas were counted in the uterus from $AS^{+/+}$ (n = total number of fetuses and placentas from 8 females) and $AS^{-/-}$ dams (n = total number of fetuses and placentas from 15 females). (B) Photos of fetuses and placentas in the uterus from $AS^{+/+}$ and $AS^{-/-}$ dams and comparison of healthy and necrotic placenta. (C) Mean litter and mean placenta weight vs. litter size in $AS^{+/+}$ (n = 8 litters) and $AS^{-/-}$ dams (n = 12 litters). Values are mean ± SEM. $^{**}P < 0.005$, $^{***}P < 0.001$ *vs.* $AS^{+/+}$.

When the mean litter and placenta weights were plotted against litter sizes (figure 32C), it became evident that the data for the $AS^{-/-}$ mice were not only shifted to smaller litter sizes but also to reduced litter and placenta weights. This is most evident when litters of the same sizes in $AS^{-/-}$ and in $AS^{+/+}$ are compared (i.e. litter sizes of 5 and 7 pups in figure 32C). In contrast, in very small litters (n = 1-3), placental weight appeared to be normal. Histological examination of the placentas further confirmed the reduced size of placentas in $AS^{-/-}$ dams, but did also reveal that most of the placentas were otherwise healthy with a similar structural organization of decidua basalis, junctional zone, and labyrinth as in $AS^{+/+}$ dams (figure 33A and 33B, left and middle section). Only dark placentas from $AS^{-/-}$ dams showed severe coagulative necrosis with lymphocyte infiltrations in all three layers of the placenta (figure 33A and B, right section).

4.2.3 High salt diet does not increase intrauterine survival, but improves fetal growth in $AS^{-/-}$ mice and lowered systolic blood pressure irrespective of the presence of aldosterone

Based on the assumption that aldosterone deficiency in $AS^{-/-}$ mice might compromise placental perfusion, we tested if replacing renal sodium losses by feeding a high salt diet (5% NaCl) before and during pregnancy improve the SBP, the weight of placentas and of pups, and the litter sizes. $AS^{+/+}$ and $AS^{-/-}$ females were fed a high salt diet starting 12 days before until the end of pregnancy. After 4 days on a high salt diet, the SBP rose in both groups of mice, but this increase occurred in parallel and hence $AS^{-/-}$ female mice continued to have lower SBP than $AS^{+/+}$ female mice (figure 34A). During the first days (days 5-7) of pregnancy, the SBP dropped significantly in both $AS^{+/+}$ and $AS^{-/-}$ dams, but the decrease of SBP was much more pronounced in $AS^{+/+}$ mice than in $AS^{-/-}$ mice. Therefore, the BP difference between genotypes became very small (days 5-7) and was no longer significant on days 15 to 17. This is in contrast to the measurements in dams on standard chow, where a significant difference in SBP was maintained throughout the entire pregnancy (figure 31A). In $AS^{-/-}$, blood pressure lower towards the end of gestation irrespective of the salt intake (figure 34B). In $AS^{+/+}$ mice, the SBP did not drop significantly in pregnancy on a normal salt diet. However, if a high salt diet was provided, the blood pressure dropped reaching the lowest levels at the end of pregnancy (figure 34C).

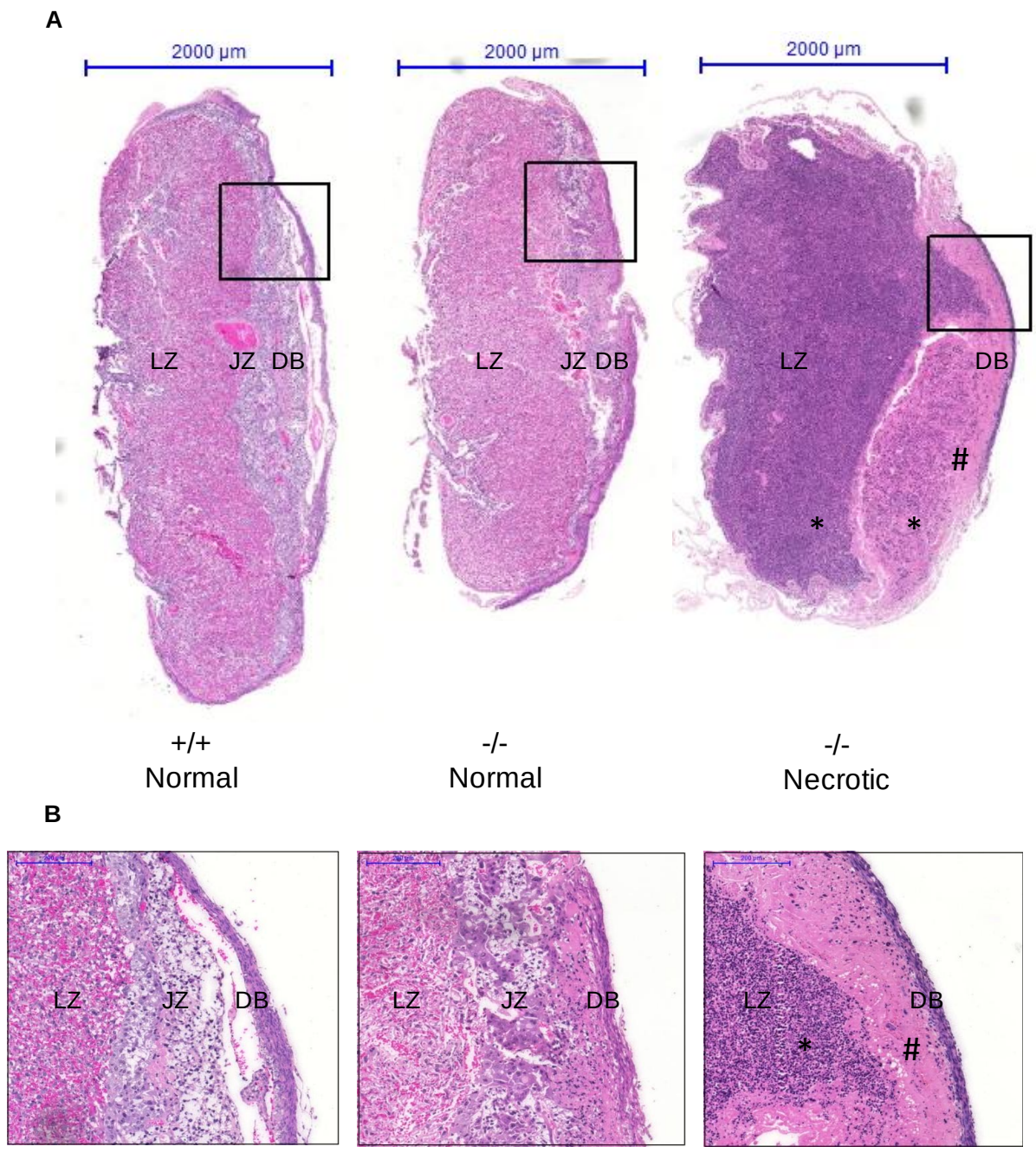

Figure 33. Histology of placentas. (A) Cross section and H&E stain of a placenta from an $AS^{+/+}$ dam and healthy and necrotic placentas from $AS^{-/-}$ dams. (B) Enlarged section of the part of healthy placenta. (C) Enlarged section of the part of the necrotic placenta. Bar = 2000 µM. DB = decidua basalis, JZ = junctional zone and LZ = labyrinth zone. * indicates lymphocyte infiltration and # indicates coagulative necrosis.

Of interest, both a low and a high volume state led to a blood pressure reduction in pregnancy with the latter being even more consistently throughout pregnancy.

The high Na^+ diet did neither increase the mean litter size nor decrease the number of necrotic placentas in $AS^{-/-}$ dams (figure 35A). However, the mean weights of litters and placentas were no longer different between the genotypes when litters of the same sizes were compared (figure 35B). This contrasts with the standard salt intake, when both mean litter and placenta weights were smaller in $AS^{-/-}$ than in $AS^{+/+}$ dams (figure 32C). Thus high salt intake does not increase the survival rate of fetuses, but appears to improve the intrauterine growth of the surviving pups.

The beneficial effect of a high salt intake was seen for both genotypes. Although the 5% NaCl intake did not increase the mean placental weight, it significantly improved the weight of the fetuses in $AS^{+/+}$ and $AS^{-/-}$ dams (figure 36A and 36B). Consistent to these differential effects on fetal and placental growth, placental efficiency (ratio of fetal weight over placental weight) was significantly increased in both $AS^{+/+}$ and $AS^{-/-}$ dams on high salt diet compared to control diet (figure 36C). Interestingly, placental efficiency was not significantly different between $AS^{+/+}$ and $AS^{-/-}$ dams, neither on control nor on high salt diet (figure 36C).

4.2.4 Expression of the hypoxia inducible factor HIF1α in the placenta

Pre-eclampsia is associated with altered expression of key anti- and pro-angiogenic factors [109]. We did not detect any differences in the mRNA expression of HIF1α (figure 37A), VEGF (figure 37B), and sFlt (figure 37C) between healthy appearing placentas from $AS^{+/+}$ and $AS^{-/-}$ dams kept on either a control or a high salt diet. Since HIF1α is mostly regulated at the post-translational level by stabilisation and degradation of the protein, we performed immunoblots. HIF1α protein abundance was significantly increased in healthy placentas from $AS^{-/-}$ dams on control diet (figure 39A). This difference disappeared on high salt diet (figure 33B). HIF1α protein was not detected in necrotic placentas (figure 39A).

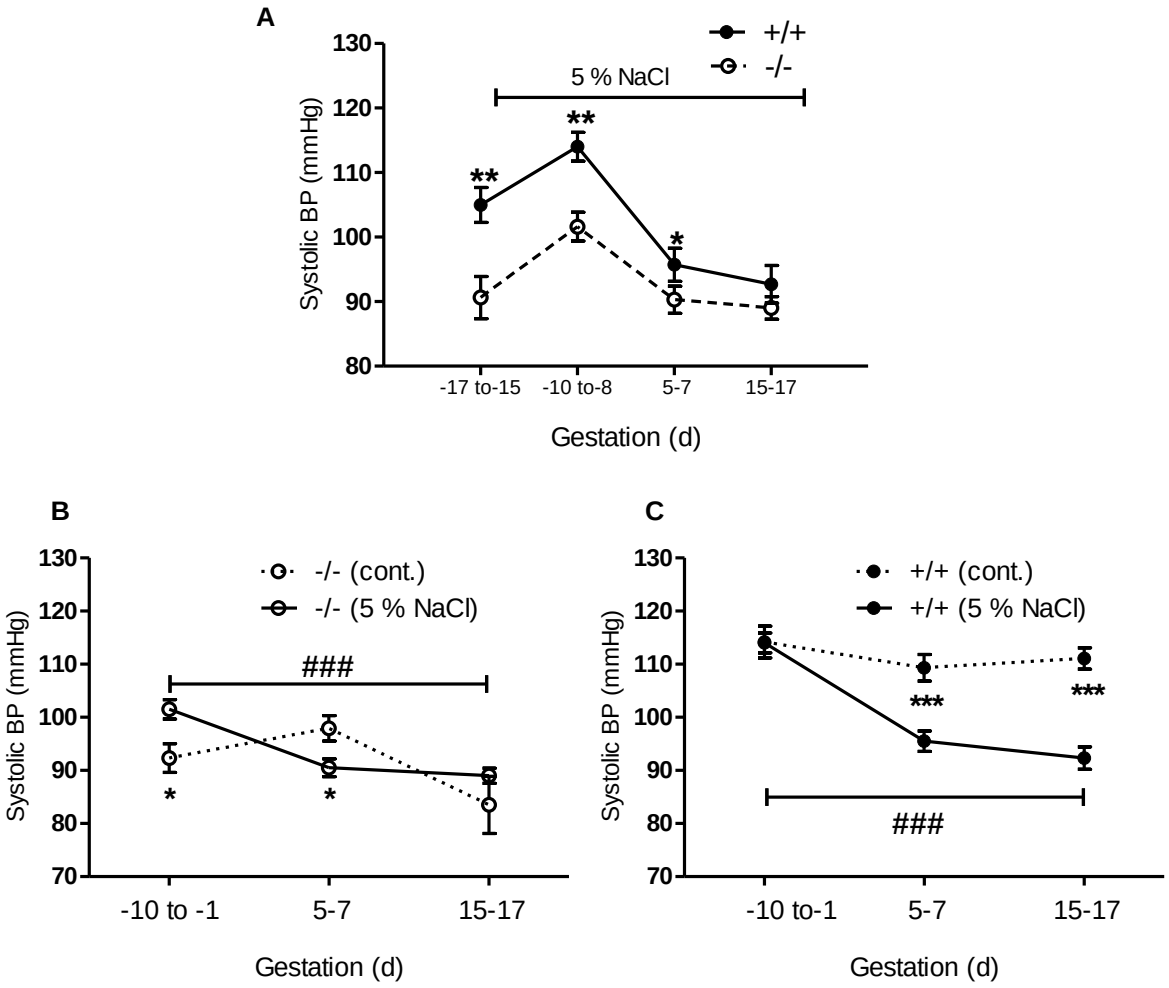

Figure 34. **Effect of high salt diet on systolic blood pressure (SBP), litter size, litter and placenta weight and necrotic placentas at day 18 of pregnancy (**A) SBP was measured at different time points (days) before and during pregnancy in $AS^{+/+}$ (n = 6-8 animals/time point) and $AS^{-/-}$ (n = 7-10 animals/ time point). (B) In $AS^{-/-}$ mice, no differences in blood pressure was observed upon salt loading in pregnancy. SBP compared between control and high salt (5% NaCl) diet at different time points just before pregnancy (-4 to -1 day for control and -10 to -8 for high salt) gestational day 5 to 7 and 15 to 17. (C) In pregnant wild-type mice, salt loading led to a significant drop in blood pressure. SBP compared between control and high salt (5% NaCl) diet at different time points just before pregnancy (-4 to -1 day for control and -10 to -8 for high salt) gestational day 5 to 7 and 15 to 17. Values are mean ± SEM. *P < 0.05, **P < 0.005, ***P < 0.001 vs. $AS^{+/+}$ (Figure 25A) or vs. control diet (Figure 25B, C), $^{###}P$ < 0.005 vs. high salt (5% NaCl) at -10 to -1 days.

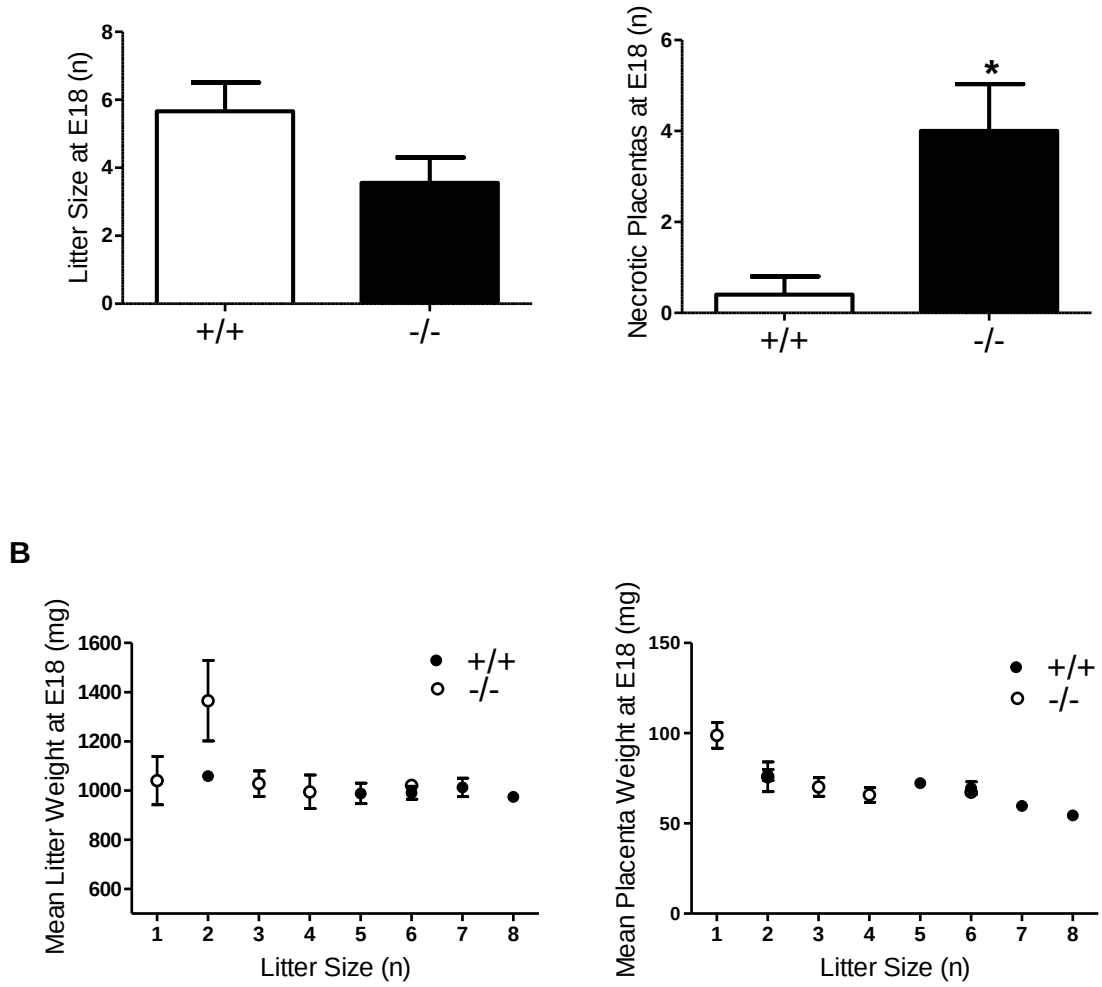

Figure 35. **Effect of high salt diet on systolic blood pressure, litter size, litter and placenta weight and necrotic placentas at day 18 of pregnancy.** (A) Number of fetuses and necrotic placentas detected in $AS^{+/+}$ (n = 6) and $AS^{-/-}$ dams (n = 9) at day 18 of pregnancy. (B) Mean litter and mean placenta weight vs. litter size in $AS^{+/+}$ (n = 6) and $AS^{-/-}$ dams (n = 9). Values are mean ± SEM. *P < 0.05 vs. $AS^{+/+}$.

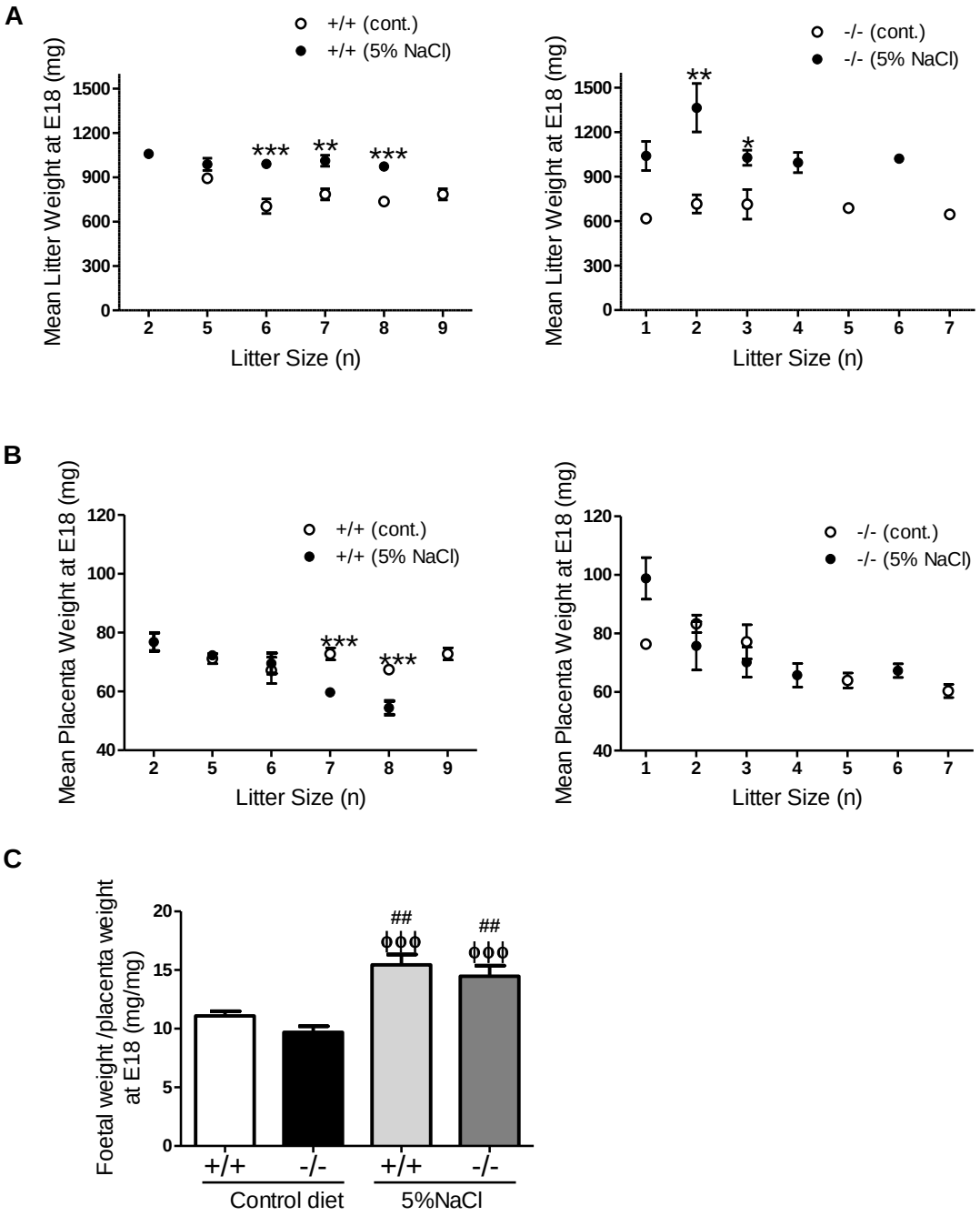

Figure 36. Comparison of litter and placenta weights, and placental efficiency between control vs. high salt diet in $AS^{+/+}$ and $AS^{-/-}$ dams. Mean litter weights (A) and mean placenta weights (B) on control diet vs. high salt diet in $AS^{+/+}$ (control diet n = 8 litters, high salt diet n = 6 litters) and $AS^{-/-}$ dams (control diet n = 12 litters, high salt diet n = 9 litters). (C) Placental efficiency in $AS^{+/+}$ (control diet n = 8 litters, high salt diet n = 6 litters) and $AS^{-/-}$ (control diet n = 13 litters, high salt diet n = 9 litters) dams on control and high salt diet. Values are mean ± SEM. **P* < 0.05, ***P* < 0.005, ****P* < 0.001 vs. control diet, ## *P* < 0.005 vs. $AS^{+/+}$ on control diet, ****P* < 0.001 vs. $AS^{-/-}$ on control diet.

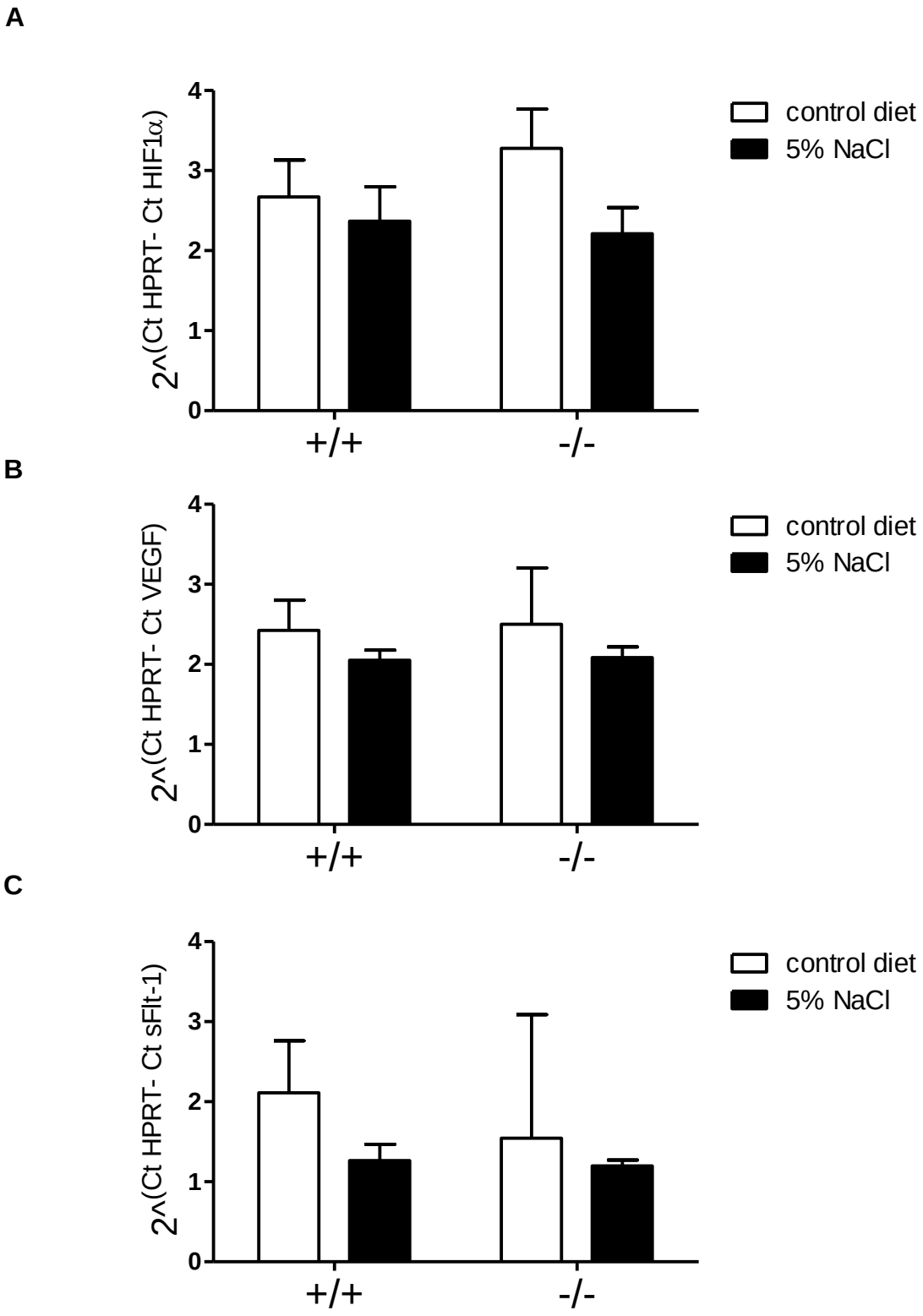

Figure 37. Expression of VEGF, sflt and HIF1α in placentas. mRNA expression of HIF1α (A) VEGF (B), and sFlt (C) in healthy placentas from $AS^{+/+}$ (n = 5) and $AS^{-/-}$ (n = 4-5) dams on control and high salt (5% NaCl) diet.

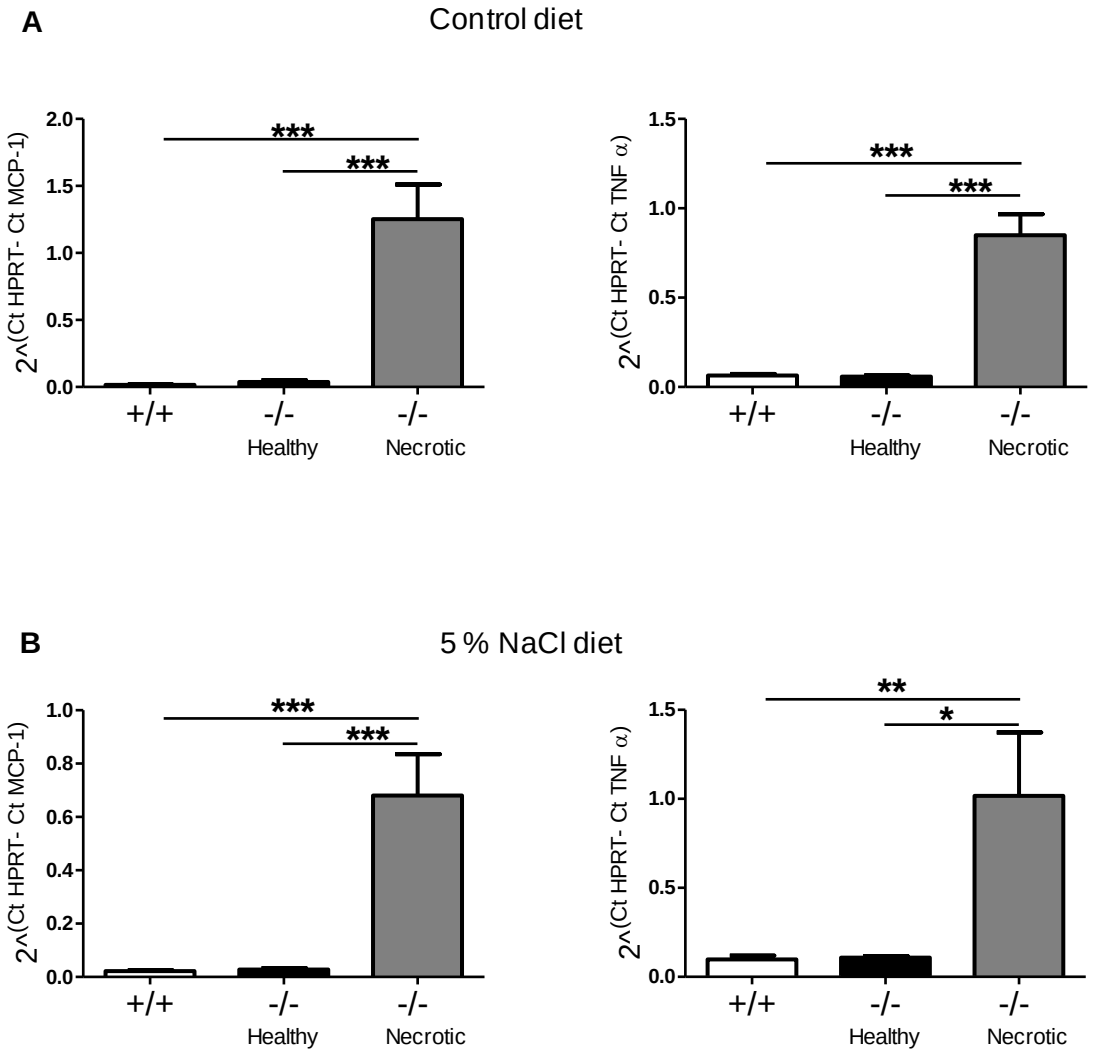

Figure 38. Expression of inflammatory markers MCP-1 and TNFα in placentas. mRNA expression of MCP-1 and TNFα was tested by qPCR in healthy placentas from $AS^{+/+}$ (n = 5), and healthy and necrotic placentas from $AS^{-/-}$ (n = 5 each) dams on control (A) and high salt (5 % NaCl) (B) diet. Values are mean ± SEM. **P* < 0.05 and ****P* < 0.001 vs. healthy placentas from $AS^{-/-}$, ***P* < 0.005 and ****P* < 0.001 vs. $AS^{+/+}$.

4.2.5 Expression of pro-inflammatory factors in necrotic placentas

MCP-1 and TNFα are key pro-inflammatory cytokines involved in inflammatory processes. Expression of MCP-1 and TNFα mRNA was significantly increased in necrotic placentas from $AS^{-/-}$ dams on control (figure 38A) and high salt diet (figure 38B) but not in healthy appearing placentas from both genotypes.

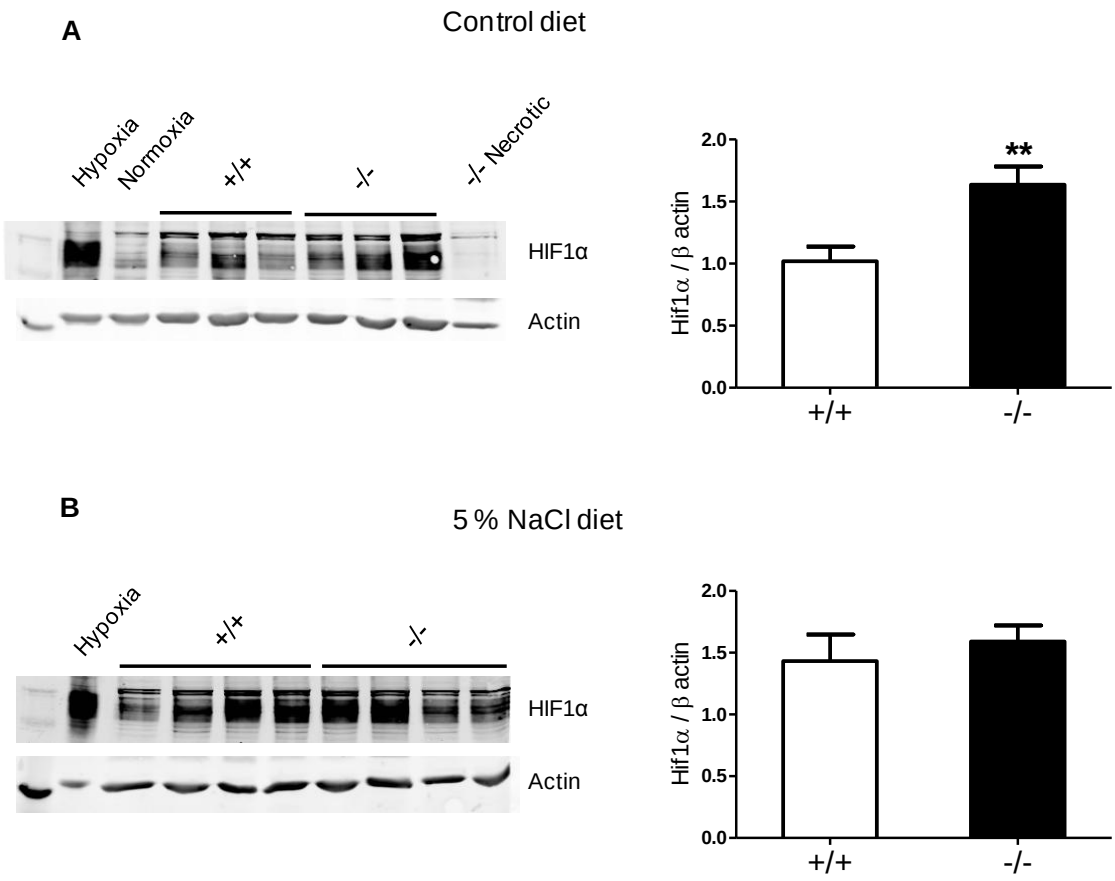

Figure 39. Protein expression of HIF1α in placentas. The protein abundance of HIF1α was examined in placentas from $AS^{+/+}$ and $AS^{-/-}$ dams on control (A) and high salt (5% NaCl) (B) diet. Hypoxic and normoxic control samples are collected from cell culture as positive and negative controls, respectively. Bar graph summarize the results from two independent blots of n= 6 normalized to β-actin measured on the same membranes. Values are mean ± SEM. $^{**}P < 0.005$ vs. $AS^{+/+}$**.**

5 DISCUSSION

5.1 Role of aldosterone in renal potassium excretion

5.1.1 Adaptation to high potassium diet is possible without aldosterone

The traditional view of the control of K^+ homeostasis assumes that increases in plasma K^+ concentrations (e.g. in response to a K^+ rich meal), directly stimulate aldosterone secretion by the adrenal glands. Then, the resulting enhanced plasma aldosterone levels stimulate renal K^+ secretion until plasma K^+ return to normal. This classical feed-back model has been challenged by studies of Rabinowitz and others [176, 177], who showed that a K^+ rich diet may provokes a kaliuretic response even before plasma K^+ and plasma aldosterone levels increase [178]. Moreover, they showed that aldosterone has very weak kaliuretic activity at normal physiological levels, and profoundly affects renal K^+ excretion only when elevated to pathological levels [176, 179]. Notably, also the well-known circadian variations of urinary K^+ excretion do not match with the diurnal changes in plasma aldosterone and K^+ [176]. Based on these observations, Rabinowitz proposed receptors in the gut, portal vein or liver responsible for the diet-induced kaliuretic reflex and suggested that the CNS and/or kaliuretic factors stimulate renal K^+ secretion independent from plasma K^+ and aldosterone. This would constitute a feed-forward control mechanism for K^+ homeostasis, which would prime the kidney to excrete K^+ to avoid high postprandial peaks of plasma K^+, with its possible detrimental effects on heart and neuronal excitability. In fact recent studies in rat further supported the idea of the existence of a gut-dependent feed-forward system that senses K^+ intake during a meal and rapidly enhances the renal clearance of plasma K^+ [180]. In our experiments, we did not test for the existence of a gut-dependent feed-forward system that regulates renal K^+ excretion. However, our data strongly support the idea of an aldosterone-independent control system. Consistent with this observation, we found increased urinary K^+ excretion and adaptation in $AS^{-/-}$ mice within a physiologically K^+-rich diet (2% K^+ diet). The increased urinary K^+ excretion might be a result of combined effects of feed-forward and feedback mechanisms. Decompensation of the system occurred at unphysiologically high K^+-intake (5% K^+ diet). The food aversion in $AS^{-/-}$ mice on this unphysiological 5% K^+ diet were consistent with previous observations in adrenalectomized rats on high K^+ diet [181]. In this previous study

adrenalectomized rats with basal or 10x times higher aldosterone infusion consumed all their diet independent of the amount of K^+ supplementation. In contrast, adrenalectomized rats with little or no aldosterone supplementation and given access to the moderately or highly K^+ supplemented diet became anorexic. Despite the reduced diet intake, the adrenalectomized rats became hyperkalemic and some of them eventually died either because of the anorexia or the hyperkalemia [181]. Consistent with these results, we found that $AS^{-/-}$ mice on 5% K^+ diet were hyperkalemic and lost body weights. The hyperkalemia and food aversion in this experiment was likely related to a decreased capacity to secrete K^+ secondary due to the lack of aldosterone.

5.1.2 Aldosterone independent regulation of ROMK and ENaC

Previous studies on adrenalectomized animals indicated that a high K^+ diet increases renal Na^+ and K^+ channel activities independent from aldosterone [166, 167]. However, adrenalectomies in rodents are often incomplete. Moreover, a physiologically relevant local renal aldosterone producing system appears to exist, which becomes activated by angiotensin II and a low salt intake in adrenalectomized rats [169]. Local synthesis of mineralcorticoids was also observed in other tissue including the heart [182]. In $AS^{-/-}$ mice, any aldosterone production in adrenal and extra-adrenal tissues is prevented due to the systemic disruption of the aldosterone-synthase gene. Thus, our experiments now conclusively demonstrate that a high K^+ intake increases Na^+ and K^+ channel activities independent from aldosterone, at least as long dietary K^+ intake is increased to the physiologically upper limit of 2% K^+. Apparently, the aldosterone precursors corticosterone [9] and deoxycorticosterone (this study) are only marginally or not elevated in $AS^{-/-}$ mice suggesting that there is no up-regulation of other members of the corticosteroid axis that could compensate for the lack of aldosterone.

In line with previous studies that suggested aldosterone-independent activation of Na^+ and K^+ channels in response to a high K^+ diet [166, 167], we show now at the molecular level a maintained K^+-diet induced regulation of ENaC and ROMK in aldosterone-deficient mice. In both $AS^{+/+}$ and $AS^{-/-}$ mice the 2% K^+ diet caused an apical translocation of ROMK and a proteolytic activation of ENaC subunits. Likewise, $AS^{-/-}$ mice showed the same natriuretic response to amiloride as

the $AS^{+/+}$ mice and showed similar ENaC sodium currents in the early ASDN segments as wild type mice. Immunohistochemistry revealed that in mice of both genotypes the K^+-diet induced activation of ROMK and ENaC predominantly occurred in the early ASDN. Given the fact that aldosterone-binding and expression of the mineralocorticoid-receptor appear to be homogenous along the entire ASDN [28], the axial gradient along the ASDN of the response of ROMK and ENaC to a high K^+ diet does already suggest that aldosterone-independent factors significantly contribute to the regulation of these two channels along the ASDN.

The axial gradient of ROMK and ENaC regulation is consistent with the idea that the early ASDN is the most critical for the maintenance of Na^+ and K^+ balance. In fact, patch clamp studies in on isolated ASDN segments of rats kept on a high K^+ diet or treated with aldosterone indicated that ENaC activity is several times larger in the CNT than in the CCD [183]. DCTs and CNTs of rats, rabbits and mice have several fold higher $Na^+/^+K$-ATPase activity than the CDs of the respective species [184]. Moreover, several regulatory proteins linked to hypertension or K^+ excretion such as WNK4, WNK1 and tissue kallikrein are localised in the DCT and CNT rather than in the CD. Tissue kallikrein, a serine protease, is a kaliuretic factor involved in renal K^+ excretion after high K^+ loads [185]. Earlier studies in collecting duct specific α-ENaC knockout mice showed the importance of the early ASDN (late DCT/CNT) for the preservation of Na^+ and K^+ balance [186]. This study indicated the importance of early ASDN (late DCT/CNT) in achieving Na^+ and K^+ balance and demonstrated that expression of ENaC in CD is not a prerequisite to maintain Na^+ and K^+ balance [186].

5.1.3 Angiotensin II dependent potassium excretion

$AS^{-/-}$ mice have very high levels of angiotensin II. AT1 receptors have been demonstrated by immunohistochemical studies in DCTs, CNTs and CDs [187]. We hypothesized that in the absence of aldosterone, the high angiotensin II levels might be important to ensure renal K^+ excretion. In fact, Inhibition of AT1 receptors for angiotensin II by losartan led to a decompensation of $AS^{-/-}$ mice on high 2% K^+ diet. The mice became severely hyperkalemic and showed a clear avoidance for the K^+ enriched food. The accompanying hyponatremia was unexpected, but might be due to a combination of reduced food intake, normal water intake, and decompensated

renal Na^+ excretion. Our immunohistochemical data suggest that the decompensation of the losartan-treated mice was related to a de-activation of ENaC which diminished the driving force for renal K^+ secretion along the ASDN. The role of angiotensin II for ENaC regulation is supported by several previous studies. Long term systemic infusion of angiotensin II increases α-ENaC expression in rat kidney cortex [188]. Likewise, AT1 receptor knockout mice have a reduced α-ENaC expression despite elevated plasma aldosterone levels [189]. Angiotensin II was shown to directly stimulate amiloride-sensitive sodium channel activity in isolated late distal tubules and initial collecting ducts. The effect could be blocked by the luminal administration of the AT1 receptor blockers candesartan or losartan [190, 191]. Furthermore, in type 2 diabetes and obesity inappropriate Na^+ retention was associated with AT1 receptor dependent activation of ENaC channels [192]. In contrast to ENaC, ROMK and SK channel activity was proposed to be inhibited by angiotensin II. During dietary K^+ restriction, inhibition of AT1 receptors by losartan augments apical K^+ channel activity likely by interfering with Src family protein tyrosine kinase (PTK) and mitogen activated protein kinase (MAPK) dependent inhibition of ROMK and BK activity, respectively. However, this effect was only evident during dietary K^+ restriction. No inhibitory effect of angiotensin II on ROMK or BK channel was observed during normal K^+ diet [193, 194]. Consistently, in our experiments on mice on standard and high K^+ diet, we did not find any evidence for an inhibitory effect of angiotensin II on ROMK. In fact, the $AS^{-/-}$ mice, which are known to have exceedingly high angiotensin II levels [9], showed a rather prominent apical ROMK localization that appeared to be even more pronounced than the one seen in wild type mice.

Interestingly, losartan caused hyperkalemia and K^+-food avoidance only in $AS^{-/-}$, but not in $AS^{+/+}$ mice suggesting that AT1 inhibition is per se not sufficient to significantly impair renal K^+ handling and hence K^+ homeostasis. Only when both aldosterone and angiotensin II actions are lacking mice appear to decompensate. Consistently, meta-analysis of clinical studies on patients with hypertension, heart failure and chronic kidney disease (CKD) demonstrated that the incidence of hyperkalemia is below 2% when only one component of the renin-angiotensin-aldosterone system (RAAS) is inhibited, but increases to about 5-10% (depending on the underlying disease) when two components of the RAAS are inhibited. In patients

with hypertension, the combination of an aldosterone receptor antagonist with an angiotensin II receptor blocker was shown to increase serum K^+ level to significantly higher values than those seen in patients with a AT1 receptor blocker mono-therapy [195].

5.1.4 Polyuria-dependent potassium excretion?

As previously reported [170], $AS^{-/-}$ mice are polyuric. This polyuria is seen already on standard diet and becomes even more prominent on a high K^+ diet. Because the activity of renal potassium channels such as maxi K/BK channels is flow-dependent, we speculated that the enhanced diuresis may contribute to the maintained renal K^+ secretion in $AS^{-/-}$ mice. However, lowering diuresis by injection of the synthetic vasopressin analogue DDAVP did not lower urinary K^+ excretion and did not increase plasma K^+ compared to wild type mice. Although we cannot exclude that under these condition a vasopressin-dependent activation of K^+ channels [196] compensated for the lowered flow-dependent K^+-channel activation, the data indicate that a high urinary flow rate is at least not critical for K^+-homeostasis in $AS^{-/-}$ mice. Moreover, we could not detect any difference in the mRNA expression of BK channel subunits β1, β2 and β4 between wild type and $AS^{-/-}$ mice suggesting that the aldosterone-deficiency did not lead to a compensatory up-regulation, at least at the mRNA level, of flow-dependent K^+-channels in the kidneys of $AS^{-/-}$ mice.

The reason for the polyuria in $AS^{-/-}$ is unclear. Theoretically, it could be the result of an increased water intake due to enhanced thirst or due to renal water loss due to an impaired urinary concentration mechanism caused by an insufficient secretion of vasopressin from the pituitary (central diabetes insipidus) or caused by an insufficient action of vasopressin on the kidney (renal diabetes insipidus). The $AS^{-/-}$ deficient mice have exceedingly high angiotensin II levels and angiotensin II is known to stimulate thirst [197]. However, previous data from Olivier Smithies group showed that $AS^{-/-}$ mice, which were restricted to the same water intake as $AS^{+/+}$ mice, still have a significantly lower urine osmolarity than wild type mice. This suggests a renal concentration defect rather than an angiotensin II-induced polydipsia as the cause for the observed polyuria [170]. Because it is technically very challenging, we did not measure vasopressin levels in our mice, but the previous studies from Olivier Smithies reported similar vasopressin levels in wild type and in

$AS^{-/-}$ mice suggesting that more likely a renal defect is responsible for the observed polyuria. In fact, there is ample evidence that aldosterone increases vasopressin mediated water transport in the renal collecting system [198, 199] either by direct effects on renal water channels such as AQP3 [200] or by increasing ENaC activity which may osmotically drive renal water reabsorption [201]. Consistent with a renal water transport defect, our immunofluorescent studies revealed a slightly reduced apical localization of the water channel AQP2 in the medullary collecting ducts of $AS^{-/-}$ mice, though the total abundance of AQP2 protein (our study) and mRNA [170] was found to be increased in $AS^{-/-}$ mice. Despite of the apparent mild trafficking defect for AQP2, $AS^{-/-}$ mice are still responsive to vasopressin. In previous studies with mice on standard diet as well as in our study on mice on 2% K^+ diet, the V2 receptor-specific agonist DDAVP increased similar urine osmolarity in both $AS^{+/+}$ and $AS^{-/-}$ mice.

5.1.5 Aldosterone-independent down regulation of NCC contributes to K^+ secretion

Previous studies showed that the thiazide-sensitive Na-Cl co-transporter is an aldosterone-induced protein [202]. Consistent with these results, we found a reduced total NCC and phospho-NCC abundance. NCC mRNA expression and the fractional volume of the DCT was similar for mice of both genotypes indicating that the NCC down-regulation occurs at the posttranscriptional level and is independent from a major epithelial remodelling of the distal nephron. Consistent with the reduced NCC phosphorylation, which is thought to be indicative for a reduced NCC activity [203], the $AS^{-/-}$ showed a reduced thiazide-sensitive natriuresis when compared to $AS^{+/+}$ mice. On a high K^+ diet, NCC expression and phosphorylation decreased in mice of both genotypes indicating that NCC-downregulation might be part of the homeostatic response of the kidney to dietary K^+ loading and that this effect is aldosterone-independent.

Although the underlying mechanism for the K^+-induced downregulation of NCC is unclear, the functional consequences are likely important for the maintenance of K^+ balance. The decreased NCC activity augments Na^+ delivery to the early ASDN where then the increased luminal Na^+ concentration increases the driving force for Na^+ reabsorption via ENaC which eventually fosters K^+ secretion via

ROMK. A strong relationship between high Na^+ delivery to the distal tubule and increased K^+ excretion is well established [22, 204]. Also patients with Gitelman's syndrome due to loss-of-function mutations in NCC tend to have an increased renal K^+ excretion leading to hypokalemia [205]. Conversely, patients with pseudohypoaldosteronism type II, having an enhanced NCC activity due to mutations in WNK kinases, develop hyperkalemia [206]. In these genetic diseases not only NCC activity, but also plasma aldosterone levels are changed and it is likely that both factors contribute to the altered renal K^+ handling. In the $AS^{-/-}$ mice, plasma aldosterone levels are constantly set to zero and it appears that K^+ homeostasis in these mice is largely achieved by adapting the Na^+ delivery to the early ASDN in which ENaC is activated via angiotensin II.

5.1.6 Potassium induced activation of Na^+ and K^+ channels in colon is aldosterone dependent

The distal colon contributes to K^+ excretion and thus to K^+ homeostasis. The distal colon is an aldosterone-sensitive segment and aldosterone is responsible for electrogenic Na^+ reabsorption through ENaC channels in the distal colon [207]. Also, aldosterone is well known to induce K^+ secretion through BK channel in the distal colon. Previous studies revealed increased mRNA expressions of BK and ENaC channels in mouse distal colon on high K^+ diet [97, 105]. Consistently, we also demonstrated K^+ induced activation of ENaC and BK channels in $AS^{+/+}$ mice but not in $AS^{-/-}$ mice indicating the necessity of aldosterone in the distal colon for stimulating Na^+ absorption and K^+ secretion. Loss of distal colon K^+ secretion activity in $AS^{-/-}$ mice was compensated at least partially by increased K^+ secretion in the kidney.

However, unlike Na^+ dependent K^+ secretion in the kidney, it is not clear if K^+ secretion in the distal colon is a Na^+ dependent process. One recent study demonstrated that BK channels are primarily expressed in crypts and γ-ENaC mainly expressed in surface cells of the distal colon. They also showed at the functional level that ENaC mediated Na^+ reabsorption and BK channels mediated K^+ secretion are two functionally independent processes [105]. In contrast, two studies with radioactive tracer flux measurements in rats with *in vivo* or *in vitro* elevated plasma aldosterone showed a ~40% reduction of serosal to mucosal tracer fluxes after luminal amiloride application indicating reduced K^+ secretion [104, 208]. This

indicates that a fraction of colonic K^+ secretion may also occur in surface epithelial cells under elevated aldosterone levels and uses Na^+ influx to drive this process or that Na^+ absorption generates a lumen-negative potential that favours K^+-secretion by crypt cells. A study using conductance scanning of epithelial surfaces concluded that aldosterone induced K^+ secretion resides in surface cells and K^+ secretion induced by adrenaline is present in both crypt as well as in surface epithelial cells [208]. It is clear that aldosterone plays an important role in K^+ secretion in the distal colon, although the exact mechanisms including its Na^+ dependency are still not clear.

Summary and perspectives

The final conclusion of this study is summarized in figure 40. In $AS^{+/+}$ mice, on control diet, the major part of the distally delivered Na^+ is reabsorbed via NCC in the DCT1 and DCT2 and a small remaining portion is reabsorbed via ENaC to maintain fluid balance as well as K^+ secretion. On the 2% K^+ diet, the expression and activity of NCC is decreased to increase Na^+ delivery to the more distal nephron segments to enhance K^+ secretion. Therefore $AS^{+/+}$ mice are able to maintain both fluid volume and K^+ secretion. Aldosterone plays an important role in ENaC regulation in $AS^{+/+}$ mice. In contrast, in $AS^{-/-}$ mice, on control diet, NCC activity is already decreased compared to $AS^{+/+}$ mice and Na^+ is reabsorbed only to some extent by NCC transporters in DCT1 and DCT2 but more Na^+ is delivered to the distal segments to be absorbed by ENaC channels in the early ASDN to maintain both Na^+ reabsorption and K^+ secretion. On the 2% K^+ diet, a further decrease in NCC expression and activity occurs to further increase Na^+ delivery to the early ASDN to stimulate K^+ secretion in order to excrete the excess K^+ load. Angiotensin II might be playing an important role for the activation of ENaC channels in the early ASDN in $AS^{-/-}$ mice in the absence of aldosterone. On the 5 % K^+ diet, residual ENaC activity only in the early ASDN in $AS^{-/-}$ mice is not sufficient to maintain the secretion of the very high load of K^+ and ultimately mice show decompensation.

In summary, we describe the aldosterone-independent activation of ENaC and ROMK in the early ASDN. The permissive effect of angiotensin II was important for the residual activity of ENaC to excrete K^+. On high K^+ diet, the downregulation of NCC is an important factor to increase Na^+ delivery to the ASDN. We speculate that

the organism of the mice prefers to downregulate Na^+ retaining mechanism on the expense of a lower blood pressure rather than to risk hyperkalemia with all its potentially deleterious effects on excitable tissues.

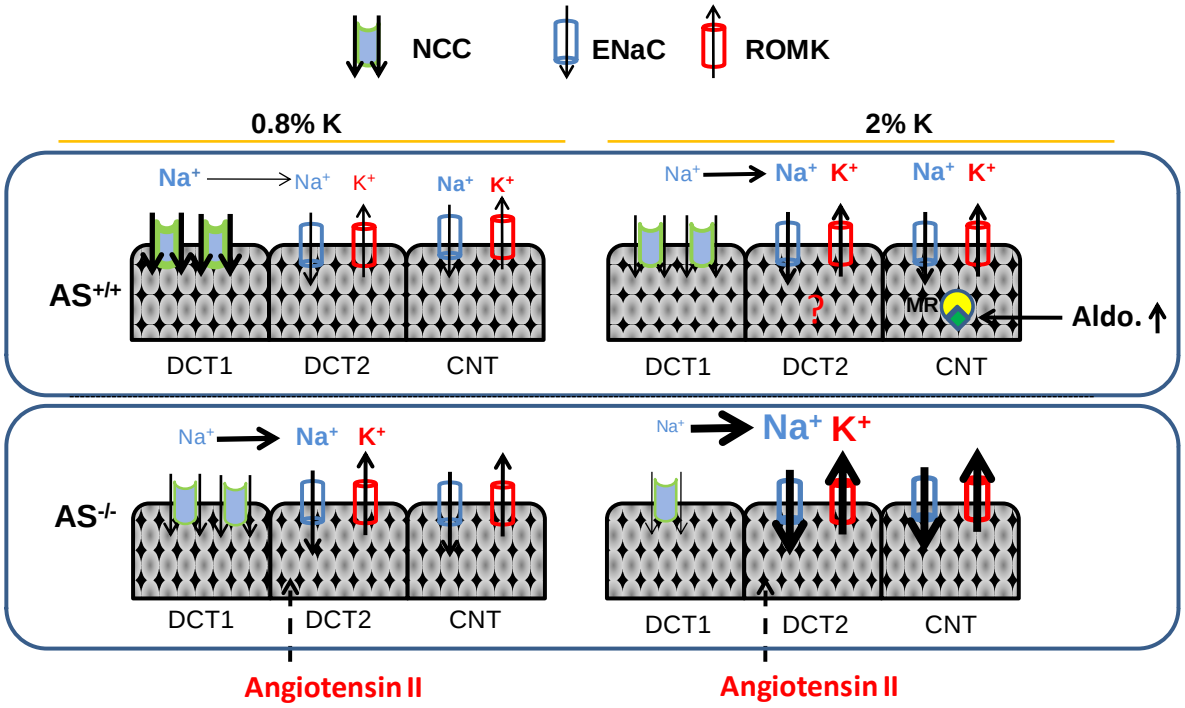

Figure 40. Model to explain aldosterone dependent and independent regulation of renal K^+-excretion in $AS^{+/+}$ and $AS^{-/-}$ mice on control and high K diet.

5.2 Role of aldosterone in pregnancy

Plasma volume expansion in the presence of high aldosterone levels is considered crucial for healthy pregnancies, both of which are low in the most severe form of hypertensive pregnancies, pre-eclampsia. In order to examine the role of aldosterone in the development of pre-eclampsia, we used an aldosterone synthase knockout mouse model ($AS^{-/-}$). $AS^{-/-}$ mice have a compensatory increase of renin and angiotensin II to supraphysiological concentrations but no aldosterone [9] allowing to independently test the role of aldosterone in pregnancy. Additional effects of these high renin and angiotensin II may occur but could not be tested because survival of $AS^{-/-}$ mice depends on high angiotensin II levels and pharmacological blockade of AT_1 receptors is lethal in $AS^{-/-}$ mice (unpublished observations).

New-onset hypertension and proteinuria with feto-placental developmental disturbances are considered to be cardinal features of pre-eclampsia [109]. We found that $AS^{-/-}$ dams did not develop preeclampsia as suggested by the absence of hypertension and proteinuria during pregnancy. A previous study measured SBP by telemetry during pregnancy and showed no change in SBP during the first 5 days, followed by a drop in SBP from days 6 to12, and again from day 15 to 17 of pregnancy [209]. In our hands, using the less sensitive tail cuff method, we found reduced SBP in wild type mice during pregnancy in response to salt loading. Though contra-intuitive, this observation is in line with some clinical observations during salt loading in pregnancy suggesting a beneficial systemic feedback on maternal hemodynamics upon optimal placental perfusion [163, 164]. Thus, pre-eclampsia is not caused by a lack of aldosterone alone, at least in mice.

However, the mouse model revealed a number of other interesting observations demonstrating an important role of aldosterone in normal pregnancy. $AS^{-/-}$ dams were hypotensive before pregnancy and became even more hypotensive during mid to term pregnancy. The resulting feto-placental phenotype of a decreased litter size and smaller or necrotic placentas without fetuses at term suggests a severe placental hypoperfusion. The sum of intact fetuses and necrotic placentas in $AS^{-/-}$ mice was similar to the average number of fetuses in $AS^{+/+}$ dams, indicating that $AS^{-/-}$ dams were able to conceive normally but had impaired placental development and function, predisposing to intrauterine death. The few normal weight

placentas and fetuses observed in $AS^{-/-}$ dams carrying small litters would such provide a residual blood and nutrient supply to the remaining placentas.

Histological examination of healthy placentas from $AS^{-/-}$ dams demonstrated normal structural patterns but reduced size. One important reason for lower placental weight might be the absence of direct effects of aldosterone on the placenta in $AS^{-/-}$ dams. *In vitro* experiments have revealed a direct role for aldosterone in the modulation of trophoblast growth and placental size [5] and *in vivo* studies in ewes suggested a role of aldosterone in placental growth [162]. Placental size in rats and humans is positively correlated with plasma levels of aldosterone [5]. Thus, aldosterone may positively modulate placental growth, similar to its proliferative capabilities in organs such as the heart and the kidney [210, 211].

Reduced fetal weight in $AS^{-/-}$ dams might thus be due to placental insufficiency. In normal human pregnancy, plasma volume expansion is associated with increased plasma aldosterone level whereas both were decreased in pregnancies with intrauterine growth restriction and pre-eclampsia [146]. Pre-eclampsia is characterised by extracellular volume expansion but low intravascular volume which is caused at least in part by a shift of fluid from the intravascular to the interstitial fluid space due to vasoconstriction and leaky endothelium [212-214]. Lack of aldosterone in $AS^{-/-}$ dams might thus critically impair plasma volume expansion and thereby cause reduced uterine blood supply similar to functional aldosterone deficiency in mice chronically exposed to the mineralocorticoid receptor antagonist spironolactone during pregnancy which led to reduced fetal umbilical blood flow [5]. Moreover, modelling a reduced uterine blood supply by constriction of the uterine artery in rats from gestational day 14 caused placental insufficiency resulting in low-birth weight [215].

One common cause for the decreased litter size, reduced fetal and placental weight, and necrotic and inflammatory placentas in $AS^{-/-}$ dams could be hypoxia. In rats, hypoxia during the last 11 days of pregnancy results in smaller sized litters, decreased placental and fetal weights, and placental resorption [216]. Low oxygen tension affects cytotrophoblast proliferation and invasion and ultimately fetal growth [116]. Consistently, the hypoxia-induced factor HIF1α, a master regulator in the adaption to hypoxia, is essential for mammalian placentation [217]. HIF1α protein

abundance was significantly higher in $AS^{-/-}$ mice on control diet, but was reduced to control levels on 5% NaCl diet in the normal appearing placentas suggesting hypoxia and rescue by high NaCl intake. Consequently, $AS^{-/-}$ necrotic placentas showed coagulative necrosis and severe lymphocyte infiltration and elevated levels of pro-inflammatory cytokines MCP-1 and TNFα.

Aldosterone plays a central role in the long-term control of extracellular volume by adapting renal and extrarenal reabsorption of sodium to blood pressure [17]. Thereby, extracellular NaCl and volume is enlarged, blood pressure and organ perfusion increased. $AS^{-/-}$ mice are hypotensive despite highly elevated levels of renin and angiotensin II. High salt diet reverses renin and angiotensin II abnormalities without increasing blood pressure indicating that the extracellular volume status is at least partially normalized [218]. To rescue the possibly reduced plasma volume and lower uterine blood flow in $AS^{-/-}$ dams, we treated mice with high salt for 12 days before pregnancy until gestational day 18. Both $AS^{+/+}$ and $AS^{-/-}$ mice responded by increasing SBP suggesting that $AS^{-/-}$ dams also retained salt and fluid even though plasma volume was not directly measured.

High salt diet had several interesting implications. Next to the blood pressure lowering potency in pregnant wild type mice, it partially rescued the fetal phenotype with a substantial effect on fetal weight, placental hypoxia, and placental efficiency in both $AS^{+/+}$ and $AS^{-/-}$ dams. Placental efficiency can be altered experimentally by manipulation of uterine blood flow, oxygen availability, and by the intake and composition of maternal diet. Increased efficiency is also seen in naturally small relative to large placentas in pigs, sheep, goats, rats and mice. Placental efficiency in these polytocous species is positively related to litter size [132]. We found that smaller placentas in $AS^{+/+}$ dams on high salt diet and $AS^{-/-}$ dams were associated with larger litter size indicating positive correlation between placental efficiency and litter size. Decreased placenta weight with larger litter size in $AS^{+/+}$ dams on high salt diet also suggests increased placental efficiency thus supporting an unrestricted fetal growth. While small, dark placentas were still observed in $AS^{-/-}$ dams on high salt diet similar to control diet it remains amenable a consequence of altered local aldosterone availability to support placental development.

Limitations of this model of aldosterone deficiency are the high renin and angiotensin II levels which may trigger local dysregulatory events in pre-eclampsia. In the absence of aldosterone synthase, deoxycorticosterone, corticosterone and some 18-hydroxycorticosterone are still synthesized via 11β-hydroxylase activity. Thus, the live-long inhibition of aldosterone synthesis in these animals potentially allowing for alternative mineralocorticoid active steroid hormones might have supplemented some extrarenal aldosterone effects or even enhanced the inhibition of proliferation of trophoblasts via the activation of glucocorticoid receptors.

Aldosterone availability appears an important prerequisite to support normal feto-placental development. $AS^{-/-}$ dams had a feto-placental phenotype with decreased litter size, smaller placentas and fetuses, yet no overt pre-eclampsia. In the absence of aldosterone, the fetal phenotype might be rescued in part by high salt diet. In wild type mice, the high salt diet led to profound blood pressure reduction in pregnancy which suggests an important role of plasma volume and placental perfusion for maternal well-being. Thus, the absence of aldosterone cannot trigger preeclampsia-like symptoms in mice, but might well contribute to the development of pre-eclampsia-related intrauterine growth restriction while pre-eclampsia needs to be triggered by additional factors. Thus, our study supports the importance of aldosterone in placental function *in vivo* and a possible role for high salt supplementation in pregnancies specifically associated with hypoaldosteronism or reduced plasma volume expansion to maintain feto-placental integrity. In contrast, in pre-eclampsia, the benefits of salt supplementation are still controversial and appears have no major impact on outcome as indicated by a recent meta-analysis.

6 PERSPECTIVES

Aldosterone availability appears to be an important prerequisite to support normal feto-placental development. This hypothesis is based on the observations that $AS^{-/-}$ dams had a feto-placental phenotype with decreased litter size, smaller placentas and fetuses, yet no overt pre-eclampsia. In the absence of aldosterone, the fetal phenotype might be rescued in part by the restoration of a higher plasma volume by the addition of a high salt diet. In wild type mice, the addition of a high salt diet led to profound blood pressure reduction in pregnancy which suggests an important role of plasma volume and placental perfusion for maternal well-being. Thus, the absence of aldosterone cannot trigger pre-eclampsia-like symptoms in mice, but might well contribute to the development of pre-eclampsia-related intrauterine growth restriction while pre-eclampsia needs to be triggered by additional factors. These data support an important role of aldosterone in the placental development as suggested by smaller weight and sized placentas, and necrotic and inflammatory placentas in $AS^{-/-}$ dams. Thus, our study supports the importance of aldosterone in placental function *in vivo* and a possible role for high salt supplementation in pregnancies specifically associated with hypoaldosteronism or reduced plasma volume expansion to maintain the feto-placental integrity. Aldosterone deficiency aids to explain reduced placental size and decreased fetal weight in pregnancy disorders such as intrauterine growth restriction and pre-eclampsia.

REFERENCES

1. Walter F. Boron, E.L.B., *Medical Physiology*. 1st ed. 2003, Philadelphia: Saunders.
2. Takeda, Y., et al., *Production of aldosterone in isolated rat blood vessels.* Hypertension, 1995. **25**(2): p. 170-3.
3. Silvestre, J.S., et al., *Myocardial production of aldosterone and corticosterone in the rat. Physiological regulation.* J Biol Chem, 1998. **273**(9): p. 4883-91.
4. Gomez-Sanchez, C.E., et al., *Aldosterone biosynthesis in the rat brain.* Endocrinology, 1997. **138**(8): p. 3369-73.
5. Gennari-Moser, C., et al., *Regulation of placental growth by aldosterone and cortisol.* Endocrinology, 2011. **152**(1): p. 263-71.
6. Chapman, A.B., et al., *Temporal relationships between hormonal and hemodynamic changes in early human pregnancy.* Kidney Int, 1998. **54**(6): p. 2056-63.
7. Zennaro, M.C., M. Caprio, and B. Feve, *Mineralocorticoid receptors in the metabolic syndrome.* Trends Endocrinol Metab, 2009. **20**(9): p. 444-51.
8. Boon, W.C., et al., *Aldosterone secretion: a molecular perspective.* Trends Endocrinol Metab, 1997. **8**(9): p. 346-54.
9. Lee, G., et al., *Homeostatic responses in the adrenal cortex to the absence of aldosterone in mice.* Endocrinology, 2005. **146**(6): p. 2650-6.
10. Arriza, J.L., et al., *Cloning of human mineralocorticoid receptor complementary DNA: structural and functional kinship with the glucocorticoid receptor.* Science, 1987. **237**(4812): p. 268-75.
11. Farman, N. and M.E. Rafestin-Oblin, *Multiple aspects of mineralocorticoid selectivity.* Am J Physiol Renal Physiol, 2001. **280**(2): p. F181-92.
12. Funder, J.W., et al., *Mineralocorticoid action: target tissue specificity is enzyme, not receptor, mediated.* Science, 1988. **242**(4878): p. 583-5.
13. Funder, J.W., *Glucocorticoid and mineralocorticoid receptors: biology and clinical relevance.* Annu Rev Med, 1997. **48**: p. 231-40.
14. Lombes, M., et al., *Prerequisite for cardiac aldosterone action. Mineralocorticoid receptor and 11 beta-hydroxysteroid dehydrogenase in the human heart.* Circulation, 1995. **92**(2): p. 175-82.
15. Takeda, Y., et al., *Expression of 11 beta-hydroxysteroid dehydrogenase mRNA in rat vascular smooth muscle cells.* Life Sci, 1994. **54**(4): p. 281-5.
16. Robson, A.C., et al., *11 Beta-hydroxysteroid dehydrogenase type 2 in the postnatal and adult rat brain.* Brain Res Mol Brain Res, 1998. **61**(1-2): p. 1-10.
17. Booth, R.E., J.P. Johnson, and J.D. Stockand, *Aldosterone.* Adv Physiol Educ, 2002. **26**(1-4): p. 8-20.
18. Briet, M. and E.L. Schiffrin, *Aldosterone: effects on the kidney and cardiovascular system.* Nat Rev Nephrol, 2010. **6**(5): p. 261-73.
19. Nguyen Dinh Cat, A. and F. Jaisser, *Extrarenal effects of aldosterone.* Curr Opin Nephrol Hypertens, 2012. **21**(2): p. 147-56.
20. Hirasawa, G., et al., *11Beta-hydroxysteroid dehydrogenase type II and mineralocorticoid receptor in human placenta.* J Clin Endocrinol Metab, 2000. **85**(3): p. 1306-9.
21. Wang, W., *Regulation of renal K transport by dietary K intake.* Annu Rev Physiol, 2004. **66**: p. 547-69.
22. Giebisch, G., *Renal potassium transport: mechanisms and regulation.* Am J Physiol, 1998. **274**(5 Pt 2): p. F817-33.
23. Giebisch, G.H., *A trail of research on potassium.* Kidney Int, 2002. **62**(5): p. 1498-512.
24. Wang, W.H. and G. Giebisch, *Regulation of potassium (K) handling in the renal collecting duct.* Pflugers Arch, 2009. **458**(1): p. 157-68.
25. O'Neil, R.G. and R.A. Hayhurst, *Functional differentiation of cell types of cortical collecting duct.* Am J Physiol, 1985. **248**(3 Pt 2): p. F449-53.

26. Frindt, G. and L.G. Palmer, *Apical potassium channels in the rat connecting tubule.* Am J Physiol Renal Physiol, 2004. **287**(5): p. F1030-7.
27. Giebisch, G., S.C. Hebert, and W.H. Wang, *New aspects of renal potassium transport.* Pflugers Arch, 2003. **446**(3): p. 289-97.
28. Loffing, J. and C. Korbmacher, *Regulated sodium transport in the renal connecting tubule (CNT) via the epithelial sodium channel (ENaC).* Pflugers Arch, 2009. **458**(1): p. 111-35.
29. Grimm, P.R. and S.C. Sansom, *BK channels in the kidney.* Curr Opin Nephrol Hypertens, 2007. **16**(5): p. 430-6.
30. Hebert, S.C., et al., *Molecular diversity and regulation of renal potassium channels.* Physiol Rev, 2005. **85**(1): p. 319-71.
31. Palmer, L.G. and G. Frindt, *Na+ and K+ transport by the renal connecting tubule.* Curr Opin Nephrol Hypertens, 2007. **16**(5): p. 477-83.
32. Meneton, P., J. Loffing, and D.G. Warnock, *Sodium and potassium handling by the aldosterone-sensitive distal nephron: the pivotal role of the distal and connecting tubule.* Am J Physiol Renal Physiol, 2004. **287**(4): p. F593-601.
33. Doucet, A. and S. Marsy, *Characterization of K-ATPase activity in distal nephron: stimulation by potassium depletion.* Am J Physiol, 1987. **253**(3 Pt 2): p. F418-23.
34. DuBose, T.D., Jr., J. Gitomer, and J. Codina, *H+,K+-ATPase.* Curr Opin Nephrol Hypertens, 1999. **8**(5): p. 597-602.
35. Okusa, M.D., et al., *Active potassium absorption by the renal distal tubule.* Am J Physiol, 1992. **262**(3 Pt 2): p. F488-93.
36. Jasti, J., et al., *Structure of acid-sensing ion channel 1 at 1.9 A resolution and low pH.* Nature, 2007. **449**(7160): p. 316-23.
37. Bhalla, V. and K.R. Hallows, *Mechanisms of ENaC regulation and clinical implications.* J Am Soc Nephrol, 2008. **19**(10): p. 1845-54.
38. Kellenberger, S. and L. Schild, *Epithelial sodium channel/degenerin family of ion channels: a variety of functions for a shared structure.* Physiol Rev, 2002. **82**(3): p. 735-67.
39. Rossier, B.C. and L. Schild, *Epithelial sodium channel: mendelian versus essential hypertension.* Hypertension, 2008. **52**(4): p. 595-600.
40. Canessa, C.M., et al., *Amiloride-sensitive epithelial Na+ channel is made of three homologous subunits.* Nature, 1994. **367**(6462): p. 463-7.
41. Canessa, C.M., *Structural biology: unexpected opening.* Nature, 2007. **449**(7160): p. 293-4.
42. Garty, H. and L.G. Palmer, *Epithelial sodium channels: function, structure, and regulation.* Physiol Rev, 1997. **77**(2): p. 359-96.
43. Shigaev, A., et al., *Regulation of sgk by aldosterone and its effects on the epithelial Na(+) channel.* Am J Physiol Renal Physiol, 2000. **278**(4): p. F613-9.
44. Soundararajan, R., et al., *A novel role for glucocorticoid-induced leucine zipper protein in epithelial sodium channel-mediated sodium transport.* J Biol Chem, 2005. **280**(48): p. 39970-81.
45. Kleyman, T.R., S.A. Ernst, and B. Coupaye-Gerard, *Arginine vasopressin and forskolin regulate apical cell surface expression of epithelial Na+ channels in A6 cells.* Am J Physiol, 1994. **266**(3 Pt 2): p. F506-11.
46. Snyder, P.M., *Liddle's syndrome mutations disrupt cAMP-mediated translocation of the epithelial Na(+) channel to the cell surface.* J Clin Invest, 2000. **105**(1): p. 45-53.
47. Yamada, T., et al., *Frog atrial natriuretic peptide and cGMP activate amiloride-sensitive Na(+) channels in urinary bladder cells of Japanese tree frog, Hyla japonica.* J Comp Physiol B, 2007. **177**(5): p. 503-8.
48. Blazer-Yost, B.L., M.A. Esterman, and C.J. Vlahos, *Insulin-stimulated trafficking of ENaC in renal cells requires PI 3-kinase activity.* Am J Physiol Cell Physiol, 2003. **284**(6): p. C1645-53.
49. Gilmore, E.S., M.J. Stutts, and S.L. Milgram, *SRC family kinases mediate epithelial Na+ channel inhibition by endothelin.* J Biol Chem, 2001. **276**(45): p. 42610-7.

50. Drummond, H.A., et al., *A molecular component of the arterial baroreceptor mechanotransducer.* Neuron, 1998. **21**(6): p. 1435-41.
51. Drummond, H.A., D. Gebremedhin, and D.R. Harder, *Degenerin/epithelial Na+ channel proteins: components of a vascular mechanosensor.* Hypertension, 2004. **44**(5): p. 643-8.
52. Satlin, L.M., et al., *Epithelial Na(+) channels are regulated by flow.* Am J Physiol Renal Physiol, 2001. **280**(6): p. F1010-8.
53. Carattino, M.D., S. Sheng, and T.R. Kleyman, *Mutations in the pore region modify epithelial sodium channel gating by shear stress.* J Biol Chem, 2005. **280**(6): p. 4393-401.
54. Carattino, M.D., S. Sheng, and T.R. Kleyman, *Epithelial Na+ channels are activated by laminar shear stress.* J Biol Chem, 2004. **279**(6): p. 4120-6.
55. Althaus, M., et al., *Mechano-sensitivity of epithelial sodium channels (ENaCs): laminar shear stress increases ion channel open probability.* FASEB J, 2007. **21**(10): p. 2389-99.
56. Kleyman, T.R., M.M. Myerburg, and R.P. Hughey, *Regulation of ENaCs by proteases: An increasingly complex story.* Kidney Int, 2006. **70**(8): p. 1391-2.
57. Carattino, M.D., et al., *The epithelial Na+ channel is inhibited by a peptide derived from proteolytic processing of its alpha subunit.* J Biol Chem, 2006. **281**(27): p. 18901-7.
58. Sheng, S., et al., *Furin cleavage activates the epithelial Na+ channel by relieving Na+ self-inhibition.* Am J Physiol Renal Physiol, 2006. **290**(6): p. F1488-96.
59. Bruns, J.B., et al., *Epithelial Na+ channels are fully activated by furin- and prostasin-dependent release of an inhibitory peptide from the gamma-subunit.* J Biol Chem, 2007. **282**(9): p. 6153-60.
60. Bruns, J.B., et al., *Multiple epithelial Na+ channel domains participate in subunit assembly.* Am J Physiol Renal Physiol, 2003. **285**(4): p. F600-9.
61. Shimkets, R.A., R.P. Lifton, and C.M. Canessa, *The activity of the epithelial sodium channel is regulated by clathrin-mediated endocytosis.* J Biol Chem, 1997. **272**(41): p. 25537-41.
62. Hicke, L. and R. Dunn, *Regulation of membrane protein transport by ubiquitin and ubiquitin-binding proteins.* Annu Rev Cell Dev Biol, 2003. **19**: p. 141-72.
63. Staub, O. and D. Rotin, *Role of ubiquitylation in cellular membrane transport.* Physiol Rev, 2006. **86**(2): p. 669-707.
64. Liang, X., et al., *AS160 modulates aldosterone-stimulated epithelial sodium channel forward trafficking.* Mol Biol Cell, 2010. **21**(12): p. 2024-33.
65. Diakov, A. and C. Korbmacher, *A novel pathway of epithelial sodium channel activation involves a serum- and glucocorticoid-inducible kinase consensus motif in the C terminus of the channel's alpha-subunit.* J Biol Chem, 2004. **279**(37): p. 38134-42.
66. Loffing, J., S.Y. Flores, and O. Staub, *Sgk kinases and their role in epithelial transport.* Annu Rev Physiol, 2006. **68**: p. 461-90.
67. Vandenbosche, R.C. and J.T. Kirchner, *Intrauterine growth retardation.* Am Fam Physician, 1998. **58**(6): p. 1384-90, 1393-4.
68. Nichols, C.G. and A.N. Lopatin, *Inward rectifier potassium channels.* Annu Rev Physiol, 1997. **59**: p. 171-91.
69. Doyle, D.A., et al., *The structure of the potassium channel: molecular basis of K+ conduction and selectivity.* Science, 1998. **280**(5360): p. 69-77.
70. Minor, D.L., Jr., et al., *Transmembrane structure of an inwardly rectifying potassium channel.* Cell, 1999. **96**(6): p. 879-91.
71. Choe, H., et al., *A conserved cytoplasmic region of ROMK modulates pH sensitivity, conductance, and gating.* Am J Physiol, 1997. **273**(4 Pt 2): p. F516-29.
72. Rapedius, M., et al., *Structural and functional analysis of the putative pH sensor in the Kir1.1 (ROMK) potassium channel.* EMBO Rep, 2006. **7**(6): p. 611-6.
73. Wang, W.H., A. Schwab, and G. Giebisch, *Regulation of small-conductance K+ channel in apical membrane of rat cortical collecting tubule.* Am J Physiol, 1990. **259**(3 Pt 2): p. F494-502.

74. Ali, S., et al., *The A kinase anchoring protein is required for mediating the effect of protein kinase A on ROMK1 channels.* Proc Natl Acad Sci U S A, 1998. **95**(17): p. 10274-8.
75. McNicholas, C.M., et al., *Regulation of ROMK1 K+ channel activity involves phosphorylation processes.* Proc Natl Acad Sci U S A, 1994. **91**(17): p. 8077-81.
76. O'Connell, A.D., et al., *Phosphorylation-regulated endoplasmic reticulum retention signal in the renal outer-medullary K+ channel (ROMK).* Proc Natl Acad Sci U S A, 2005. **102**(28): p. 9954-9.
77. Yoo, D., et al., *A phosphorylation-dependent export structure in ROMK (Kir 1.1) channel overrides an endoplasmic reticulum localization signal.* J Biol Chem, 2005. **280**(42): p. 35281-9.
78. Liou, H.H., S.S. Zhou, and C.L. Huang, *Regulation of ROMK1 channel by protein kinase A via a phosphatidylinositol 4,5-bisphosphate-dependent mechanism.* Proc Natl Acad Sci U S A, 1999. **96**(10): p. 5820-5.
79. Huang, C.L., S. Feng, and D.W. Hilgemann, *Direct activation of inward rectifier potassium channels by PIP2 and its stabilization by Gbetagamma.* Nature, 1998. **391**(6669): p. 803-6.
80. Yoo, D., et al., *Cell surface expression of the ROMK (Kir 1.1) channel is regulated by the aldosterone-induced kinase, SGK-1, and protein kinase A.* J Biol Chem, 2003. **278**(25): p. 23066-75.
81. Loo, T.W. and D.M. Clarke, *Location of the rhodamine-binding site in the human multidrug resistance P-glycoprotein.* J Biol Chem, 2002. **277**(46): p. 44332-8.
82. Zeng, W.Z., et al., *Protein kinase C inhibits ROMK1 channel activity via a phosphatidylinositol 4,5-bisphosphate-dependent mechanism.* J Biol Chem, 2003. **278**(19): p. 16852-6.
83. Pluznick, J.L. and S.C. Sansom, *BK channels in the kidney: role in K(+) secretion and localization of molecular components.* Am J Physiol Renal Physiol, 2006. **291**(3): p. F517-29.
84. Schlatter, E., *Regulation of ion channels in the cortical collecting duct.* Ren Physiol Biochem, 1993. **16**(1-2): p. 21-36.
85. Schlatter, E., et al., *pH dependence of K+ conductances of rat cortical collecting duct principal cells.* Pflugers Arch, 1994. **428**(5-6): p. 631-40.
86. Taniguchi, J. and M. Imai, *Flow-dependent activation of maxi K+ channels in apical membrane of rabbit connecting tubule.* J Membr Biol, 1998. **164**(1): p. 35-45.
87. Woda, C.B., et al., *Flow-dependent K+ secretion in the cortical collecting duct is mediated by a maxi-K channel.* Am J Physiol Renal Physiol, 2001. **280**(5): p. F786-93.
88. Rieg, T., et al., *The role of the BK channel in potassium homeostasis and flow-induced renal potassium excretion.* Kidney Int, 2007. **72**(5): p. 566-73.
89. Bailey, M.A., et al., *Maxi-K channels contribute to urinary potassium excretion in the ROMK-deficient mouse model of Type II Bartter's syndrome and in adaptation to a high-K diet.* Kidney Int, 2006. **70**(1): p. 51-9.
90. Gamba, G., *The thiazide-sensitive Na+-Cl- cotransporter: molecular biology, functional properties, and regulation by WNKs.* Am J Physiol Renal Physiol, 2009. **297**(4): p. F838-48.
91. Vallon, V., *Regulation of the Na+-Cl- cotransporter by dietary NaCl: a role for WNKs, SPAK, OSR1, and aldosterone.* Kidney Int, 2008. **74**(11): p. 1373-5.
92. Frindt, G. and L.G. Palmer, *Effects of dietary K on cell-surface expression of renal ion channels and transporters.* Am J Physiol Renal Physiol, 2010. **299**(4): p. F890-7.
93. Ko, B. and R.S. Hoover, *Molecular physiology of the thiazide-sensitive sodium-chloride cotransporter.* Curr Opin Nephrol Hypertens, 2009. **18**(5): p. 421-7.
94. Gordon, R.D. and G.P. Hodsman, *The syndrome of hypertension and hyperkalaemia without renal failure: long term correction by thiazide diuretic.* Scott Med J, 1986. **31**(1): p. 43-4.
95. Gitelman, H.J., J.B. Graham, and L.G. Welt, *A new familial disorder characterized by hypokalemia and hypomagnesemia.* Trans Assoc Am Physicians, 1966. **79**: p. 221-35.
96. Lin, S.H., et al., *Phenotype and genotype analysis in Chinese patients with Gitelman's syndrome.* J Clin Endocrinol Metab, 2005. **90**(5): p. 2500-7.

97. Sorensen, M.V., et al., *Colonic potassium handling.* Pflugers Arch, 2010. **459**(5): p. 645-56.
98. Agarwal, R., R. Afzalpurkar, and J.S. Fordtran, *Pathophysiology of potassium absorption and secretion by the human intestine.* Gastroenterology, 1994. **107**(2): p. 548-71.
99. Foster, E.S., J.P. Hayslett, and H.J. Binder, *Mechanism of active potassium absorption and secretion in the rat colon.* Am J Physiol, 1984. **246**(5 Pt 1): p. G611-7.
100. Foster, E.S., et al., *Corticosteroid alteration of active electrolyte transport in rat distal colon.* Am J Physiol, 1983. **245**(5 Pt 1): p. G668-75.
101. Foster, E.S., et al., *Role of aldosterone and dietary potassium in potassium adaptation in the distal colon of the rat.* Gastroenterology, 1985. **88**(1 Pt 1): p. 41-6.
102. Foster, E.S., et al., *Dietary potassium modulates active potassium absorption and secretion in rat distal colon.* Am J Physiol, 1986. **251**(5 Pt 1): p. G619-26.
103. Halm, D.R. and D.C. Dawson, *Potassium transport by turtle colon: active secretion and active absorption.* Am J Physiol, 1984. **246**(3 Pt 1): p. C315-22.
104. Sweiry, J.H. and H.J. Binder, *Characterization of aldosterone-induced potassium secretion in rat distal colon.* J Clin Invest, 1989. **83**(3): p. 844-51.
105. Sorensen, M.V., et al., *The secretory KCa1.1 channel localises to crypts of distal mouse colon: functional and molecular evidence.* Pflugers Arch, 2011. **462**(5): p. 745-52.
106. Edmonds, C.J., *Amiloride sensitivity of the transepithelial electrical potential and of sodium and potassium transport in rat distal colon in vivo.* J Physiol, 1981. **313**: p. 547-59.
107. Fromm, M. and S.G. Schultz, *Potassium transport across rabbit descending colon in vitro: evidence for single-file diffusion through a paracellular pathway.* J Membr Biol, 1981. **63**(1-2): p. 93-8.
108. Binder, H.J., sandle, G.I., *Electrolyte transport in the mammalian colon*. 1994, New York.
109. Young, B.C., R.J. Levine, and S.A. Karumanchi, *Pathogenesis of preeclampsia.* Annu Rev Pathol, 2010. **5**: p. 173-92.
110. Noris, M., N. Perico, and G. Remuzzi, *Mechanisms of disease: Pre-eclampsia.* Nat Clin Pract Nephrol, 2005. **1**(2): p. 98-114; quiz 120.
111. Briana, D.D. and A. Malamitsi-Puchner, *Intrauterine growth restriction and adult disease: the role of adipocytokines.* Eur J Endocrinol, 2009. **160**(3): p. 337-47.
112. Rosenberg, A., *The IUGR newborn.* Semin Perinatol, 2008. **32**(3): p. 219-24.
113. Moffett-King, A., *Natural killer cells and pregnancy.* Nat Rev Immunol, 2002. **2**(9): p. 656-63.
114. Kaufmann, P., S. Black, and B. Huppertz, *Endovascular trophoblast invasion: implications for the pathogenesis of intrauterine growth retardation and preeclampsia.* Biol Reprod, 2003. **69**(1): p. 1-7.
115. Brosens, I.A., W.B. Robertson, and H.G. Dixon, *The role of the spiral arteries in the pathogenesis of preeclampsia.* Obstet Gynecol Annu, 1972. **1**: p. 177-91.
116. Genbacev, O., et al., *Regulation of human placental development by oxygen tension.* Science, 1997. **277**(5332): p. 1669-72.
117. Genbacev, O., et al., *Hypoxia alters early gestation human cytotrophoblast differentiation/invasion in vitro and models the placental defects that occur in preeclampsia.* J Clin Invest, 1996. **97**(2): p. 540-50.
118. Ness, R.B. and B.M. Sibai, *Shared and disparate components of the pathophysiologies of fetal growth restriction and preeclampsia.* Am J Obstet Gynecol, 2006. **195**(1): p. 40-9.
119. Caniggia, I., et al., *Hypoxia-inducible factor-1 mediates the biological effects of oxygen on human trophoblast differentiation through TGFbeta(3).* J Clin Invest, 2000. **105**(5): p. 577-87.
120. Caniggia, I., et al., *Inhibition of TGF-beta 3 restores the invasive capability of extravillous trophoblasts in preeclamptic pregnancies.* J Clin Invest, 1999. **103**(12): p. 1641-50.
121. Pijnenborg, R., et al., *Immunolocalization of tumour necrosis factor-alpha (TNF-alpha) in the placental bed of normotensive and hypertensive human pregnancies.* Placenta, 1998. **19**(4): p. 231-9.

122. Caniggia, I. and J.L. Winter, *Adriana and Luisa Castellucci Award lecture 2001. Hypoxia inducible factor-1: oxygen regulation of trophoblast differentiation in normal and pre-eclamptic pregnancies--a review.* Placenta, 2002. **23 Suppl A**: p. S47-57.
123. Tazuke, S.I., et al., *Hypoxia stimulates insulin-like growth factor binding protein 1 (IGFBP-1) gene expression in HepG2 cells: a possible model for IGFBP-1 expression in fetal hypoxia.* Proc Natl Acad Sci U S A, 1998. **95**(17): p. 10188-93.
124. Kingdom, J.C. and P. Kaufmann, *Oxygen and placental vascular development.* Adv Exp Med Biol, 1999. **474**: p. 259-75.
125. Hodgkinson, C.P., A. Hodari, and F.M. Bumpus, *Experimental hypertensive disease of pregnancy.* Obstet Gynecol, 1967. **30**(3): p. 371-80.
126. Combs, C.A., et al., *Experimental preeclampsia produced by chronic constriction of the lower aorta: validation with longitudinal blood pressure measurements in conscious rhesus monkeys.* Am J Obstet Gynecol, 1993. **169**(1): p. 215-23.
127. Villar, J., et al., *Preeclampsia, gestational hypertension and intrauterine growth restriction, related or independent conditions?* Am J Obstet Gynecol, 2006. **194**(4): p. 921-31.
128. Salafia, C. and K. Shiverick, *Cigarette smoking and pregnancy II: vascular effects.* Placenta, 1999. **20**(4): p. 273-9.
129. McDonald, A.D., B.G. Armstrong, and M. Sloan, *Cigarette, alcohol, and coffee consumption and prematurity.* Am J Public Health, 1992. **82**(1): p. 87-90.
130. Conde-Agudelo, A., et al., *Cigarette smoking during pregnancy and risk of preeclampsia: a systematic review.* Am J Obstet Gynecol, 1999. **181**(4): p. 1026-35.
131. Barker, D.J. and P.M. Clark, *Fetal undernutrition and disease in later life.* Rev Reprod, 1997. **2**(2): p. 105-12.
132. Fowden, A.L., et al., *Placental efficiency and adaptation: endocrine regulation.* J Physiol, 2009. **587**(Pt 14): p. 3459-72.
133. Wilson, M.E. and S.P. Ford, *Comparative aspects of placental efficiency.* Reprod Suppl, 2001. **58**: p. 223-32.
134. Baur, R., *Morphometry of the placental exchange area.* Adv Anat Embryol Cell Biol, 1977. **53**(1): p. 3-65.
135. Mellor, D.J., *Nutritional and placental determinants of foetal growth rate in sheep and consequences for the newborn lamb.* Br Vet J, 1983. **139**(4): p. 307-24.
136. Fowden, A.L., et al., *Programming placental nutrient transport capacity.* J Physiol, 2006. **572**(Pt 1): p. 5-15.
137. Fowden, A.L. and A.J. Forhead, *Endocrine mechanisms of intrauterine programming.* Reproduction, 2004. **127**(5): p. 515-26.
138. Jones, H.N., T.L. Powell, and T. Jansson, *Regulation of placental nutrient transport--a review.* Placenta, 2007. **28**(8-9): p. 763-74.
139. Levine, R.J., et al., *Circulating angiogenic factors and the risk of preeclampsia.* N Engl J Med, 2004. **350**(7): p. 672-83.
140. Maynard, S.E., et al., *Excess placental soluble fms-like tyrosine kinase 1 (sFlt1) may contribute to endothelial dysfunction, hypertension, and proteinuria in preeclampsia.* J Clin Invest, 2003. **111**(5): p. 649-58.
141. Venkatesha, S., et al., *Soluble endoglin contributes to the pathogenesis of preeclampsia.* Nat Med, 2006. **12**(6): p. 642-9.
142. Shah, D.M., *The role of RAS in the pathogenesis of preeclampsia.* Curr Hypertens Rep, 2006. **8**(2): p. 144-52.
143. Shah, D.M., *Preeclampsia: new insights.* Curr Opin Nephrol Hypertens, 2007. **16**(3): p. 213-20.
144. Nolten, W.E., et al., *Desoxycorticosterone in normal pregnancy. I. Sequential studies of the secretory patterns of desoxycorticosterone, aldosterone, and cortisol.* Am J Obstet Gynecol, 1978. **132**(4): p. 414-20.

145. Hays, P.M., D.P. Cruikshank, and L.J. Dunn, *Plasma volume determination in normal and preeclamptic pregnancies.* Am J Obstet Gynecol, 1985. **151**(7): p. 958-66.
146. Salas, S.P., et al., *Time course of maternal plasma volume and hormonal changes in women with preeclampsia or fetal growth restriction.* Hypertension, 2006. **47**(2): p. 203-8.
147. Wacker, J., et al., *Increased aldosterone-18-glucuronide/tetrahydroaldosterone ratios in pregnancy.* Endocr Res, 1995. **21**(1-2): p. 197-202.
148. Gallery, E.D., S.N. Hunyor, and A.Z. Gyory, *Plasma volume contraction: a significant factor in both pregnancy-associated hypertension (pre-eclampsia) and chronic hypertension in pregnancy.* Q J Med, 1979. **48**(192): p. 593-602.
149. Escher, G. and M. Mohaupt, *Role of aldosterone availability in preeclampsia.* Mol Aspects Med, 2007. **28**(2): p. 245-54.
150. Symonds, E.M., F. Broughton Pipkin, and D.J. Craven, *Changes in the renin-angiotensin system in primigravidae with hypertensive disease of pregnancy.* Br J Obstet Gynaecol, 1975. **82**(8): p. 643-50.
151. Shojaati, K., et al., *Evidence for compromised aldosterone synthase enzyme activity in preeclampsia.* Kidney Int, 2004. **66**(6): p. 2322-8.
152. Pascoe, L., et al., *Mutations in the human CYP11B2 (aldosterone synthase) gene causing corticosterone methyloxidase II deficiency.* Proc Natl Acad Sci U S A, 1992. **89**(11): p. 4996-5000.
153. Nicod, J., et al., *A biallelic gene polymorphism of CYP11B2 predicts increased aldosterone to renin ratio in selected hypertensive patients.* J Clin Endocrinol Metab, 2003. **88**(6): p. 2495-500.
154. Escher, G., et al., *High aldosterone-to-renin variants of CYP11B2 and pregnancy outcome.* Nephrol Dial Transplant, 2009.
155. Rossant, J. and J.C. Cross, *Placental development: lessons from mouse mutants.* Nat Rev Genet, 2001. **2**(7): p. 538-48.
156. Driver, P.M., et al., *Expression of 11 beta-hydroxysteroid dehydrogenase isozymes and corticosteroid hormone receptors in primary cultures of human trophoblast and placental bed biopsies.* Mol Hum Reprod, 2001. **7**(4): p. 357-63.
157. Driver, P.M., et al., *Characterization of human trophoblast as a mineralocorticoid target tissue.* Mol Hum Reprod, 2003. **9**(12): p. 793-8.
158. Schoof, E., et al., *Decreased gene expression of 11beta-hydroxysteroid dehydrogenase type 2 and 15-hydroxyprostaglandin dehydrogenase in human placenta of patients with preeclampsia.* J Clin Endocrinol Metab, 2001. **86**(3): p. 1313-7.
159. del Monaco, S., et al., *[Characterization of the epithelial sodium channel in human pre-eclampsia syncytiotrophoblast].* Medicina (B Aires), 2006. **66**(1): p. 31-5.
160. Del Monaco, S.M., et al., *[Preeclampsia, cellular migration and ion channels].* Medicina (B Aires), 2008. **68**(5): p. 405-10.
161. Grifoni, S.C., et al., *ENaC proteins contribute to VSMC migration.* Am J Physiol Heart Circ Physiol, 2006. **291**(6): p. H3076-86.
162. Jensen, E., C.E. Wood, and M. Keller-Wood, *Reduction of maternal adrenal steroids results in increased VEGF protein without increased eNOS in the ovine placenta.* Placenta, 2007. **28**(7): p. 658-67.
163. Robinson, M., *Salt in pregnancy.* Lancet, 1958. **1**(7013): p. 178-81.
164. Farese, S., et al., *Blood pressure reduction in pregnancy by sodium chloride.* Nephrol Dial Transplant, 2006. **21**(7): p. 1984-7.
165. Duley, L., D. Henderson-Smart, and S. Meher, *Altered dietary salt for preventing pre-eclampsia, and its complications.* Cochrane Database Syst Rev, 2005(4): p. CD005548.
166. Muto, S., S. Sansom, and G. Giebisch, *Effects of a high potassium diet on electrical properties of cortical collecting ducts from adrenalectomized rabbits.* J Clin Invest, 1988. **81**(2): p. 376-80.

167. Palmer, L.G., L. Antonian, and G. Frindt, *Regulation of apical K and Na channels and Na/K pumps in rat cortical collecting tubule by dietary K.* J Gen Physiol, 1994. **104**(4): p. 693-710.
168. Stanton, B., et al., *Effects of adrenalectomy and chronic adrenal corticosteroid replacement on potassium transport in rat kidney.* J Clin Invest, 1985. **75**(4): p. 1317-26.
169. Xue, C. and H.M. Siragy, *Local renal aldosterone system and its regulation by salt, diabetes, and angiotensin II type 1 receptor.* Hypertension, 2005. **46**(3): p. 584-90.
170. Makhanova, N., et al., *Disturbed homeostasis in sodium-restricted mice heterozygous and homozygous for aldosterone synthase gene disruption.* Hypertension, 2006. **48**(6): p. 1151-9.
171. Seaton, B. and A. Ali, *Simplified manual high performance clinical chemistry methods for developing countries.* Med Lab Sci, 1984. **41**(4): p. 327-36.
172. Nowik, M., et al., *Renal phosphaturia during metabolic acidosis revisited: molecular mechanisms for decreased renal phosphate reabsorption.* Pflugers Arch, 2008. **457**(2): p. 539-49.
173. Nowik, M., et al., *Genome-wide gene expression profiling reveals renal genes regulated during metabolic acidosis.* Physiol Genomics, 2008. **32**(3): p. 322-34.
174. Dawson, T.P., et al., *Ecto-5'-nucleotidase: localization in rat kidney by light microscopic histochemical and immunohistochemical methods.* J Histochem Cytochem, 1989. **37**(1): p. 39-47.
175. Krege, J.H., et al., *A noninvasive computerized tail-cuff system for measuring blood pressure in mice.* Hypertension, 1995. **25**(5): p. 1111-5.
176. Rabinowitz, L., *Aldosterone and potassium homeostasis.* Kidney Int, 1996. **49**(6): p. 1738-42.
177. Rabinowitz, L., *Model of homeostatic regulation of potassium excretion in sheep.* Am J Physiol, 1988. **254**(2 Pt 2): p. R381-8.
178. Rabinowitz, L., et al., *Homeostatic potassium excretion in fed and fasted sheep.* Am J Physiol, 1988. **254**(2 Pt 2): p. R357-80.
179. Rabinowitz, L., R.L. Sarason, and H. Yamauchi, *Effects of KCl infusion on potassium excretion in sheep.* Am J Physiol, 1985. **249**(2 Pt 2): p. F263-71.
180. Lee, F.N., et al., *Evidence for gut factor in K+ homeostasis.* Am J Physiol Renal Physiol, 2007. **293**(2): p. F541-7.
181. Rabinowitz, L., T.W. Castonguay, and J.C. Rutledge, *Aldosterone reverses potassium-induced food aversions in adrenalectomized rats.* Physiol Behav, 1988. **42**(2): p. 137-40.
182. Taves, M.D., C.E. Gomez-Sanchez, and K.K. Soma, *Extra-adrenal glucocorticoids and mineralocorticoids: evidence for local synthesis, regulation, and function.* Am J Physiol Endocrinol Metab, 2011. **301**(1): p. E11-24.
183. Frindt, G. and L.G. Palmer, *Na channels in the rat connecting tubule.* Am J Physiol Renal Physiol, 2004. **286**(4): p. F669-74.
184. Katz, A.I., A. Doucet, and F. Morel, *Na-K-ATPase activity along the rabbit, rat, and mouse nephron.* Am J Physiol, 1979. **237**(2): p. F114-20.
185. El Moghrabi, S., et al., *Tissue kallikrein permits early renal adaptation to potassium load.* Proc Natl Acad Sci U S A, 2010. **107**(30): p. 13526-31.
186. Rubera, I., et al., *Collecting duct-specific gene inactivation of alphaENaC in the mouse kidney does not impair sodium and potassium balance.* J Clin Invest, 2003. **112**(4): p. 554-65.
187. Harrison-Bernard, L.M., et al., *Immunohistochemical localization of ANG II AT1 receptor in adult rat kidney using a monoclonal antibody.* Am J Physiol, 1997. **273**(1 Pt 2): p. F170-7.
188. Beutler, K.T., et al., *Long-term regulation of ENaC expression in kidney by angiotensin II.* Hypertension, 2003. **41**(5): p. 1143-50.
189. Brooks, H.L., et al., *Targeted proteomic profiling of renal Na(+) transporter and channel abundances in angiotensin II type 1a receptor knockout mice.* Hypertension, 2002. **39**(2 Pt 2): p. 470-3.
190. Peti-Peterdi, J., D.G. Warnock, and P.D. Bell, *Angiotensin II directly stimulates ENaC activity in the cortical collecting duct via AT(1) receptors.* J Am Soc Nephrol, 2002. **13**(5): p. 1131-5.

191. Wang, T. and G. Giebisch, *Effects of angiotensin II on electrolyte transport in the early and late distal tubule in rat kidney.* Am J Physiol, 1996. **271**(1 Pt 2): p. F143-9.
192. Madala Halagappa, V.K., et al., *Chronic candesartan alters expression and activity of NKCC2, NCC, and ENaC in the obese Zucker rat.* Am J Physiol Renal Physiol, 2008. **294**(5): p. F1222-31.
193. Wei, Y., et al., *Angiotensin II inhibits the ROMK-like small conductance K channel in renal cortical collecting duct during dietary potassium restriction.* J Biol Chem, 2007. **282**(9): p. 6455-62.
194. Jin, Y., et al., *Inhibition of angiotensin type 1 receptor impairs renal ability of K conservation in response to K restriction.* Am J Physiol Renal Physiol, 2009. **296**(5): p. F1179-84.
195. Weir, M.R. and M. Rolfe, *Potassium homeostasis and renin-angiotensin-aldosterone system inhibitors.* Clin J Am Soc Nephrol, 2010. **5**(3): p. 531-48.
196. Wang, W.H., *Two types of K+ channel in thick ascending limb of rat kidney.* Am J Physiol, 1994. **267**(4 Pt 2): p. F599-605.
197. Fitzsimons, J.T., *Angiotensin, thirst, and sodium appetite.* Physiol Rev, 1998. **78**(3): p. 583-686.
198. Schwartz, M.J. and J.P. Kokko, *Urinary concentrating defect of adrenal insufficiency. Permissive role of adrenal steroids on the hydroosmotic response across the rabbit cortical collecting tubule.* J Clin Invest, 1980. **66**(2): p. 234-42.
199. Chen, L., S.K. Williams, and J.A. Schafer, *Differences in synergistic actions of vasopressin and deoxycorticosterone in rat and rabbit CCD.* Am J Physiol, 1990. **259**(1 Pt 2): p. F147-56.
200. Kwon, T.H., et al., *Regulation of collecting duct AQP3 expression: response to mineralocorticoid.* Am J Physiol Renal Physiol, 2002. **283**(6): p. F1403-21.
201. Bankir, L., *Antidiuretic action of vasopressin: quantitative aspects and interaction between V1a and V2 receptor-mediated effects.* Cardiovasc Res, 2001. **51**(3): p. 372-90.
202. Kim, G.H., et al., *The thiazide-sensitive Na-Cl cotransporter is an aldosterone-induced protein.* Proc Natl Acad Sci U S A, 1998. **95**(24): p. 14552-7.
203. Richardson, C., et al., *Activation of the thiazide-sensitive Na+-Cl- cotransporter by the WNK-regulated kinases SPAK and OSR1.* J Cell Sci, 2008. **121**(Pt 5): p. 675-84.
204. Weinstein, A.M., *A mathematical model of rat distal convoluted tubule. I. Cotransporter function in early DCT.* Am J Physiol Renal Physiol, 2005. **289**(4): p. F699-720.
205. Knoers, N.V. and E.N. Levtchenko, *Gitelman syndrome.* Orphanet J Rare Dis, 2008. **3**: p. 22.
206. Mayan, H., et al., *Pseudohypoaldosteronism type II: marked sensitivity to thiazides, hypercalciuria, normomagnesemia, and low bone mineral density.* J Clin Endocrinol Metab, 2002. **87**(7): p. 3248-54.
207. Kunzelmann, K. and M. Mall, *Electrolyte transport in the mammalian colon: mechanisms and implications for disease.* Physiol Rev, 2002. **82**(1): p. 245-89.
208. Grotjohann, I., et al., *Localization of cAMP- and aldosterone-induced K+ secretion in rat distal colon by conductance scanning.* J Physiol, 1998. **507 (Pt 2)**: p. 561-70.
209. Burke, S.D., et al., *Spiral arterial remodeling is not essential for normal blood pressure regulation in pregnant mice.* Hypertension, 2010. **55**(3): p. 729-37.
210. Sohn, H.J., et al., *Aldosterone modulates cell proliferation and apoptosis in the neonatal rat heart.* J Korean Med Sci, 2010. **25**(9): p. 1296-304.
211. Yim, H.E., et al., *Aldosterone regulates cellular turnover and mitogen-activated protein kinase family expression in the neonatal rat kidney.* J Cell Physiol, 2009. **219**(3): p. 724-33.
212. Gallery, E.D. and M.A. Brown, *Control of sodium excretion in human pregnancy.* Am J Kidney Dis, 1987. **9**(4): p. 290-5.
213. Gallery, E.D., *Pregnancy-associated hypertension: interrelationships of volume and blood pressure changes.* Clin Exp Hypertens B, 1982. **1**(1): p. 39-47.
214. Puschett, J.B., *The role of excessive volume expansion in the pathogenesis of preeclampsia.* Med Hypotheses, 2006. **67**(5): p. 1125-32.

215. Alexander, B.T., *Placental insufficiency leads to development of hypertension in growth-restricted offspring.* Hypertension, 2003. **41**(3): p. 457-62.
216. Huang, S.T., et al., *Developmental response to hypoxia.* FASEB J, 2004. **18**(12): p. 1348-65.
217. Adelman, D.M., et al., *Placental cell fates are regulated in vivo by HIF-mediated hypoxia responses.* Genes Dev, 2000. **14**(24): p. 3191-203.
218. Makhanova, N., et al., *Kidney function in mice lacking aldosterone.* Am J Physiol Renal Physiol, 2006. **290**(1): p. F61-9.

ACKNOWLEDGEMENTS

I would like to thank:

- Prof. Carsten Wagner and Prof. Johannes Loffing, my thesis supervisors and bosses for giving me the opportunity to work in their groups, their valuable guidance and support throughout the years of my thesis;

- Prof. François Verrey and Prof. Dominique Eladari, members of my thesis committee, for valuable suggestions and advice concerning my project;

- All the people who contributed to the project with their work and expertise- Nicolas Picard, Dominique Loffing-Cueni, Mariana Di Chiara, Mads Sorensen, Monique Carrel, Nicole Kampik, Carla Bettoni, Marija Mihailova;

- Our collaborators Prof. Christoph Korbmacher and Viatcheslav Nesterov; Prof. Felix Frey and Bernhard Dick for their work and expertise contributing to this project;

- Prof. Gerhard Rogler, Isabelle Frey-Wagner and Yu Wang for supply of few primers and probes

- All the people working on J-floor in the Institutes of Physiology and Anatomy for creating great working atmosphere;

- My parents (Pandurang and Jyotsna Todkar), Amit and Aparna for their great support during all the years of my studies and my PhD;

- My wife Prajakta for her love and especially for her patience during tough time of my PhD;

- My cousine Kiran and friends Pankaj, Nikhil, Manoj, Dheeraj, Pallavi, Samyuktha and Alok for making my life easier in Zurich during PhD;

Further I would like to thank:

- Zurich Center for Integrative Human Physiology “ZIHP”, for the PhD student fellowship.

CURRICULUM VITAE

Name	Abhijeet Pandurang Todkar
Nationality	Indian
Marital status	Married
Date of Birth	20th January 1980
E-mail	abhijeet.todkar@access.uzh.ch
Mobile	(041) 789299135

EDUCATION

Since Oct 2007

PhD fellow**,** Institute of Physiology and Institute of Anatomy),
University of Zurich, Switzerland
Title of Projects: 1.Aldosterone dependent and independent regulation of potassium homeostasis.
2. Role of aldosterone in pregnancy

Project advisors: Prof. Carsten Wagner and Prof. Johannes Loffing

Jan 2006 to Aug 2007

M.Sc. Molecular Biology**, University of Skovde, Sweden** and **Eberhard Kares University of Tübingen, Germany**

Title of thesis: Transdifferentiation of vascular smooth muscle cells.

Project Advisor: Prof. Robert Feil, (Department of Signal Transduction-Transgene Models)

Jan 2003 to Feb 2005

Master of Veterinary Science (M.V.Sc.) - Veterinary Pathology.
Bombay Veterinary College (BVC), India.

Title of thesis: Pathology of Streptozotocin (STZ) induced hyperglycemia in rat and effect of herbal medicine.

Project advisor: Prof. P.L. Lonkar

Sept 2007- Sept 2002

Bachelor of Veterinary science (B.V. Sc.)
K.N.P. College of veterinary Science, Shirwal Satara
MAFSU University, Satara

PUBLICATIONS

Papers

1. Abhijeet Todkar, Marianna Di Chiara, Dominique Loffing-Cueni, Carla Bettoni, Markus Mohaupt, Johannes Loffing, Carsten A Wagner. Aldosterone deficiency adversely affects pregnancy outcome in mice. Pflügers Arch, in press

2. Abhijeet Todkar, Nicolas Picard, Dominique Loffing-Cueni, Mads Sorensen, Marija Mihailova, Christoph Korbmacher, Natalia Makhanova, Oliver Smithies, Carsten Wagner, Johannes Loffing. Aldosterone is dispensable for renal but not for colonic regulation of potassium homeostasis. (In preparation).

Abstracts (Poster and Oral Presentations)

Abhijeet Todkar, Nicolas Picard, Dominique Loffing-Cueni, Marija Mihailova, Carsten A. Wagner, Johannes Loffing. Expression of Na^+-Cl^- cotransporter (NCC) and Cl^-/anion exchanger pendrin in aldosterone-deficient mice. Poster presented in Transporter 2008 meeting, Murten, August 2008, Switzerland.

Abhijeet Todkar, Jana Kovacikova, Marija Mihailova, Natalia Makhanova, Olivier Smithies, Johannes Loffing, Carsten A Wagner. Acidosis in mice lacking aldosterone synthase. 5th symposium of ZHIP (Zurich Center for integrative human Physiology), 30 August 2009, University Hospital, Zurich, Switzerland.

Abhijeet Todkar, Jana Kovacikova, Marija Mihailova, Natalia Makhanova, Olivier Smithies, Johannes Loffing, Carsten A Wagner. Acidosis in mice lacking aldosterone synthase.ISN Forefronts Symposium on Renal and Extrarenal Control of Acid-base Homeostasis in Health and Disease, 17 - 20 September 2009, Florence, Italy.

Abhijeet Todkar, Jana Kovacikova, Marija Mihailova, Natalia Makhanova, Olivier Smithies, Johannes Loffing, Carsten A Wagner. Acidosis in mice lacking aldosterone synthase.American Society of Nephrology (ASN) Renal Week, 27.10 to 1.11. 2009, San Diego, CA, USA.

Abhijeet Todkar, Jana Kovacikova, Marija Mihailova, Natalia Makhanova, Olivier Smithies, Johannes Loffing, Carsten A Wagner. Acidosis in mice lacking aldosterone synthase.Joint Meeting of the Scandinavian and German Physiological Societies, 27-30 September, 2010, Copenhagen, Denmark.

Abhijeet Todkar, N Picard, D Loffing-Cueni, M Mihailova, N Makhanova[3], O Smithies, CA Wagner, J Loffing. Aldosterone-dependent and -independent regulation of renal potassium excretion. Poster presented in 4th symposium of ZHIP (Zurich

Center for Integrative Human Physiology), 22 August 2008, University Hospital, Zurich, Switzerland.

A Todkar, M Di Chiara, D Loffing-Cueni, C Bettoni, N Makhanova, O Smithies, J Loffing, CA Wagner. Aldosterone deficiency during pregnancy does not lead to preeclampsia but results in placenta dysfunction, reduced litter size, and smaller pups. Poster presented in 7th International Symposium on Aldosterone and the ENaC/Degenerin Family of Ion Channels: Molecular Mechanisms and Pathophysiology, September 18-22, 2011. Pacific Grove, CA.

Abhijeet Todkar, Nicolas Picard, Mads Sorensen, Natalia Makhanova, OliverSmithies, Carsten Wagner, Johannes Loffing. Aldosterone is diepensable for renal but not for colonic regulation of potassium homeostasis. Oral presentation in 7th International Symposium on Aldosterone and the ENaC/Degenerin Family of Ion Channels: Molecular Mechanisms and Pathophysiology, September 18-22, 2011. Pacific Grove, CA.

A. Todkar, M. Di Chiara, D. Loffing-Cueni, C. Bettoni, M. G. Mohaupt, J. Loffing, C. Wagner. Aldosterone deficiency adversely affects pregnancy outcome in mice. Accepted for oral presentation in XVIII International Society for the Study of Hypertension in Pregnancy (ISSHP) World Congress, 9th to 12th July, 2012, Geneva, Switzerland.